

NASA CR-152139

SYSTEMS TECHNOLOGY, INC.

2672 BAYSHORE FRONTAGE ROAD • MOUNTAIN VIEW, CALIFORNIA 94043 • PHONE [415] 961-4874

STI Technical Report No 1095-1

(NASA-CR-152139)	STUDY OF A SAFETY MARGIN	N78-24117
	SYSTEM FOR POWERED-LIFT STOL AIRCRAFT Final	
	Report, Dec. 1976. - Jan. 1978 (Systems	
	Technology, Inc., Mountain View, Calif.)	Unclas
160 p HC A08/MF A01	CSCL 01C G3/05	21440

Study of a Safety Margin System
For Powered-Lift STOL Aircraft

Robert K Heffley
Wayne F. Jewell

May 1978

Contract NAS2-9418
National Aeronautics and Space Administration
Ames Research Center
Moffett Field, CA 94035

1 Report No NASA CR-152139	2 Government Accession No	3 Recipient's Catalog No	
4 Title and Subtitle STUDY OF A SAFETY MARGIN SYSTEM FOR POWERED-LIFT STOL AIRCRAFT		5 Report Date May 1978	6 Performing Organization Code
		8 Performing Organization Report No. SIT TR-1095-1	10 Work Unit No
7 Author(s) Robert K. Heffley and Wayne F. Jewell	9 Performing Organization Name and Address Systems Technology, Inc. 2672 Bayshore-Frontage Road, Suite 505 Mountain View, California 94043		11 Contract or Grant No NAS2-9418
12 Sponsoring Agency Name and Address National Aeronautics and Space Administration Ames Research Center Moffett Field, California 94035			13 Type of Report and Period Covered Final Report
15 Supplementary Notes		14 Sponsoring Agency Code	
16 Abstract A study was conducted to explore the feasibility of a safety margin system for powered-lift aircraft which require a backside piloting technique. The objective of the safety margin system was to present multiple safety margin criteria as a single variable which could be tracked manually or automatically and which could be monitored for the purpose of deriving safety margin status. The study involved a pilot-in-the-loop analysis of several safety margin system concepts and a simulation experiment to evaluate those concepts which showed promise of providing a good solution. A system was ultimately configured which offered reasonable compromises in controllability, status information content, and the ability to regulate the safety margin at some expense of the allowable low speed flight path envelope.			
17 Key Words (Suggested by Author(s)) Powered Lift STOL Safety Margins Airworthiness Criteria		18 Distribution Statement	
19 Security Classif (of this report)	20 Security Classif (of this page)	21. No of Pages 158	22 Price*

SYSTEMS TECHNOLOGY, INC.

Technical Report No. 1095-1

STUDY OF A SAFETY MARGIN SYSTEM FOR POWERED-LIFT STOL AIRCRAFT

Robert K. Heffley
Wayne F. Jewell

May 1978

Contract NAS2-9418

National Aeronautics and Space Administration
Ames Research Center
Moffett Field, CA 94035

ABSTRACT

A study was conducted to explore the feasibility of a safety margin system for powered-lift aircraft which require a backside piloting technique. The objective of the safety margin system was to present multiple safety margin criteria as a single variable which could be tracked manually or automatically and which could be monitored for the purpose of deriving safety margin status. The study involved a pilot-in-the-loop analysis of several safety margin system concepts and a simulation experiment to evaluate those concepts which showed promise of providing a good solution. A system was ultimately configured which offered reasonable compromises in controllability, status information content, and the ability to regulate the safety margin at some expense of the allowable low speed flight path envelope.

FOREWORD

The research reported here was performed under NASA Contract NAS2-9418. The NASA Contract Technical Monitor was Donald W. Smith of Ames Research Center, and the Systems Technology, Inc., Project Engineer was Robert K. Heffley. STOLAND simulator modification and checkout was supervised by Wayne F. Jewell of Systems Technology, Inc. The primary research pilot was Gordon H. Hardy of Ames Research Center. Work on this project was accomplished during the period from December 1976 to January 1978.

The authors wish to acknowledge the valuable contributions made by Robert L. Stapleford, Roger H. Hoh, and Warren F. Clement of Systems Technology, Inc., William S. Hindson of the National Aeronautical Establishment (Canada), and the careful preparation of the report manuscript by Sharon A. Duerksen of Systems Technology, Inc.

PRECEDING PAGE BLANK NOT FILMED

TABLE OF CONTENTS

Section	Page	
I	INTRODUCTION	1
	A. Background	1
	B. Program Objective	4
	C. Technical Approach	5
	D. Report Organization	6
II	DEFINITION OF SAFETY MARGIN SYSTEM CONCEPTS	7
	A. Safety Margin Criteria	7
	B. Cockpit Instrument Display Concepts	9
	1. Flight Reference (FR)	9
	2. Safety Reference (SR)	9
	C. Safety Margin System Implementation Concepts	10
	1. Safety Margin System	10
	2. Dynamic Safety Margin	10
	3. Static Safety Margin	12
	4. Lift Margin	12
III	ANALYTICAL INVESTIGATION	17
	A. Analysis of Approach	17
	B. Survey of Implementation Concepts	22
	1. Flight Reference Based on Dynamic Safety Margin	25
	2. Flight References Based on Static Safety Margin	36
	3. Flight Reference Based on Lift Margin	42
	C. Implications for the Experimental Investigation	45

TABLE OF CONTENTS (Continued)

Section		Page
IV	EXPERIMENTAL INVESTIGATION	49
A.	Experimental Procedure	49
B.	Investigation of Display Features	53
	1. Flight Reference Indication	53
	2. Safety Reference Indication	56
	3. Flight Reference Status Lights	57
	4. Other Features	58
C.	Preliminary Evaluation of Safety Margin System Concepts	58
	1. Evaluation of FR[DSM]	60
	2. Evaluation of FR[SSM _{u,θ}]	63
	3. Evaluation of FR[SSM _{u,θ}] and SR[DSM]	64
	4. Evaluation of FR[DSM+f($\dot{\theta}$)]	65
	5. Evaluation of FR[DSM+k _θ $\dot{\theta}$] and SR[DSM]	67
	6. Evaluation of a Flight Path Reference, GR (Gamma Reference)	67
	7. Conclusions from the Preliminary System Evaluations	68
D.	Investigation of FR Design Adjustments	68
	1. Alleviation of Adverse γ - θ Cross Coupling in High Thrust Region	68
	2. Evaluation of a General u,w Flight Reference (with Implications for the Use of Lift Margin)	70
E.	Compatibility of Manual, Automatic, and Flight Director Functions — Implementation and Operation	72
	1. System Implementation	72
	2. System Operation	73
F.	Evaluation of a Refined System Configuration	75
	1. System Description	75
	2. System Analysis	79
	3. Simulator Results	80
	4. Departure From a Fixed Configuration System	82

TABLE OF CONTENTS (Concluded)

Section	Page
V CONCLUSIONS AND RECOMMENDATIONS	85
A. Summary of System Objectives and Design Constraints	85
B. Definition of Recommended Safety Margin System . . .	86
C. System Benefits	87
D. Implementation Considerations	88
E. Recommendations for Further Study	89
REFERENCES	91
 Appendix	
A AERODYNAMIC CHARACTERISTICS OF THE NASA AUGMENTOR WING AIRPLANE	93
B SUMMARY OF MULTILoop SYSTEM RELATIONSHIPS	95
C DETAILED ANALYSIS OF FLIGHT REFERENCES BASED ON STATIC SAFETY MARGIN	101
D FLIGHT REFERENCE LOOP PARAMETER COMPUTATION	121
E SPERRY 1819A DIGITAL COMPUTER SOFTWARE MODIFICATIONS	125

LIST OF FIGURES

		Page
I-1	Examples of Safety Margins for Conventional and Powered-Lift Aircraft	2
I-2	An Example of the Determination of the Minimum Safe Flight Envelope by Various Safety Margin Criteria	3
II-1	$\gamma - V$ Plot Showing Conditions of 100% Dynamic Safety Margin for the Powered-Lift Airplane Example Used in this Study	11
II-2	$\gamma - V$ Plot with Trajectories of Constant θ , N_H and SSM	13
II-3	Mapping of SSM as a Function of V and θ	14
II-4	$\gamma - V$ Plot Showing Contour of Constant Lift Margin	16
III-1	$\gamma - V$ Curve Showing Steady State Trajectory for DSM = 100%	27
III-2	DSM Control Response Asymptotes (With and Without Flight Path Regulation)	30
III-3	Regions of Varying $\gamma - \theta$ Cross Coupling	32
III-4	Pitch Attitude Required to Maintain Flight Reference During a Step Change in Flight Path	34
III-5	Effect of Regulating DSM on Reducing Safety Margin Excursion	35
IV-1	Simulator Block Diagram	50
IV-2	Assumed Loop Structure for Pilot Identification	55
IV-3	STOLAND EADI Display for Safety Margin Evaluation	59
IV-4	Illustration of DSM Regulation in Sustained Wind Shears	62
IV-5	$\gamma - V$ Plot Showing Trajectory for $FR[DSM+k_\theta] = 100\%$. . .	78

LIST OF FIGURES (Concluded)

	Page
IV-6	Relative Effectiveness of $FR[DSM+k_{\theta}]$ in Maintaining Dynamic Safety Margin 81
IV-7	Comparative Effectiveness of $FR[DSM+k_{\theta}]$ in Regulating DSM in Wind Shears 83
C-1	Reduction in Flight Path Overshoot Using $u-\theta$ Static Safety Margin 103
C-2	Behavior of $SSM_{u,\theta}$ to Gusts with Pilot Holding Pitch Attitude Where the Vertical Gust Margin is Critical 105
C-3	Ineffectiveness of $SSM_{u,\delta}$ in Eliminating Flight Path Overshoot 108
C-4	Ineffectiveness of $SSM_{w,\theta}$ in Regulating DSM 113
C-5	Frequency Response of DSM/u_g with $FR = SSM_{w,\theta}$ Compared to $FR = DSM$ 114
E-1	Flow Chart of 1819A Computer Program for Calculating SR, FR, and GR 126

LIST OF TABLES

		Page
III-1	List of Features Considered in the Safety Margin System Survey	19
III-2	Summary of Flight Path/Flight Reference Dynamics	23
III-3	Definition of FR[DSM]	26
III-4	Summary of Linearized Safety Margin Functions	40
III-5	Summary of Static Safety Margin Analysis	43
III-6	Summary of the Survey of Flight Reference Implementation Concepts	46
IV-1	Strip Chart Recorder Assignments	54
IV-2	Flight Reference Based on DSM and $f(\dot{\theta})$	66
IV-3	Refined Safety Margin System	76
A-1	Basic Flight Condition Parameters — NASA Augmentor Wing Airplane	94
E-1	Listing of Sperry 1819A Assembly Language Code	128

LIST OF ABBREVIATIONS

cg	Center of gravity
CTOL	Conventional Takeoff and Landing
DSM	Dynamic Safety Margin
EADI	Electronic Attitude Director Indicator
EAI	Electronics Associates, Inc.
FAA	Federal Aviation Administration
FR	Flight Reference
GR	Gamma Reference
ILS	Instrument Landing System
LM	Lift Margin
MFD	Multifunction Display
NASA	National Aeronautics and Space Administration
PIO	Pilot Induced Oscillation
PLSDWG	Powered-Lift Standards Development Working Group
rpm	Revolutions per minute
SAS	Stability Augmentation System
SR	Safety Reference
SSM	Static Safety Margin
STOL	Short Takeoff and Landing

LIST OF SYMBOLS

\bar{d}	Distance of cg above and normal to glide slope
$\dot{\bar{d}}$	Inertial velocity normal to glide slope
FR	Flight reference
GR	Gamma reference
h	Altitude
\dot{h}	Altitude rate
k_d	Flight reference partial derivative with respect to $\dot{\bar{d}}$
k_u	Flight reference partial derivative with respect to u
k_w	Flight reference partial derivative with respect to w
k_δ	Flight reference partial derivative with respect to δ
k_θ	Flight reference partial derivative with respect to θ
k_u^r	Dynamic safety margin partial derivative with respect to u
k_w^r	Dynamic safety margin partial derivative with respect to w
k_δ^r	Dynamic safety margin partial derivative with respect to δ
K_{FRI}	Pilot gain for integral flight reference error
K_ϵ	Pilot gain for glide slope error
K_θ	Pilot gain for pitch attitude error
$N_{\delta_1}^{x_1}$	Numerator for state x_1 and control δ_1
$N_{\delta_1 \delta_2}^{x_1 x_2}$	Coupling numerator for states x_1, x_2 and controls δ_1, δ_2
N_H	Engine rpm
s	Laplace operator
SR	Safety reference

LIST OF SYMBOLS (Continued)

t	Time
T_F	Flight reference filter time constant
$T_{\theta 1}$	Long term time constant associated with θ -fixed response
$T_{\theta 2}$	Short term time constant associated with θ -fixed response
$T_{\gamma 1}$	Inverse of numerator zero appearing in \dot{d}/θ or γ/θ numerator
u	Inertial velocity perturbation
u_a	Airspeed perturbation
u_g	Horizontal gust velocity perturbation
\dot{u}_g	Horizontal gust velocity rate or shear
V	True airspeed
V_{min}	Minimum speed at approach thrust
V_{min_m}	Minimum speed at maximum thrust
w_g	Vertical gust velocity
W	Weight
X_u	Partial derivative of x-force with respect to u
X_w	Partial derivative of x-force with respect to w
X_δ	Partial derivative of x-force with respect to thrust
Y_d	Pilot compensation in flight path feedback loop
Y_{FR}	Pilot compensation in flight reference feedback loop
Z_u	Partial derivative of z-force with respect to u
Z_w	Partial derivative of z-force with respect to w
Z_w^\dagger	Partial derivative of z-force with respect to w with θ constrained $\triangleq Z_w (1 - Z_{\delta_e} M_w / M_{\delta_e} Z_w)$

LIST OF SYMBOLS (Concluded)

Z_{δ}	Partial derivative of z-force with respect to thrust with θ constrained $\triangleq Z_w (1 - Z_{\delta_e} M_w / M_{\delta_e} Z_w)$
Z_{α}	Partial derivative of z-force with respect to α
α	Angle of attack
α_{\max}	Maximum allowable angle of attack
γ	Flight path angle
γ_{\max}	Maximum flight path angle
γ_{\min}	Minimum flight path angle
δ	Throttle deflection
δ_c	Control column deflection
δ_e	Elevator deflection
δ_F	Flap deflection
δ_v	Nozzle deflection
Δ	Denominator in θ -constrained equations of motion
ϵ_{GS}	Glide slope error
θ	Pitch attitude, pitch attitude perturbation
θ_c	Pitch attitude command
θ_o	Flight reference constant
σ_{u_g}	Standard deviation of u_g
ω_c	Crossover frequency
ω_{cFR}	Flight reference crossover frequency

SECTION I
INTRODUCTION

A. BACKGROUND

Safety margins for powered-lift aircraft are inherently different from their counterparts for conventional aircraft both in how they are defined and in how they are controlled. This is illustrated by the low speed flight path versus airspeed envelopes shown in Fig. I-1. While both the conventional and powered-lift examples possess a common idle-thrust stall speed, their minimum safe target speeds vary greatly. As demonstrated in Refs. 1 through 3, powered-lift safety margins can involve several criteria including various explicit forms of airspeed, angle of attack relationships, and lift margin — not just a simple proportion of stall speed. Also, when operating under multiple margin criteria, the pilot or autopilot is confronted with either (i) evaluating and maintaining several airspeed and angle of attack functions simultaneously or (ii) utilizing conservative margins and tracking a nearly constant airspeed or angle of attack.

In addition to the complex nature of powered-lift safety margins, some powered-lift aircraft require a different piloting technique from that of conventional aircraft. Where flight path changes cannot be easily sustained using pitch attitude commands, it is necessary to vary the magnitude of a vertically inclined thrust vector to regulate flight path and to vary pitch attitude to maintain safety margins — the so-called backside or STOL technique.

The implication of the above ideas is that it may be difficult to utilize the minimum allowable safety margins of a given powered-lift aircraft and thereby to take full advantage of its short landing capability. Consider an example. For a given powered-lift airplane, several safety margin criteria combine to establish a maximum safe flight envelope as shown in Fig. I-2 in the form of a $\gamma - V$ envelope. The problem is how to utilize effectively the

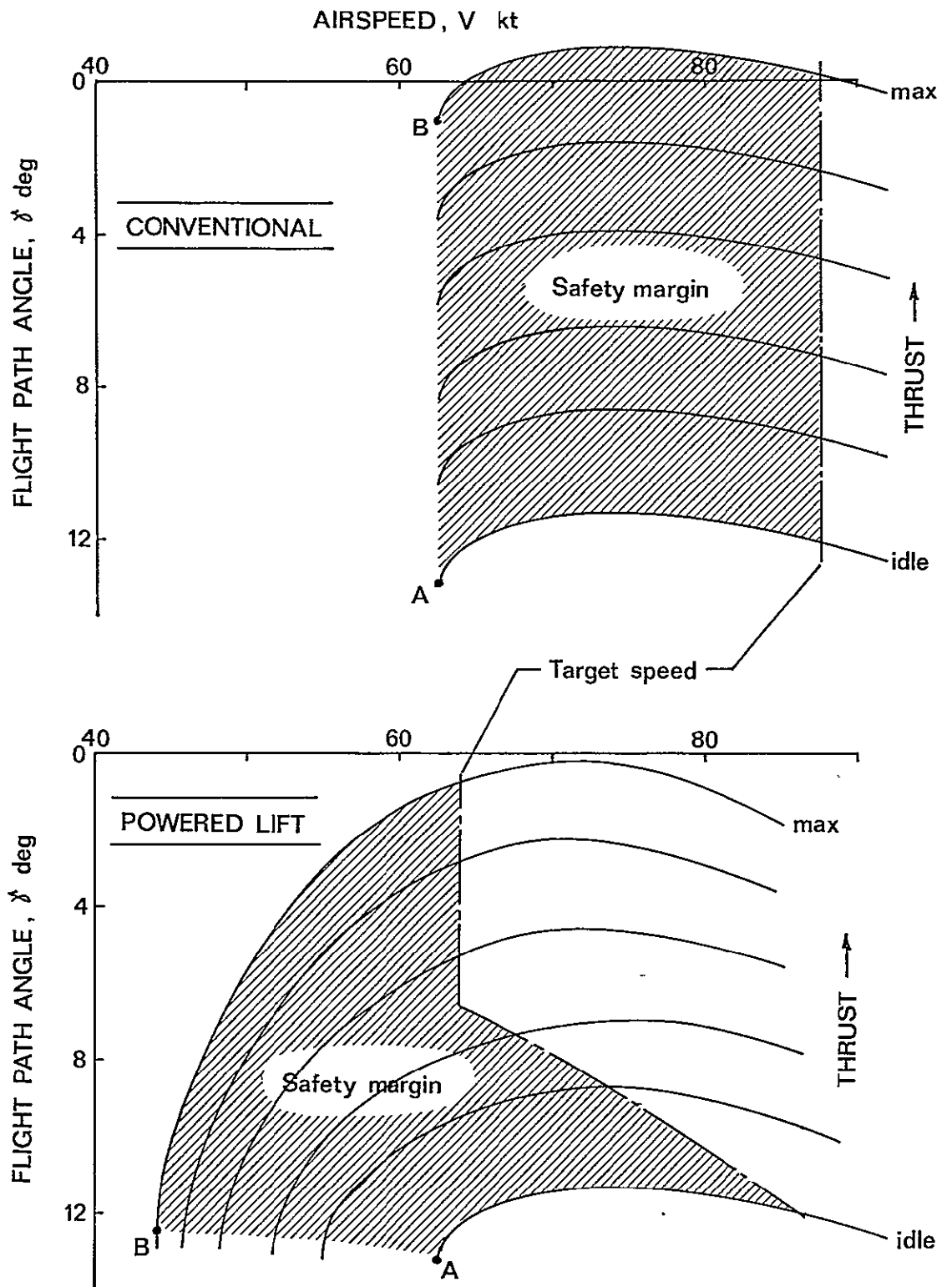


Figure I-1. Examples of Safety Margins for Conventional and Powered-Lift Aircraft

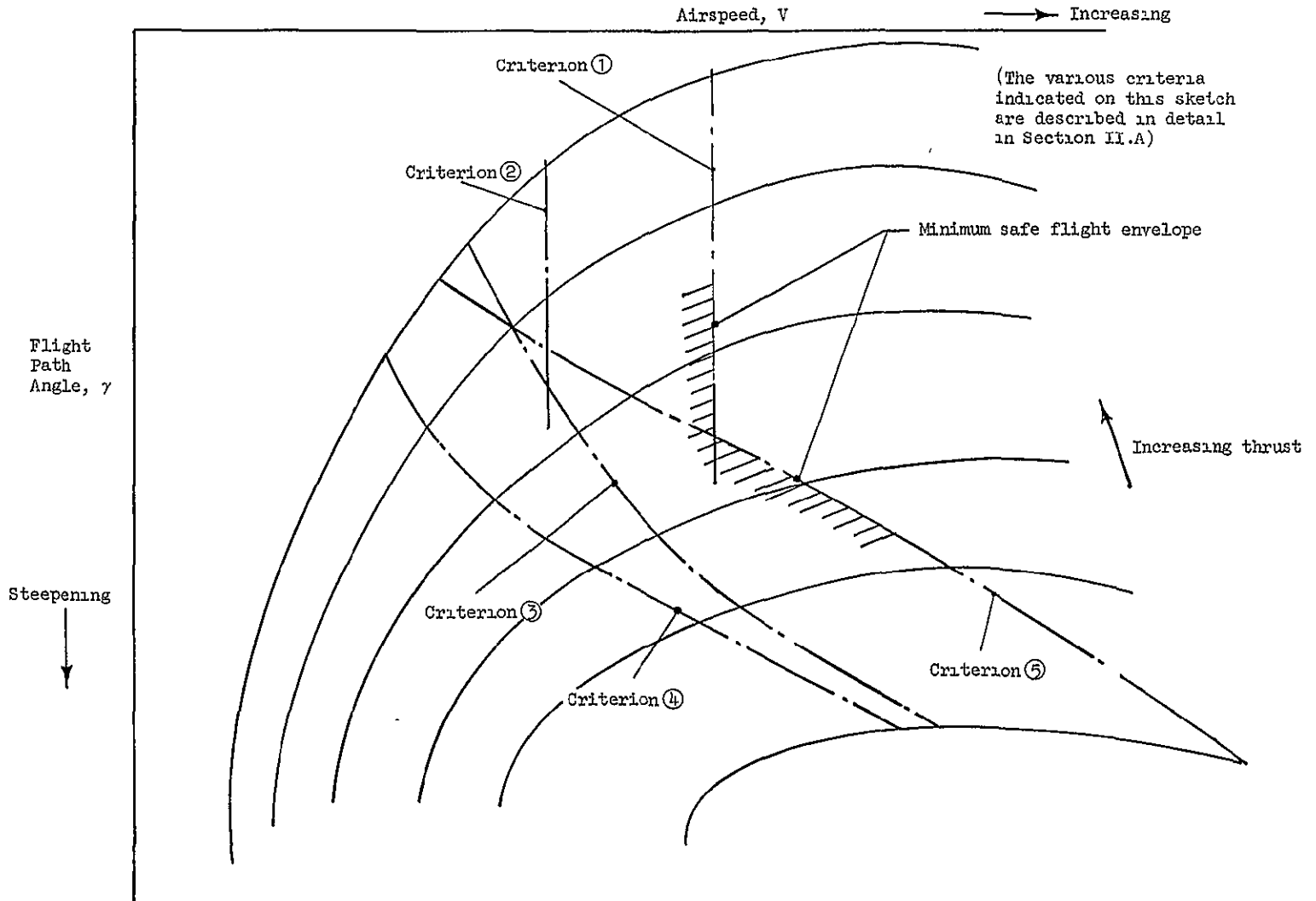


Figure I-2: An Example of the Determination of the Minimum Safe Flight Envelope by Various Safety Margin Criteria

lowest speed defined by the safety margin criteria consistent with suitable manual or automatic operation. There is no obvious solution to safe operation and maximum utilization of the low speed flight envelope through use of existing displays such as pitch attitude, indicated airspeed, or angle of attack. Therefore, we must examine more sophisticated alternatives.

These ideas are based, in part, on the results from a series of simulator experiments to explore airworthiness criteria needs for powered-lift aircraft as summarized in Ref. 4. As a result of the FAA-sponsored Powered-Lift Standards Development Working Group (PLSDWG), a set of tentative standards was produced and presented in Ref. 1.

The problem of how to maintain a minimum allowable margin using a special cockpit gauge was addressed briefly on an experimental basis in Ref. 5. A more general treatment was given in Ref. 6 which, in turn, led to the program reported here.

B. PROGRAM OBJECTIVE

The objective of this study was to investigate safety margin system concepts which would (i) provide the pilot with crucial information regarding the state of the aircraft with respect to its flight envelope, and (ii) maintain a level of safety consistent with present-day standards.

The fundamental safety margin for a powered-lift aircraft was assumed to be composed of the speed and angle of attack margins recommended by the Powered-Lift Standards Development Working Group (Ref. 1). These margins are a function of angle of attack, airspeed, and thrust for given configuration conditions, e.g., flap angle, nozzle angle, and weight. The criteria can be interpreted as defining safety margins in both unaccelerated and accelerated flight.

Some of the problem areas and tradeoffs which were considered in the selection and development of a safety margin system included the following:

- Performance in maintaining safety margins while utilizing a display which may not show margins directly

- Ease of both automatic and manual aircraft control in tracking a given safety margin error
- Ease of system monitoring on reversion from automatic to manual operation
- System mechanizations as they relate to sensor requirements and computer requirements
- Envelope tradeoffs when backing off from the minimum allowable margins in order to enhance characteristics of a safety margin system.

The effort undertaken in this program was primarily a feasibility study of the problem. In order to minimize cost and time, the NASA Augmentor Wing aircraft was used as the subject of the study, and the flight phase was limited to final landing approach. The Sperry STOLAND system was used to fill basic computational and display needs.

C. TECHNICAL APPROACH

The approach used to study a safety margin system for powered-lift STOL aircraft was both analytical and experimental. The analytical portion of the study primarily involved examination of a large number of possible mechanizations which made full use of multiloop control system analysis methods. This analysis considered ease of control, display of safety margin status, and performance in maintaining safety margins. The analysis also considered implementation of the system in an airborne digital computer. The ultimate goal of the analysis was to sort a large number of possibilities and to find a few which would be worth examining experimentally on a ground-based simulator.

The objective of the experimental program was to study safety margin system concepts in a realistic environment taking into account the complexities of the aircraft, its systems, and a human pilot. Assuming that a feasible safety margin system were found, the ultimate goal would be to propose further developmental work including experiments which could be flight tested on the NASA Augmentor Wing aircraft in order to verify and expand on the simulator results.

D. REPORT ORGANIZATION

The chronological progress of the safety margin system program is reflected in the organization of this report. Section II contains the definition of a number of important concepts which form the basis of this study. These include definition of the assumed safety margin criteria, special terms which are useful in dealing with safety margin systems, and finally, a list of useful implementation concepts. Section III describes the analytical investigation which includes a systematic survey of implementation concepts followed by a discussion of implications for the experimental investigation. Section IV then describes the experimental investigation with a description of the simulation and the results obtained from viewing preliminary system configurations, various design adjustments, implementation matters, and a refined safety margin system. Finally, in Section V, conclusions and recommendations are presented. Appendix A contains aircraft stability and control data used in the system analysis. For a concise summary of multiloop analysis relationships, Appendix B is offered. Appendix C gives a detailed analysis of a class of safety margin system concepts. Appendix D provides a description of an on-line pilot identification procedure used during the simulator experiment. Finally, Appendix E presents airborne digital computer modifications used in the system implementation.

The reader who wishes to obtain an overview of the program and a thorough account of the refined system configuration ultimately developed should consult Sections II and IV with particular emphasis on Subsection IV.F. The reader interested in understanding the conceptual development should study Section III in addition. Finally, for a detailed treatment of the closed loop analysis methods, Appendices B and C should be studied in conjunction with Section III.

SECTION II

DEFINITION OF SAFETY MARGIN SYSTEM CONCEPTS

It is convenient to precede the reporting of analytical and experimental efforts with a definition of various concepts connected with safety margins of powered-lift aircraft. We shall begin by citing the safety margin criteria which are to be addressed. Next, important cockpit instrument display concepts will be identified. Finally, we shall define certain safety margin system implementation concepts which are relatively unconventional and may require clarification.

A. SAFETY MARGIN CRITERIA

The safety margin criteria addressed in our safety margin system design were those recommended by the FAA-sponsored PLSDWG and which are presented in Ref. 1. In order to avoid unnecessary complexity, the condition of inoperative power units was set aside. The following applicable criteria thus remained:

1. Percent airspeed margin relative to minimum airspeed at approach thrust†:

$$\frac{V - V_{\min}}{V_{\min}} \geq 15\%$$

2. Absolute airspeed margin relative to minimum airspeed at approach thrust:

$$V - V_{\min} \geq 10 \text{ kt}$$

* The term "safety margin system" itself will be defined shortly in II.C.1.

† According to Ref. 1, "approach thrust" refers to the trim thrust for a given approach flight path angle. In order to facilitate implementation, we chose to interpret "approach thrust" as the instantaneous thrust setting.

3. Percent airspeed margin relative to minimum airspeed at maximum thrust:

$$\frac{V - V_{\min_m}}{V_{\min_m}} \geq 30\%$$

4. Absolute airspeed margin relative to minimum airspeed at maximum thrust:

$$V - V_{\min_m} \geq 20 \text{ kt}$$

5. Instantaneous vertical gust margin at approach thrust:

$$V \sin (\alpha_{\max} - \alpha) \geq 20 \text{ kt}$$

In effect, these criteria combined to form an operating envelope in terms of any three independent flight condition variables (e.g., θ , V , and α); or, if constrained to steady unaccelerated flight, any pair of independent flight condition variables (e.g., V and α or V and θ). We shall make use of these relationships shortly.

In addition to the above safety margin criteria, we must also mention the flight path control power criteria because they were included in our consideration of a design example. Simply stated, Ref. 1 suggests that for any specified nominal operating condition (normally in terms of V and γ), the aircraft shall be capable of an upward flight path angle increment of 4 deg or level flight, whichever is larger, and a flight path angle decrement of 4 deg. Hence, if the aircraft were to operate at 65 kt on a nominal 7.5 deg glide slope in headwinds from zero to 35 kt, it must have a flight path angle capability of:

$$\gamma_{\min} \leq -7.5 - 4 = -11.5 \text{ deg}$$

and

$$\gamma_{\max} \geq -7.5(1 - 35/65) + 4 = +.5 \text{ deg } (> \text{ level flight})$$

B. COCKPIT INSTRUMENT DISPLAY CONCEPTS

It was convenient to employ two display concepts in the implementation of a safety margin system. One was used as an object to track in either a manual or automatic mode, and the other was used in a monitoring role.

1. Flight Reference (FR)

In conventional aircraft, airspeed is normally regulated in order to maintain adequate margins; however, as discussed in Refs. 1 and 4, powered-lift aircraft require a more general label for the variable to be regulated. The variable could be airspeed, angle of attack, pitch attitude, or a combination of each. Hence, the term "flight reference" was used as a general term to describe that quantity which is actively regulated to maintain a given flight condition. This concept was originally proposed for use in Ref. 7, and adopted by the PLSDWG.

2. Safety Reference (SR)

The "safety reference" was a newly defined term (as opposed to FR) to represent a displayed quantity to be primarily monitored rather than tracked or regulated as the FR.

An example of an SR could be an angle of attack gauge monitored only to detect proximity to stall (while the airspeed indicator would represent the FR which was actively tracked).

The concepts of FR and SR apply to both manual and automatic operation. In the case of an autopilot, the FR would be the outer loop variable regulated by the autopilot and the SR would be whatever the pilot actively monitored for an indication of safe operation.

Under some conditions, FR and SR could be one-in-the-same, for example indicated airspeed frequently serves both purposes in conventional aircraft.

C. SAFETY MARGIN SYSTEM IMPLEMENTATION CONCEPTS

1. Safety Margin System

We shall use the term "safety margin system" to describe the specific implementation of a flight reference and a safety reference. The purpose of such a system is to provide for safe manual or automatic operation while simultaneously serving as an aid to maintaining a given target operating point or flight condition.

2. Dynamic Safety Margin

The dynamic safety margin (DSM) is the true, instantaneous, critical safety margin as defined by any given set of safety margin criteria. If the individual criteria are represented by the set $[DSM_1, DSM_2, \dots, DSM_n]$, then the DSM equals the minimum numerical member of the set, i.e.:

$$DSM = \min(DSM_1, DSM_2, \dots, DSM_n)$$

In this study we found that only two safety margin criteria applied to the airplane example used*, the absolute airspeed margin relative to minimum airspeed at maximum thrust and the instantaneous vertical gust margin at approach thrust. Hence,

$$DSM_1 \triangleq \frac{V - V_{min_m}}{20 \text{ kt}} \times 100\%$$

and

$$DSM_2 \triangleq \frac{\alpha_{max} - \alpha}{\sin^{-1} \frac{20 \text{ kt}}{V}}$$

The combined minimum allowable margin (DSM = 100%) is plotted in Fig. II-1 for the powered-lift airplane example used in this study.

* Nevertheless, the other margins were computed during the simulator experiments in order to monitor and thus verify their insignificance.

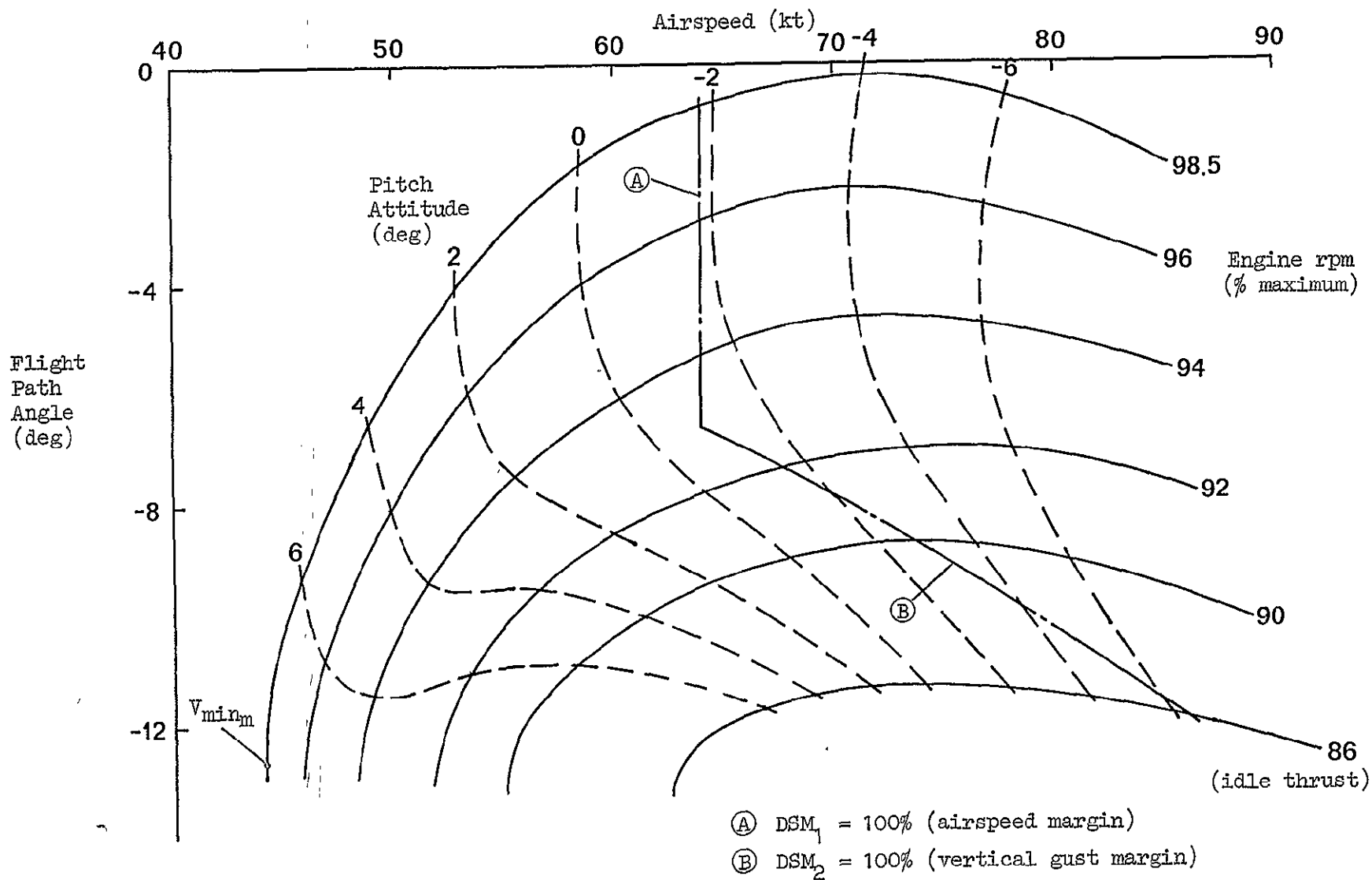


Figure II-1. γ -V Plot Showing Conditions of 100% Dynamic Safety Margin For the Powered-Lift Airplane Example Used in This Study.

3. Static Safety Margin

The term static safety margin (SSM) is a general term which applies to mappings of any pair of state variables into a steady state safety margin for the purpose of forming a flight reference or safety reference. The $\gamma - V$ plot of dynamic safety margin in Fig. II-2 could be, for example, conformally transformed into SSM as a function of (V and γ), or (V and N_H), or (θ and N_H), etc. Figure II-3 shows a static safety margin as a function of V and θ (or $SSM_{V,\theta}$).

If we were to consider the five directly measurable variables θ , N_H , V , α , and \dot{h} we could formulate $\binom{5}{2}$, i.e., ten safety margin schemes, namely:

$$SSM_{\theta, N_H}$$

$$SSM_{\theta, V}$$

$$SSM_{\theta, \alpha}$$

$$SSM_{\theta, \dot{h}}$$

$$\vdots$$

$$SSM_{\alpha, \dot{h}}$$

The significance of a static safety margin formulation is that only two input variables are required compared to three for the dynamic safety margin (V , α , N_H). Also, the static safety margin, by definition, equals the dynamic safety margin in 1 g steady flight. Without careful examination, the unknown aspect is how useful a particular SSM is under non-steady conditions. This was the subject of much of the analysis effort and some simulation.

4. Lift Margin

Another safety margin system concept is lift margin (LM). Lift margin refers to the capability to produce a given level of normal acceleration

TR 1095-1

13

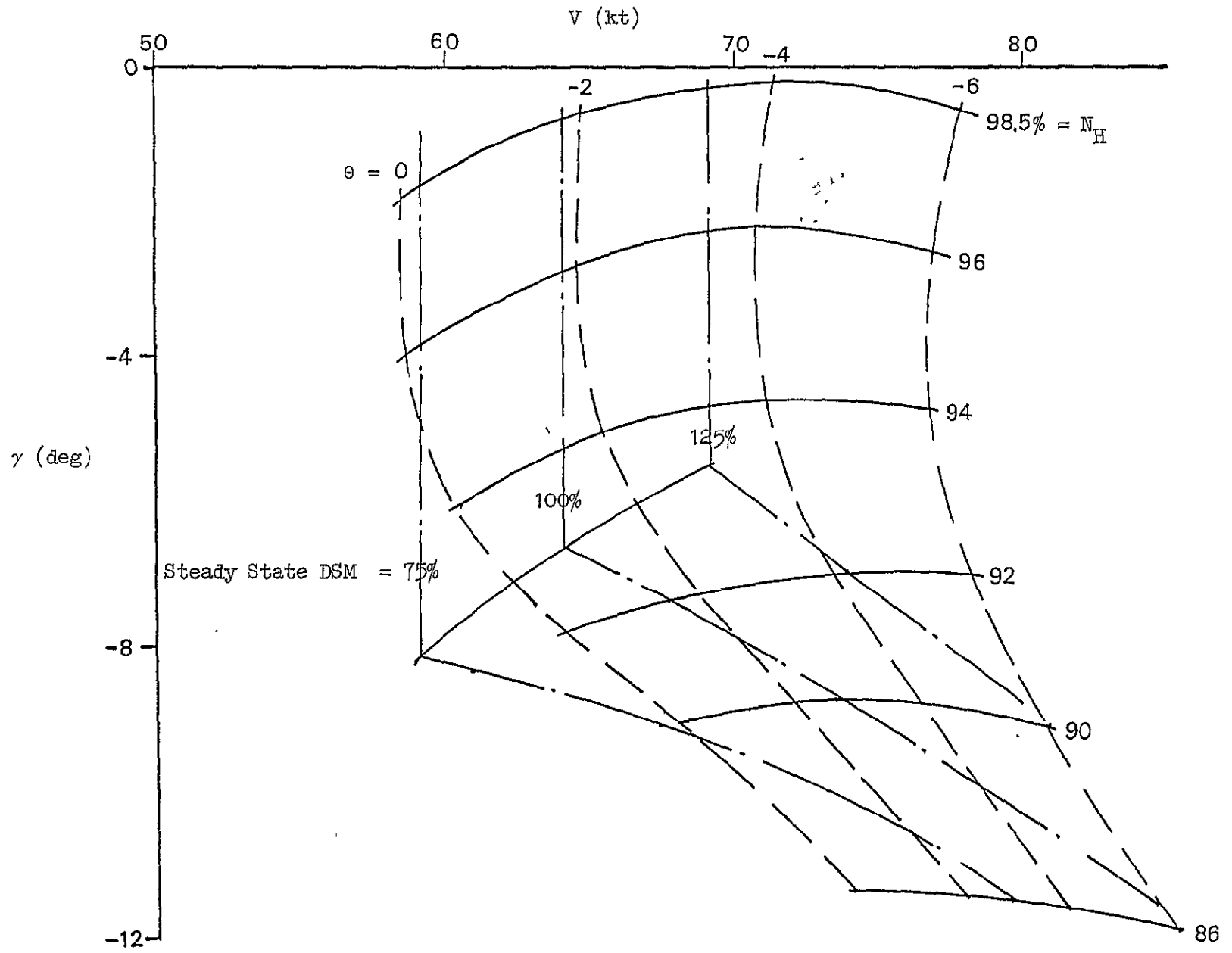


Figure II-2. $\gamma - V$ Plot with Trajectories of Constant θ , N_H , and SSM

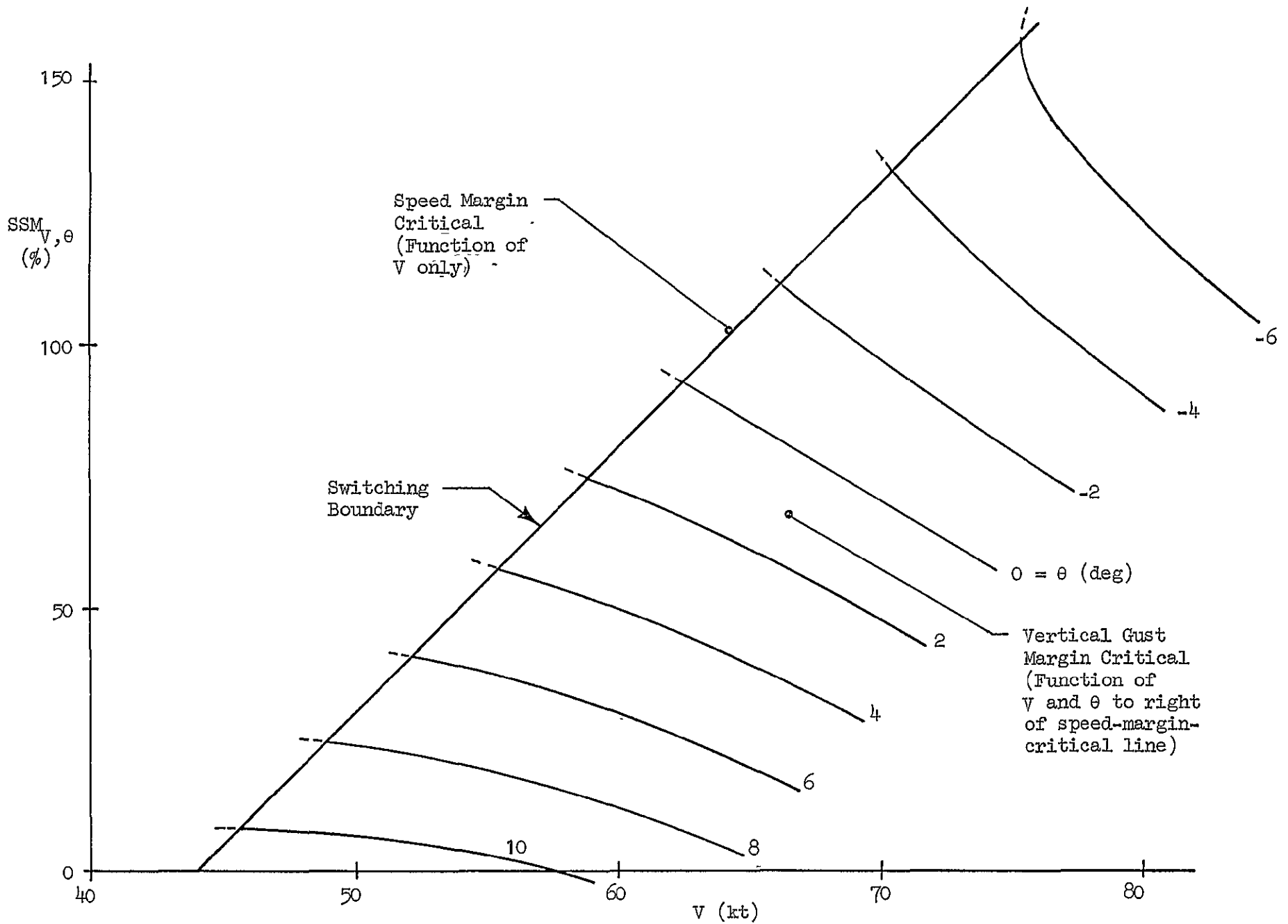


Figure II-3. Mapping of SSM as a Function of V and θ

by increasing pitch attitude up to the point of α_{\max} . It involves angle of attack margin combined with the ability to produce lift by increasing angle of attack.

A lift margin criterion was not included in the list of criteria composing dynamic safety margin but could be, if desired. In this study lift margin was considered as a separate possibility for a safety margin flight reference. Its main advantage was that it consisted of a continuous function compared to the aforementioned multifunctioned dynamic safety margin or static safety margins. A $\gamma - V$ plot showing a steady state contour of constant lift margin is shown in Fig. II-4.

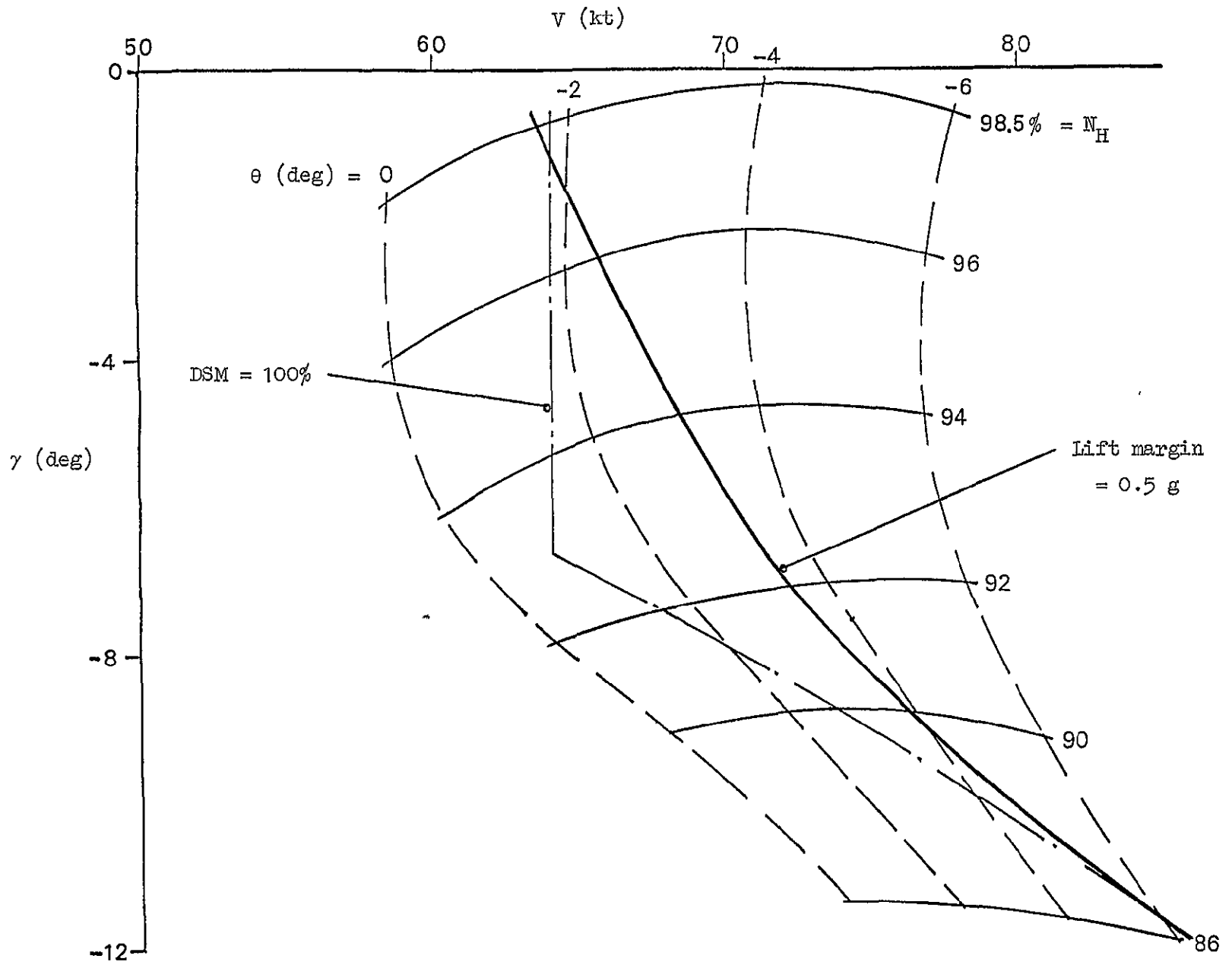


Figure II-4. $\gamma - V$ Plot Showing Contour of Constant Lift Margin

SECTION III

ANALYTICAL INVESTIGATION

A large number of possible ways of implementing a safety margin system exist even though the safety margin criteria are specific in terms of the allowable flight envelope. The first possibility considered was, of course, use of the dynamic safety margin itself as a flight reference. There was also a large number of static safety margin combinations which were attractive from the standpoint of minimizing the sensed states and therefore minimizing sensor hardware. Finally, there was a possibility of using lift margin as the basic flight reference although it would require a reduction in available flight envelope.

For each safety margin system implementation possibility it was necessary to consider at least two flight conditions, a high thrust condition for which airspeed margin was critical and a low thrust region for which vertical gust margin was critical. In all, 23 separate safety margin/flight condition combinations were analyzed prior to the experimental phase.

In this section we shall first present the analytical approach used to perform the system analysis on the large number of possibilities. Next, we shall present the results of this survey of implementation concepts. Finally we shall discuss the implications of the analytical investigation for the subsequent experimental investigation.

A. ANALYSIS APPROACH

The systems analysis which was carried out to survey the large number of implementation possibilities made full use of the multiloop analysis methods described in Ref. 8. Further simplification of analysis methods was obtained using the simplified longitudinal equations of motion described in Ref. 4. The primary advantage in these multiloop analysis methods was that they revealed characteristics of a closed-loop system without unnecessarily complex computation. Since the flight reference system involved

outer loop regulation, it was generally convenient to assume that pitch attitude was well regulated. Also, because flight path, like flight reference, was regulated by an outer feedback loop, it was desirable to look at the pilot-vehicle dynamics with and without flight path regulation.

The major considerations in our analysis of various system concepts included the following:

- ⊗ Controllability — manual or automatic
- ⊗ Effectiveness in maintaining margins
- ⊗ Indication of margin status
- ⊗ Compatibility between manual and automatic operation
- ⊗ Ease of implementation — hardware and software.

Some of these items could be assessed directly from appropriate transfer function relationships, in particular the first three. Compatibility between manual and automatic operation was addressed by striving for a system in which the automatic mode could mimic manual operation, i.e., the autopilot feedbacks and gains would be similar to those of a pilot. Ease of implementation was evaluated subjectively in terms of sensor and computation requirements necessary for implementation in an operational system.

A number of the closed-loop transfer functions which were considered in our systems survey are listed in Table III-1, along with comments on their specific value. Features of particular interest included direct control response, i.e., FR/ θ command, cross-coupling effects between the flight path and flight reference loops, gust response effects, and performance in terms of safety margin regulation.

The analytic approach centered around pitch-attitude-constrained equations of motion because of the greatly reduced complexity with virtually no compromise in computational accuracy in the spectral region of interest, i.e., below 1 rad/sec.

TABLE III-1

LIST OF FEATURES CONSIDERED IN
THE SAFETY MARGIN SYSTEM SURVEY

1. Direct Controllability

Response of flight reference, FR, to pitch attitude, θ

$$\frac{FR}{\theta} = \frac{N_{\theta}^{FR}}{\Delta}$$

or, if a flight path loop is closed ($d \rightarrow \delta$):

$$\left. \frac{FR}{\theta} \right|_{d \rightarrow \delta} = \frac{N_{\theta}^{FR} + Y_d N_{\theta}^{FR} d}{\Delta + Y_d N_{\delta}^d}$$

* The multiloop analysis notation is explained in Appendix B, however, a concise definition of symbols is.

$\Delta \triangleq$ characteristic polynomial

$\frac{x_i}{N_{\delta_j}} \triangleq$ control or gust numerator

$\frac{x_i x_j}{N_{\delta_k \delta_l}} \triangleq$ control or gust coupling numerator

$Y_{x_i} \triangleq$ loop gain and associated compensation

$\frac{x_i}{\delta_k} \triangleq$ transfer function between δ_k and x_i

$\left. \frac{x_i}{\delta_k} \right|_{x_j \rightarrow \delta_l} \triangleq$ transfer function between δ_k and x_i with the x_j loop closed using δ_l

where x_i, x_j are dependent variables

and δ_k, δ_l are independent variables, i.e., control or gust inputs.

(Continued)

TABLE III-1 (Continued)

2. Cross Coupling Effects

Response of flight reference to throttle, δ , compared to response of dynamic safety margin, DSM:

$$\frac{FR}{\delta} = \frac{N_{\delta}^{FR}}{\Delta} \text{ compared to } \frac{DSM}{\delta} = \frac{N_{\delta}^{DSM}}{\Delta}$$

and, the response of flight path to throttle if flight reference is regulated:

$$\left. \frac{\dot{d}}{\delta} \right|_{FR \rightarrow \theta} = \frac{N_{\delta}^{\dot{d}} + Y_{FR} N_{\theta}^{FR} \dot{d}}{\Delta + Y_{FR} N_{\theta}^{FR}}$$

3. Response of flight reference to horizontal and vertical gusts, u_g and w_g .

$$\frac{FR}{u_g} = \frac{N_{u_g}^{FR}}{\Delta}, \quad \frac{FR}{w_g} = \frac{N_{w_g}^{FR}}{\Delta}$$

or, if a flight path loop is closed:

$$\left. \frac{FR}{u_g} \right|_{d \rightarrow \delta} = \frac{N_{u_g}^{FR} + Y_d N_{u_g}^{FR} \dot{d}}{\Delta + Y_d N_{\delta}^{\dot{d}}},$$

similarly for w_g .

REPRODUCIBILITY OF THE ORIGINAL PAGE IS POOR.

(Continued)

TABLE III-1 (Concluded)

4. Safety margin status given by flight reference:

$$\frac{FR}{u_g}, \frac{FR}{w_g}, \frac{FR}{\delta} \text{ compared to:}$$

$$\frac{DSM}{u_g}, \frac{DSM}{w_g}, \frac{DSM}{\delta}, \text{ respectively}$$

REPRODUCIBILITY OF THE
ORIGINAL PAGE IS POOR

5. Closed loop regulation of dynamic safety margin performance with flight reference loop closed.

$$\left. \frac{DSM}{u_g} \right|_{FR \rightarrow \theta} = \frac{N_{u_g}^{DSM}}{\Delta} \frac{\left[1 + \frac{Y_{FR} N_{FR}^{FR}}{\Delta} \left(1 - \frac{N_{u_g}^{FR} N_{\theta}^{DSM}}{N_{u_g}^{DSM} N_{\theta}^{FR}} \right) \right]}{\left(1 + \frac{Y_{FR} N_{FR}^{FR}}{\Delta} \right)}$$

where the term:

$$1 - \frac{N_{u_g}^{FR} N_{\theta}^{DSM}}{N_{u_g}^{DSM} N_{\theta}^{FR}}$$

is an indicator of effectiveness of DSM regulation.

Table III-2 summarizes the key relationships used which are based on (i) basic aircraft equations of motion, and (ii) a linearized general flight reference equation. The elements of (i) and (ii) are combined system equations of motion from which important transfer functions are derived. It is important to recognize that only a few system parameters are involved:

Aircraft parameters consist of the dimensional stability derivatives:

$$X_u, X_w, Z_u, Z_w, \frac{X_\delta}{Z_\delta}, \text{ and } V^-$$

Flight reference parameters are: $k_u, k_w, k_d^i, k_\theta,$ and k_δ

As shown in Ref. 4 the above aircraft parameters are relatively invariant for powered-lift aircraft, and the Augmentor Wing airplane is, hence, representative. The flight reference parameters depend upon specific safety margin criteria and implementation concepts as we shall describe next.

B. SURVEY OF IMPLEMENTATION CONCEPTS

The survey of implementation concepts was carried out to establish likely system candidates which would then be examined on the simulator. It is important to note that this survey did not directly provide the system ultimately recommended, but it did serve as an instructive exercise which led to a useful simulation effort. The survey began with consideration of the dynamic safety margin (DSM) as the flight reference, but certain undesirable features prompted further study of alternatives. One large group of alternatives consisted of the various static safety margin (SSM) combinations. These were attractive because they offered the potential for operating at the minimum allowable safety margin at least for steady

* The derivative Z_w^i represents the effective heave damping when the elevator is used to balance the pitching moment equation.

$$Z_w^i \triangleq Z_w \left(1 - \frac{M_w}{Z_w} \frac{Z_{\delta e}}{M_{\delta e}} \right) \doteq Z_w$$

TABLE III-2

SUMMARY OF FLIGHT PATH/FLIGHT REFERENCE DYNAMICS

AIRCRAFT EQUATIONS OF MOTION

$$\begin{bmatrix} s - X_u & X_w \\ Z_u & s - Z_w^* \end{bmatrix} \begin{bmatrix} u_a \\ d \end{bmatrix} = \begin{bmatrix} (X_\alpha - g) & X_\delta \\ -Z_\alpha & -Z_\delta \end{bmatrix} \begin{bmatrix} \theta \\ \delta \end{bmatrix} + \begin{bmatrix} -s & -X_w \\ 0 & +Z_w \end{bmatrix} \begin{bmatrix} u_g \\ w_g \end{bmatrix}$$

FLIGHT REFERENCE EQUATION

$$FR = k_u u_a + k_w w_a + k_d d + k_\theta \theta + k_\delta \delta$$

COMBINED AIRCRAFT AND FLIGHT REFERENCE EQUATIONS

$$\begin{bmatrix} s - X_u & X_w & 0 \\ Z_u & (s - Z_w) & 0 \\ -k_u & (k_w - k_d) & 1 \end{bmatrix} \begin{bmatrix} u_a \\ d \\ FR \end{bmatrix} = \begin{bmatrix} (X_\alpha - g) & X_\delta \\ -Z_\alpha & -Z_\delta \\ (k_\theta + k_w V) & k_\delta \end{bmatrix} \begin{bmatrix} \theta \\ \delta \end{bmatrix} + \begin{bmatrix} -s & -X_w \\ 0 & +Z_w \\ 0 & -k_w \end{bmatrix} \begin{bmatrix} u_g \\ w_g \end{bmatrix}$$

AUXILIARY RELATIONSHIPS

$$u_a = u - u_g$$

$$w_a = w - w_g$$

$$\alpha = \frac{1}{V} w_a$$

$$\dot{d} = V \theta - w$$

$$\gamma = \frac{1}{V} \dot{d}$$

REPRODUCIBILITY OF THE ORIGINAL PAGE IS POOR

$\gamma - V$ SLOPES

$$\left. \frac{\partial u}{\partial \gamma} \right|_{FR} = \frac{V N_\theta^{FR} u}{N_\theta^{FR} \dot{d}} \Big|_{s=0} = \frac{(k_\theta + k_w V)(X_u Z_\delta - Z_w X_\delta) + (k_w - k_d)[X_\delta Z_\alpha - Z_\delta(X_\alpha - g)] - k_\delta g Z_w}{k_u [X_\delta Z_w - Z_\delta(X_w - \frac{g}{V})] + (k_w + \frac{k_\theta}{V})(X_u Z_\delta - Z_u X_\delta) + k_\delta [Z_u(X_w - \frac{g}{V}) - X_u Z_w]}$$

$$\left. \frac{\partial \theta}{\partial \gamma} \right|_{FR} = \frac{V N_\delta^{FR} \theta}{N_\delta^{FR} \dot{d}} \Big|_{s=0} = \frac{k_u (X_w Z_\delta - Z_w X_\delta) + (k_w - k_d)(X_\delta Z_u - Z_\delta X_u) + k_\delta (X_u Z_w - Z_u X_w)}{k_u [(X_w - \frac{g}{V}) Z_\delta - Z_w X_\delta] + (\frac{k_\theta}{V} + k_w)(X_\delta Z_u - Z_\delta X_u) + k_\delta [X_u Z_u - Z_u (X_w - \frac{g}{V})]}$$

TABLE III-2 (Concluded)

TRANSFER FUNCTIONS

$$\Delta = s^2 + (-X_u - Z_w)s + X_u Z_w - X_w Z_u = (s + \frac{1}{T_{\theta 1}})(s + \frac{1}{T_{\theta 2}})$$

$$N_{\theta}^{\dot{\delta}} = -Z_{\alpha} \left[s - X_u + \frac{X_{\alpha} - g}{Z_{\alpha}} Z_u \right] = -Z_{\alpha} (s + \frac{1}{T_{\gamma 1}})$$

$$N_{\delta}^{\dot{\delta}} = -Z_{\delta} \left[s - X_u + \frac{X_{\delta}}{Z_{\delta}} Z_u \right]$$

$$N_{\theta}^{FR} = k_u [(X_{\alpha} - g)s + gZ_w] + (k_w - k_d)[Z_{\alpha}(s - X_u) + (X_{\alpha} - g)Z_u] + (k_{\theta} + k_w V)[(s - X_u)(s - Z_w) - X_w Z_u]$$

$$N_{\delta}^{FR} = k_u [X_{\delta}(s - Z_w) + Z_{\delta} X_w] + (k_w - k_d)[Z_{\delta}(s - X_u) + X_{\delta} Z_u] + k_{\delta} [(s - X_u)(s - Z_w) - X_w Z_u]$$

$$N_{\theta}^{FR} \frac{u_{\delta}}{\delta} = (k_w - k_d)[X_{\delta} Z_{\alpha} - Z_{\delta}(X_{\alpha} - g)] + (k_{\theta} + k_w V)[X_{\delta}(s - Z_w) + Z_{\delta} X_w] - k_{\delta} [(X_{\alpha} - g)s + gZ_w]$$

$$N_{\theta}^{FR} \frac{d}{\delta} = k_u [X_{\delta} Z_{\alpha} - Z_{\delta}(X_{\alpha} - g)] - (k_{\theta} + k_w V)[X_{\delta} Z_u + Z_{\delta}(s - X_u)] + k_{\delta} [(X_{\alpha} - g)Z_u + Z_{\alpha}(s - X_u)]$$

$$N_{u_g}^{FR} = -k_u s(s - Z_w) - k_w Z_u s + k_d Z_u s$$

$$N_{u_g}^{FR} \frac{\dot{\delta}}{\delta} = k_u Z_{\delta} s - k_{\delta} Z_u s$$

$$N_{w_g}^{FR} = -k_w s(s - X_u) - k_u X_w s + k_d Z_w (s - X_u + \frac{X_u Z_u}{Z_w})$$

REPRODUCIBILITY OF THE ORIGINAL PAGE IS POOR

state conditions. In addition, a lift margin (LM)-based flight reference was considered although it involved a loss of available flight envelope.

In the following pages we shall present the results of the survey of the above-mentioned implementation concepts beginning with a flight reference based on the dynamic safety margin, i.e., FR[DSM].

1. Flight Reference Based on Dynamic Safety Margin

The most direct solution for a safety margin system was considered to be a flight reference exactly equal to the dynamic safety margin. The advantages were that (i) true safety margin status would be displayed on the same symbol which the pilot or autopilot tracks and (ii) the full flight envelope potential would be realized. In effect, the DSM represented an ideal. The question which was addressed in this study, however, was how serious would be the disadvantages in other features, especially controllability and the cross coupling interactions with the flight path loop.

Table III-3 gives a functional definition of FR[DSM] as implemented in the NASA Augmentor Wing airplane simulator model. Figure III-1 shows the steady state $\gamma - V$ trajectory corresponding to DSM equal to 100%.

The upper portion of the $\gamma - V$ curve was referred to as the high thrust condition and involved that portion of the DSM corresponding to constant airspeed. Tracking the flight reference in this region was equivalent to tracking indicated airspeed except for the change in scaling (the target FR was 100% or $V = V_{\min_m} + 20 \text{ kt} = 64 \text{ kt}$; and +1% FR corresponded to +.2 kt).

Similarly, the lower portion of the $\gamma - V$ curve was referred to as the low thrust condition. The DSM in this region corresponded to a constant vertical gust margin or a nearly constant angle of attack. (For an airspeed of 70 kt, 100% DSM corresponded to an angle of attack margin of $\arcsin 20/70 = 16.6 \text{ deg.}$)

TABLE III-3
DEFINITION OF FR[DSM]

$$\begin{aligned} \text{FR[DSM]} &= \text{DSM} \\ &= \min(\text{DSM}_1, \text{DSM}_2) \end{aligned}$$

$$\text{where } \text{DSM}_1 = 100\% \times \frac{V - V_{\min}}{20 \text{ kt}}$$

$$\text{and } \text{DSM}_2 = 100\% \times \frac{\alpha_{\max} - \alpha}{\sin^{-1} \frac{20 \text{ kt}}{V}}$$

For the NASA Augmentor Wing airplane with

$$W = 40,000 \text{ lb}$$

$$\delta_f = 65 \text{ deg}$$

$$\delta_v = 70 \text{ deg}$$

at sea level, standard day conditions

$$V_{\min} = 44 \text{ kt}$$

$$\begin{aligned} \alpha_{\max}(\text{deg}) &\doteq -14.466 - 0.5933 V(\text{kt}) + 0.003316 V^2(\text{kt}) \\ &\quad + 0.9773 N_H(\%) - 0.003236 N_H^2(\%)* \end{aligned}$$

* The α_{\max} function shown is fitted to a NASA-supplied plot of α_{\max} versus non-dimensional blowing coefficient.

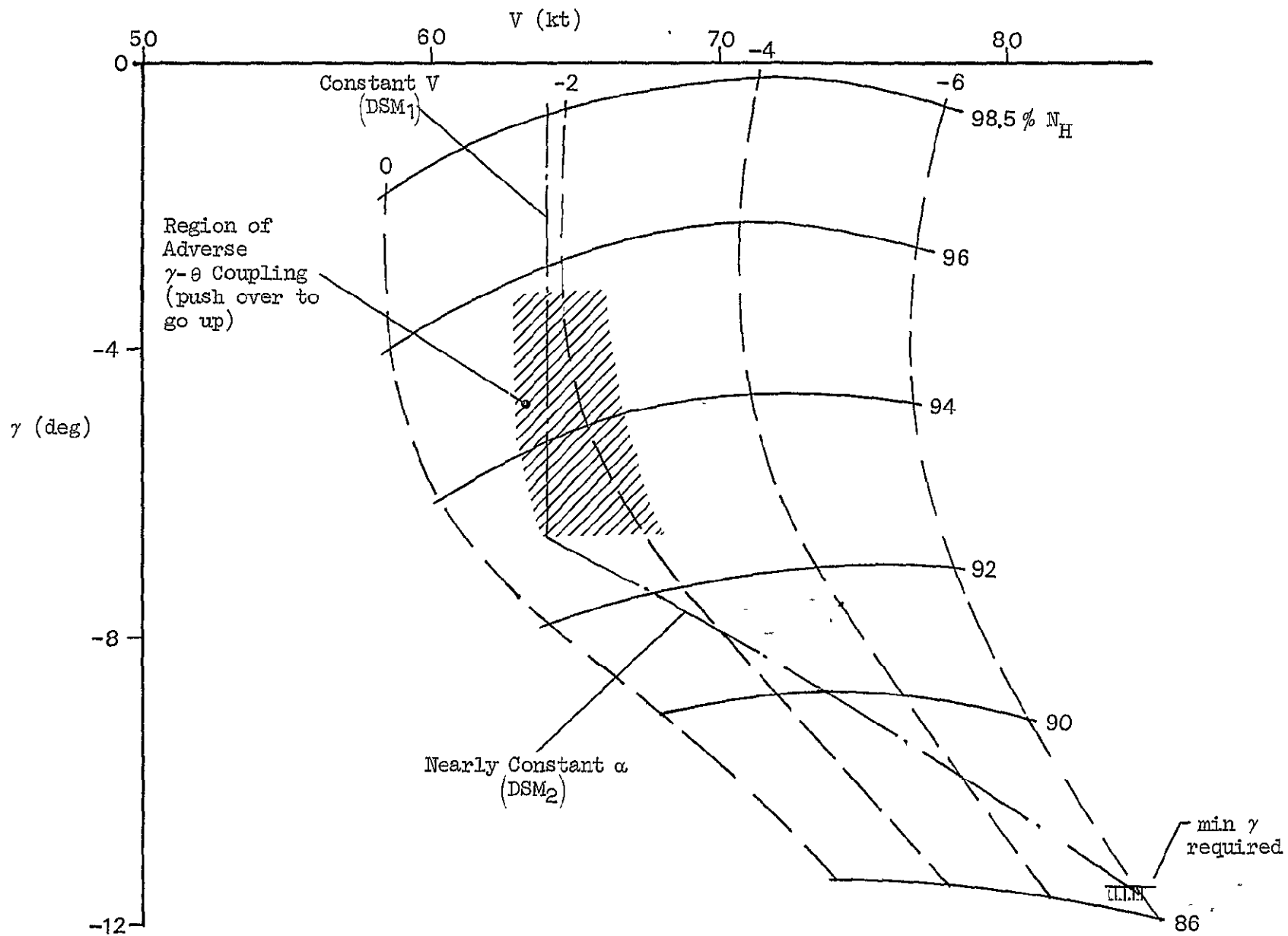


Figure III-1. $\gamma - V$ Curve Showing Steady State Trajectory for $DSM = 100\%$

The first step in analyzing the FR[DSM] was to construct a linearized small perturbation model of the flight reference and aircraft. For the flight reference:

$$DSM_1 = 100\% \times \frac{V - V_{min}}{20 \text{ kt}}$$

or

$$\underline{\Delta DSM_1 = 5\%/kt \Delta u_a \text{ (kt)}}$$

(Note that Δu_a is the airspeed perturbation.)

and

$$DSM_2 = 100\% \times \frac{\alpha_{max} - \alpha}{\sin^{-1} \frac{20 \text{ kt}}{V}}$$

or

$$\Delta DSM_2 = \frac{100\%}{\sin^{-1} \frac{20 \text{ kt}}{V}} \left[\frac{\frac{\partial \alpha_{max}}{\partial V}}{2V} \Delta u_a + \frac{\frac{\partial \alpha_{max}}{\partial N_H}}{2N_H} \Delta N_H - \Delta \alpha \right]$$

$$+ \frac{DSM_2}{\left(\sin^{-1} \frac{20 \text{ kt}}{V} \right)} \times \frac{\frac{20}{V^2}}{\left(1 - \frac{20^2}{V^2} \right)^{1/2}} \Delta u_a$$

e.g., for $DSM = DSM_2 = 100\%$ (low thrust condition)

$$\gamma = -7.5 \text{ deg}$$

$$V = 68.3 \text{ kt}$$

and

$$N_H = 91.69\%$$

$$\underline{\underline{\Delta DSM_2 = 0.68\%/kt \Delta u_a - 4.93\%/kt \Delta w_a + 2.25\%/ \Delta N_H}}$$

If we define a general linearized form for the DSM to be:

$$\Delta DSM = k_u^* \Delta u_a + k_w^* \Delta w_a + k_\delta^* \Delta N_H$$

then at any high thrust condition (where speed margin is critical) $k_u^+ = 5\%/kt$ and $k_w^+ = k_\delta^+ = 0$, exactly. Correspondingly, at the specific low thrust condition considered above

$$k_u^+ = 0.68\%/kt$$

$$k_w^- = -4.93\%/kt$$

$$k_\delta^- = 2.25\%/%$$

Note that for the low thrust condition $k_w^+ \doteq -5\%/kt$ (100% safety margin/20 kt vertical gust). The k_u^+ and k_δ^+ are nearly negligible based on their relative influence on important transfer function quantities. It was possible, in fact, to show all important characteristics of the vertical gust margin critical DSM using $k_w^+ = -5\%/kt$ and $k_u^+ = k_\delta^+ = 0$.

For the airplane dynamics, stability derivatives were obtained directly from the simulator model used in connection with the program. The derivatives for several important flight conditions are tabulated in Appendix A.

The controllability of FR[DSM] through pitch attitude was judged with and without flight path regulation using the appropriate attitude-constrained transfer functions. The results are summarized in Fig. III-2 in which the frequency response asymptotes are drawn for the amplitude of $\frac{DSM}{\theta}$ using log scales.

For the high thrust condition, where DSM is proportional to airspeed, the usual low frequency breakpoint corresponding to speed damping is evident. As flight path is regulated, that breakpoint moves to a lower frequency but the essential control features are little affected.

The corresponding $\frac{DSM}{\theta}$ plot for the low thrust condition shows a controlled element that is more nearly a pure gain, especially when the flight path loop is closed. One notable feature which does not show up in this

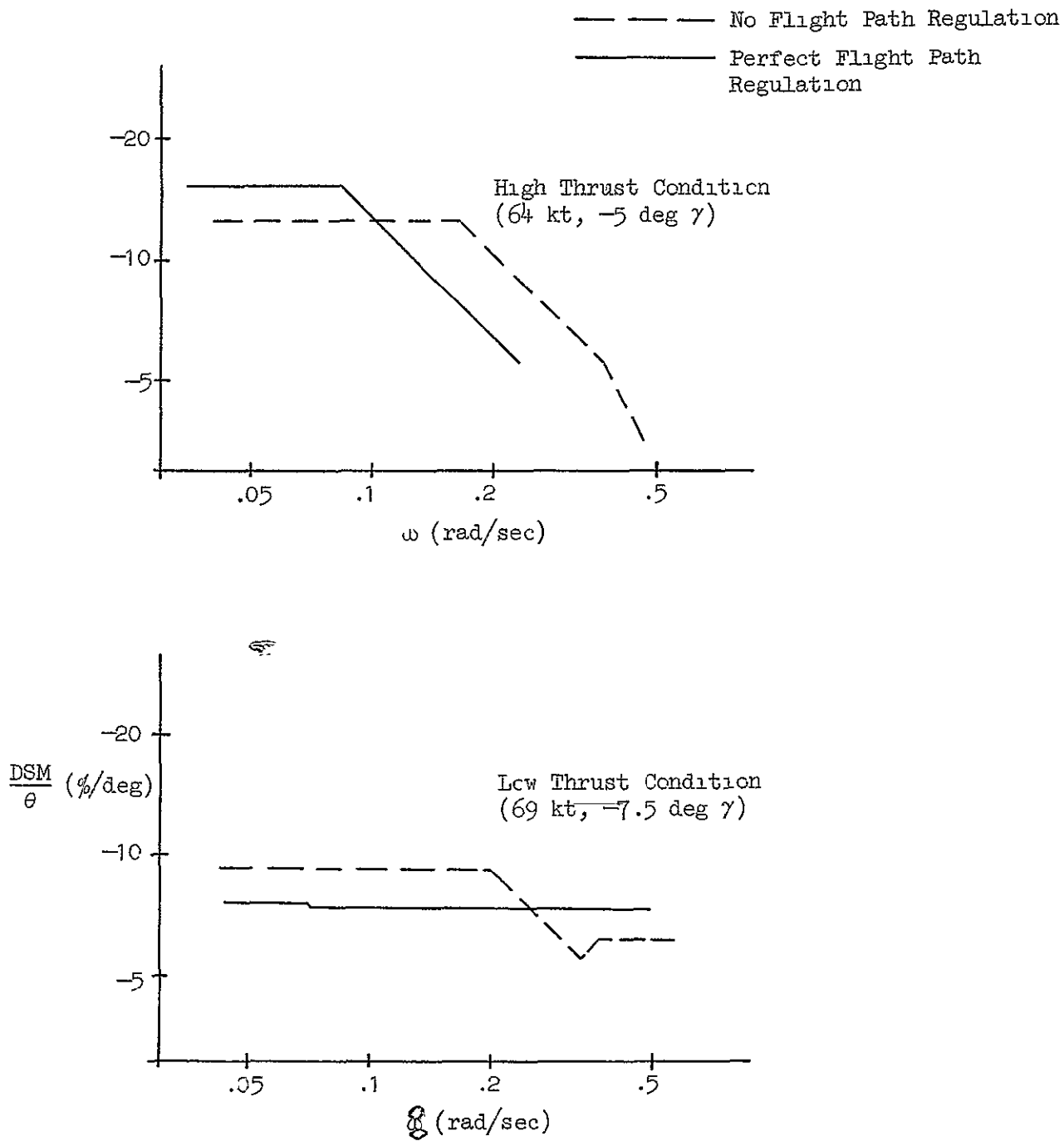


Figure III-2. DSM Control Response Asymptotes
 (With and Without Flight Path Regulation)

sketch, however, is a pair of complex zeros with low damping ratio for $\frac{DSM}{\theta}$ when flight path is not regulated:

$$\frac{DSM}{\theta} \doteq \frac{-6[0.2;0.33]}{(0.2)(0.36)} \quad (\%/rad)$$

This pair of complex zeros could produce an oscillatory condition if FR[DSM] were tracked too tightly, and the condition is present whenever angle of attack or a variable dominated by angle of attack is controlled by commanded pitch attitude. This is easily shown by considering the approximate factors[†] form of the appropriate numerator:

$$N_{\theta}^{\alpha} = \frac{1}{V} N_{\theta}^W = \left[s^2 - X_u s - \frac{g}{V} Z_u \right]$$

Since X_u is typically small, the numerator damping ratio is also small. Hence, closing a tight loop on α ($\alpha \rightarrow \theta_c$) could result in a lightly damped closed loop system as the system poles migrate toward the numerator zeros.

A cross coupling problem involving flight path and flight reference was anticipated based on the $\gamma - V$ curves for the airplane used in this study. The particular variety of cross coupling was the sense of pitch attitude change required to hold dynamic safety margin while making changes in flight path angle. We shall refer to this as $\gamma - \theta$ cross coupling.

As illustrated in Fig. III-3, for varying flight path angles in the high thrust range (96% to 98.5% N_H) no pitch attitude change is required to maintain dynamic safety margin. We shall refer to this as neutral $\gamma - \theta$ cross coupling. If operating at a lower thrust setting, say 94% N_H ,

* The following shorthand notation is used for first and second order polynomial roots:

$$(a) \triangleq (s + a) ; [\zeta, \omega] \triangleq s^2 + 2\zeta\omega s + \omega^2$$

† "Approximate factors" refers to the expression of specific transfer function quantities in terms of their dominant stability derivative factors.

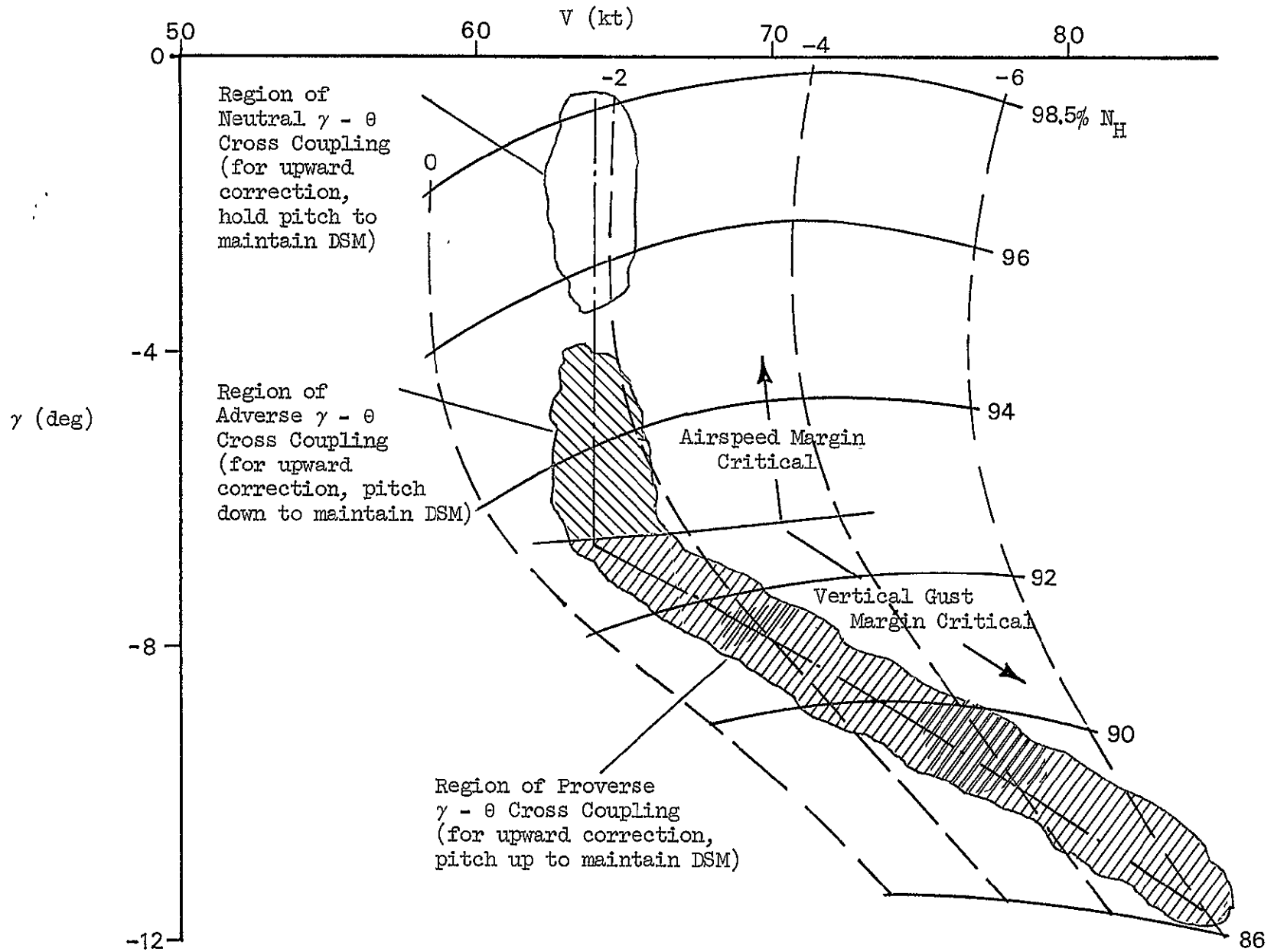


Figure III-3. Regions of Varying $\gamma - \theta$ Cross Coupling

we then encounter adverse $\gamma - \theta$ cross coupling since a pitch down is required to hold DSM during an upward flight path angle correction. Finally, if we transition into the lower half of the $\gamma - V$ curve where vertical gust margin is critical, the cross coupling becomes proverse — an increase in γ requires an increase in θ to maintain DSM.

We chose to study $\gamma - \theta$ cross coupling analytically by computing the θ time history for a given change in γ in the presence of reasonable flight reference regulation, i.e.,

$$\frac{\theta}{\gamma} = \frac{-Y_{FR} N_{\delta}^{FR}}{\bar{V} \left(N_{\delta}^{\dot{\gamma}} + Y_{FR} N_{\delta}^{\dot{\gamma}} \theta \right)}$$

where $FR = DSM$

and $Y_{FR} = \frac{K_{FRI}}{s} @ \omega_{cFR} = 0.15 \text{ rad/sec}$

Figure III-4 shows how widely the θ/γ proportion varies between holding a constant speed margin and holding a constant vertical gust margin. Accordingly, this represented a major area of interest for subsequent simulator experiments.

The effectiveness in maintaining the safety margin by directly regulating dynamic safety margin was demonstrated by computing the maximum safety margin excursion in a steady shear ($\dot{u}_g = \text{constant}$); no flight path regulation was involved. The comparison was made against the case where pitch attitude was held constant. For an integral feedback and a nominal cross-over frequency of 0.15 rad/sec (based on prior simulator observations) we obtained the time histories shown in Fig. III-5. Depending upon whether the speed margin was critical ($k_u^* = +5\%/kt$, $k_w^* = 0$) or vertical gust margin was critical ($k_w^* = -5\%/kt$, $k_u^* = 0$) the peak margin excursion was 10% to 20% for a steady 1 kt/sec shear with the margin excursion eventually washing out. Without DSM regulation the excursion ranged from 20% to 35% and the excursion persisted. Thus, the margin excursion was improved by about a factor of two.

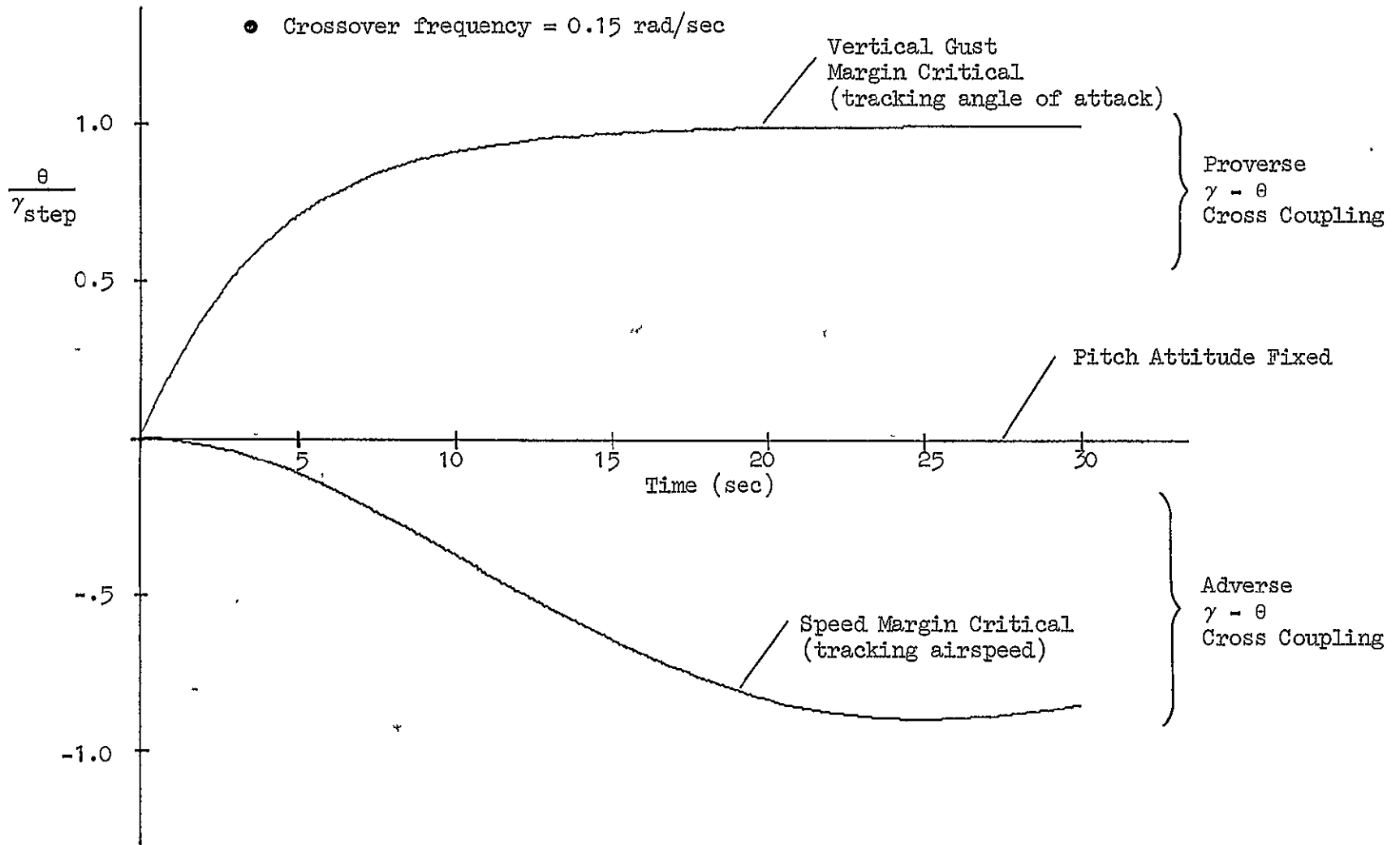


Figure III-4. Pitch Attitude Required to Maintain Flight Reference During a Step Change in Flight Path

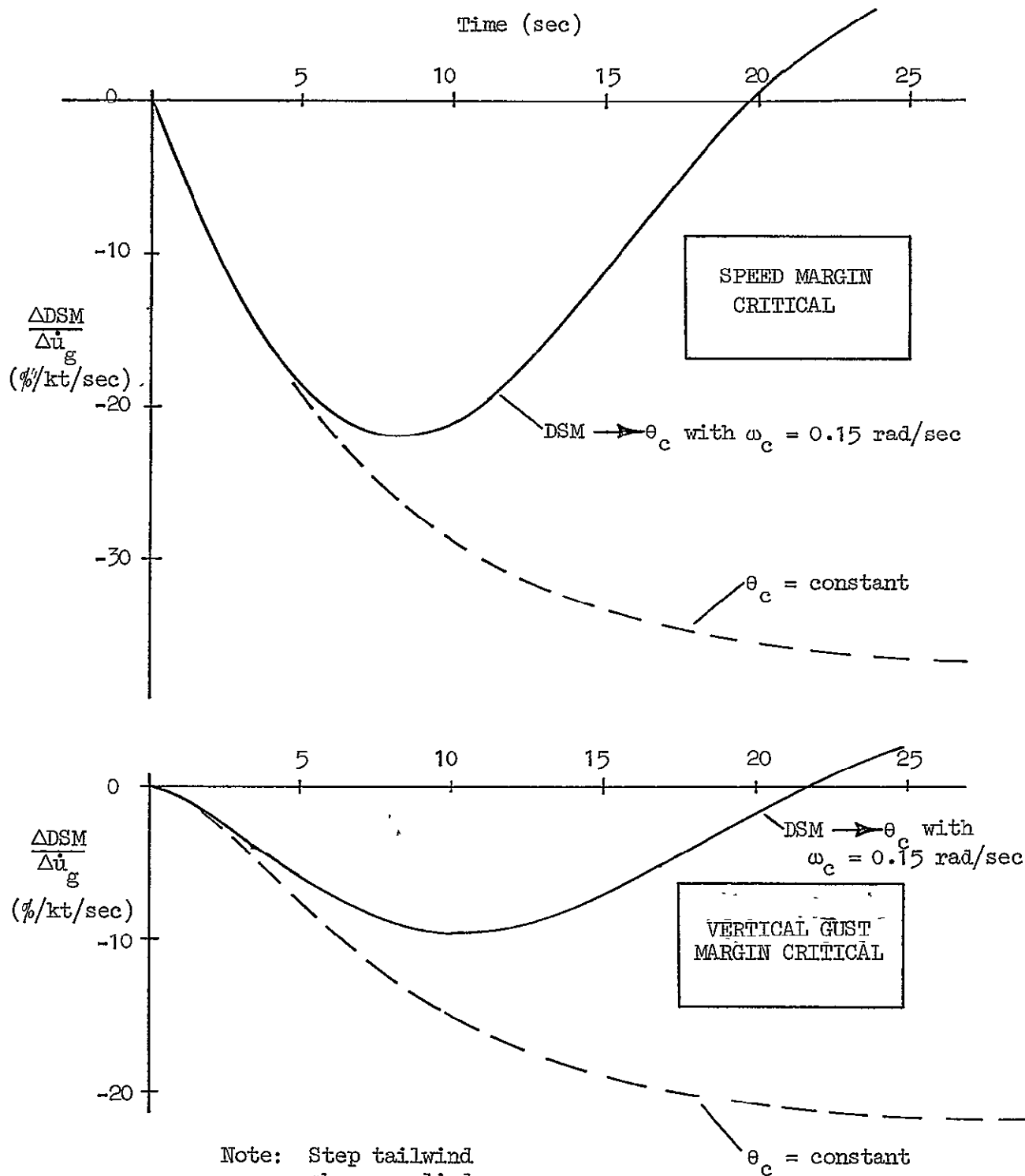


Figure III-5. Effect of Regulating DSM on Reducing Safety Margin Excursion

In summary, the analysis indicated the following characteristics for a flight reference based on dynamic safety margin:

- ④ Control varies from typical airspeed-like qualities to angle-of-attack-like in transitioning between speed-margin-critical and vertical-gust-margin-critical conditions — tight control is difficult in either case.
- ④ When the airspeed margin is critical, an adverse cross coupling between γ and θ exists, i.e., a pitch down is required for an upward flight path correction.
- ④ Margin status information is correct because the flight reference is dynamic safety margin directly.
- ④ Nominal regulation of DSM improves safety margin performance.

2. Flight References Based on Static Safety Margin

A flight reference based on the static safety margin concept appeared attractive because it would require the use of two sensors at most rather than the three required for the dynamic safety margin. Also, full use of the allowable low speed flight envelope would be possible. Thus a survey was made to determine if any of the various static safety margin combinations would also prove attractive with regard to other requirements such as controllability and status information.

The survey of SSM implementations was conducted using the same analytical approach described previously for the DSM. Ten SSM combinations were considered, each at high and low thrust conditions. Many of the combinations were redundant, however. Consequently, only five high thrust conditions (speed margin critical) and seven low thrust conditions (vertical gust margin critical) needed to be analyzed.

- a. Determination of Static Safety Margin Dynamics. The first step was to determine linearized equations for each of the SSM combinations to be considered. The general procedure consisted of:

given $DSM(V, \alpha, N_H)$,

then the differential SSM(x,y) (where x and y are the static safety margin variables to be used) is simply

$$\Delta \text{SSM}(x,y) = \left. \frac{\partial \text{DSM}}{\partial x} \right|_y \Delta x + \left. \frac{\partial \text{DSM}}{\partial y} \right|_x \Delta y$$

for steady state conditions, i.e., 1 g flight. The partial derivatives can be computed directly using steady state trim equations corresponding to the simplified longitudinal equations of motion. One simple formulation of the trim equations is:

$$\begin{bmatrix} -X_u & -X_w & 0 \\ -Z_u & -Z_w & 1 \\ -k_u^* & -k_w^* & 1 \end{bmatrix} \begin{bmatrix} u \\ w \\ \text{DSM} \end{bmatrix} = \begin{bmatrix} -g & X_\delta \\ 0 & X_\delta \\ 0 & k_\delta^* \end{bmatrix} \begin{bmatrix} \theta \\ \delta \end{bmatrix} \quad \dot{} = 0$$

An alternative with \dot{d} (or γ) in place of w is:

$$\begin{bmatrix} -X_u & X_w & 0 \\ Z_u & -Z_w & 0 \\ -k_u^* & k_w^* & 1 \end{bmatrix} \begin{bmatrix} u \\ \dot{d} \\ \text{DSM} \end{bmatrix} = \begin{bmatrix} (X_\alpha - g) & X_\delta \\ -Z_\alpha & -Z_\delta \\ k_w^* V & k_\delta^* \end{bmatrix} \begin{bmatrix} \theta \\ \delta \end{bmatrix} \quad \dot{} = 0$$

The value of using equations such as those above was that it permitted static safety margin flight reference gains to be computed as explicit functions of aircraft stability derivatives (X_u , X_w , Z_u , Z_w , and V) and dynamic safety margin flight reference gains (k_u^* , k_w^* , and k_δ^*). Consider the following example.

Suppose that we desired to compute the linearized static safety margin coefficients for $\text{SSM}(V,\theta)$, i.e., $\left. \frac{\partial \text{DSM}}{\partial u} \right|_\theta$ and $\left. \frac{\partial \text{DSM}}{\partial \theta} \right|_u$. In terms of partial derivative notation:

$$\left. \frac{\partial \text{DSM}}{\partial u} \right|_\theta = \frac{\left. \frac{\partial \text{DSM}}{\partial \delta} \right|_\theta}{\left. \frac{\partial u}{\partial \delta} \right|_\theta}$$

Solving for the numerators by forming appropriate determinants, we obtain

$$\left. \frac{\partial \text{DSM}}{\partial \delta} \right|_{\theta} = \begin{vmatrix} -X_u & -X_w & 0 \\ -Z_u & -Z_w & Z_\delta \\ -k_u^* & -k_w^* & k_\delta^- \end{vmatrix} = X_w Z_\delta \left[k_u^- - \frac{X_u}{X_w} k_w^* + \left(\frac{X_u Z_w}{X_w} - Z_u \right) \frac{k_\delta^+}{Z_\delta} \right]$$

$$\left. \frac{\partial u}{\partial \delta} \right|_{\theta} = \begin{vmatrix} 0 & -X_w & 0 \\ Z_\delta & -Z_w & 0 \\ k_\delta^* & -k_w^+ & 1 \end{vmatrix} = X_w Z_\delta$$

The partial derivative holding u fixed with δ is:

$$\left. \frac{\partial \text{DSM}}{\partial \theta} \right|_u = \begin{vmatrix} 0 & -X_w & -g \\ Z_\delta & -Z_w & 0 \\ k_\delta^+ & -k_w^- & 0 \end{vmatrix} = Z_\delta g \left(k_w^* - Z_w \frac{k_\delta^+}{Z_\delta} \right)$$

$$\text{Thus, } \left. \frac{\partial \text{DSM}}{\partial u} \right|_{\theta} = k_u = k_u^* - \frac{X_u}{X_w} k_w^+ + \left(\frac{X_u Z_w}{X_w} - Z_u \right) \frac{k_\delta^-}{Z_\delta}$$

$$\text{and } \left. \frac{\partial \text{DSM}}{\partial \theta} \right|_u = k_\theta = \frac{g}{X_w} k_w^* - \frac{g Z_w}{X_w} \frac{k_\delta^+}{Z_\delta}$$

By evaluating the above SSM gains using typical Augmentor Wing stability derivatives and the linearized DSM coefficients found previously, we could further simplify relationships:

	$k_u = \left. \frac{\partial \text{DSM}}{\partial u} \right _{\theta}$	$k_{\theta} = \left. \frac{\partial \text{DSM}}{\partial \theta} \right _u$
High Thrust (Speed Margin Critical)	k_u^*	zero
Low Thrust (Vertical Gust Margin Critical)	$-\frac{X_u}{X_w} k_w^*$	$\frac{g}{X_w} k_w^*$

Recall that for speed margin critical $k_u^* = 5\%/kt$ (k_w^* and $k_{\delta}^* = 0$) and for vertical gust margin critical $k_w^* = -5\%/kt$ (k_u^* and k_{δ}^* are small).

In the following pages we shall not develop each static safety margin in detail as was done for the V- θ combination; it suffices to say that the same procedure applies. Instead, we shall present the numerical results finally obtained for each SSM possibility linearized at a high thrust condition and low thrust condition. The respective flight reference gains are given in Tables III-4a and III-4b. Negligible gains are stricken with a diagonal line: /.

Using just the tabulated flight reference gains from Tables III-4a and III-4b it was possible to reduce significantly the cases to be analyzed.

- For speed margin critical, any static safety margin involving airspeed was equivalent to the dynamic safety margin.
- For vertical gust margin critical, all static safety margins involving vertical velocity, w (i.e., angle of attack) were equivalent and essentially depended only on k_w^* . In turn, they were also equivalent to the dynamic safety margin.
- Under all conditions, the static safety margin involving flight path angle and thrust was excessively sensitive and clearly unsatisfactory. (This was due to having an aircraft operating point at or near the minimum thrust required.)

TABLE III-4a

SUMMARY OF LINEARIZED SAFETY MARGIN FUNCTIONS
 (High Thrust Condition — Speed Margin Critical)

	k_u (%/kt)	k_w (%/kt)	k_θ (%/deg)	$k_{\dot{d}}$ ($\frac{\%}{ft/sec}$)	k_δ (%/%)
DSM	5				
$SSM_{u,w}$	5	0			
$SSM_{u,\theta}$	5		0		
$SSM_{u,\dot{d}}$	5			0	
$SSM_{u,\delta}$	5				0
$SSM_{w,\theta}$		3.7	-19.7		
$SSM_{w,\dot{d}}$		-9.6		-8	
$SSM_{w,\delta}$		-6.6			-13.7
$SSM_{\theta,\dot{d}}$			-14.2	-2.2	
$SSM_{\theta,\delta}$			-12.6		-4.9
$SSM_{\dot{d},\delta}$				17	-42.7

TABLE III-4b

(Low Thrust Condition — Vertical Gust Margin Critical)

	k_u (%/kt)	k_w (%/kt)	k_θ (%/deg)	k_d ($\frac{\%}{ft/sec}$)	k_δ (%/%)
DSM	0.7	-4.9			2.3
$SSM_{u,w}$	0/1	-6.1			
$SSM_{u,\theta}$	-3.3		-16.5		
$SSM_{u,\dot{d}}$	4.3			6.6	
$SSM_{u,\delta}$	4.3				15.2
$SSM_{w,\theta}$		-6.0	-/4		
$SSM_{w,\dot{d}}$		-6.2		-/1	
$SSM_{w,\delta}$		-6.2			-/3
$SSM_{\theta,\dot{d}}$			-9.3	2.9	
$SSM_{\theta,\delta}$			-9.3		6.7
$SSM_{\dot{d},\delta}$				-1007	2341

- b. Analysis of Static Safety Margin Dynamics. The static safety margin evaluation process thus continued with an analysis of closed loop dynamics similar to those conducted for the dynamic safety margin. The linearized flight reference gains obtained previously were combined with the linearized airplane dynamics in order to study controllability, performance, and indication of safety margin status. In Table III-5 we summarize the potential for each of the static safety margin possibilities. For a more detailed treatment of the analysis of static safety margin dynamics the reader is referred to Appendix C.

3. Flight Reference Based on Lift Margin

The potential use of lift margin as a flight reference was studied for reasons previously mentioned. Lift margin was viewed using the same approach applied to other flight reference candidates (DSM and various SSMs) and found to have certain interesting properties which would make it a safety margin system candidate if other means failed.

Implementation of a lift margin function would involve a multi-dimensional function of at least airspeed, angle of attack, and thrust, and possibly pitch rate and elevator deflection. The function would likely have no simple rational form such as DSM (i.e., the basic margin criteria) but would require either a look-up table or a fitted analytic formulation. The form of the lift margin function was not a subject of this study.

The behavior of the lift margin was examined using linearized derivatives obtained from a lift margin routine implemented in the NASA Augmentor Wing simulator model. There was no significant variation in the lift margin partial derivatives over the expected range of operating conditions between $\gamma = -5$ deg and $\gamma = -7.5$ deg. Representative values were:

$$k_u \doteq 1.2\%/kt$$

$$k_w \doteq -2.4\%/kt$$

$$k_\delta \doteq -0.3\%/^\circ$$

TABLE III-5

SUMMARY OF STATIC SAFETY MARGIN ANALYSIS (APPENDIX C)

STATIC SAFETY MARGIN	INPUTS	SPEED MARGIN CRITICAL (HIGH THRUST)	VERTICAL GUST MARGIN CRITICAL (LOW THRUST)
$SSM_{u,w}$	Airspeed and Angle of Attack	Equivalent to DSM — airspeed-like response, adverse $\gamma - \theta$ cross coupling.	Nearly equivalent to DSM — lacks relatively minor effects of airspeed and thrust.
$SSM_{u,\theta}$	Airspeed and Pitch Attitude	Ditto	Significant improvement in direct controllability and reduction of cross coupling effect in flight path response. Improvement in long term DSM regulation over θ -fixed, but incorrect margin indication in short term.
$SSM_{u,d}$	Airspeed and Flight Path Angle (or Vertical Velocity)	Ditto	Unacceptable control response — positive real zero in the flight reference numerator.
$SSM_{u,\delta}$	Airspeed and Thrust	Ditto	No direct indication of vertical gust component. An adverse cross coupling influence of thrust on flight path response.
$SSM_{w,\theta}$	Angle of Attack and Pitch Attitude	Better direct controllability than DSM, (but adverse $\gamma - \theta$ cross coupling still present). Incorrect indication of horizontal gust. Ineffective in regulating DSM.	Nearly equivalent to DSM — lacks relatively minor effects of airspeed and thrust.
$SSM_{w,d}$	Angle of Attack and Flight Path Angle (or Vertical Velocity)	Essentially equivalent to $SSM_{w,\theta}$.	Ditto
$SSM_{w,\delta}$	Angle of Attack and Thrust	Angle-of-attack like controllability (as in DSM). Large adverse cross coupling between thrust and FR.	Ditto
$SSM_{\theta,d}$	Pitch attitude and Flight Path Angle (or Vertical Velocity)	Angle-of-attack-like controllability. Inadequate margin status information. Ineffective in regulating DSM.	Same as high thrust condition.
$SSM_{\theta,\delta}$	Pitch Attitude and Thrust	Excellent controllability — one-to-one with pitch attitude. No status information. No regulation of DSM.	Same as high thrust condition.
$SSM_{d,\delta}$	Flight Path Angle (or Vertical Velocity) and Thrust	Unusable — too sensitive to thrust and flight path changes.	Same as high thrust condition.

Based on the above partial derivatives, we found the controllability of lift margin to be essentially similar to angle of attack with the characteristically low damping ratio of the complex pair of zeros, i.e.,

$$N_{\theta}^{FR} \doteq k_w V \left[s^2 + \left(-X_u + \frac{X_{\alpha} - g}{k_w/k_u V} \right) s - \frac{g}{V} Z_u + \frac{gZ_w}{k_w/k_u V} \right]$$

$$\doteq -2.9[0.2; 0.4] \% / \text{deg}$$

Thus, it was considered to be equivalent to vertical-gust-critical DSM in this respect.

The lift-margin-based flight reference was found to be effective for maintaining dynamic safety margin via an FR $\rightarrow \theta_c$ loop closure. The key expression of closed-loop effectiveness introduced previously (and explained in detail in Appendix C),

$$1 - \frac{N_{u_g}^{FR} N_{\theta}^{DSM}}{N_{u_g}^{DSM} N_{\theta}^{FR}}$$

was evaluated for a general flight reference involving u and w:

$$\frac{s \left[s^2 - (X_u + Z_w) s + X_u Z_w - X_w Z_u \right]}{(s - Z_w) \left[s^2 + \left(-X_u + \frac{X_{\alpha} - g}{k_w/k_u V} \right) s - \frac{g}{V} Z_u + \frac{gZ_w}{k_w/k_u V} \right]}$$

Thus, for lift margin, $-k_w/k_u \doteq -2$:

$$1 - \frac{N_{u_g}^{FR} N_{\theta}^{DSM}}{N_{u_g}^{DSM} N_{\theta}^{FR}} \doteq \frac{1(0)(0.15)(0.40)}{[0.20; 0.40](0.50)}$$

Since this tends to be small compared to unity for frequencies below 0.4 rad/sec we could expect the closed loop $\frac{DSM}{u_g}$ for lift margin regulation to be comparable to that of direct DSM regulation.

The main shortcoming of lift margin was that it produced a distorted indication of 'safety margin' — mainly, critical margins indicated low. This was determined by comparison of FR and DSM gust numerators:

For speed margin critical,

$$\frac{N_{u_g}^{FR}}{N_{u_g}^{DSM}} \doteq \frac{-k_u s \left(s - Z_w + \frac{k_w}{k_u} Z_u \right)}{-k_u s \left(s - Z_w \right)} \doteq \frac{0.25(1.1)}{(0.5)}$$

i.e., the indicated margin change compared to the actual was 0.5 at low frequencies and 0.25 at high frequencies

For vertical gust margin critical

$$\frac{N_{w_g}^{FR}}{N_{w_g}^{DSM}} \doteq \frac{2k_w s \left(s - X_u + \frac{k_u}{k_w} X_w \right)}{-k_w s \left(s - X_u \right)} \doteq \frac{0.5(0.02)}{(0.07)} \doteq 0.14$$

It was believed that lift margin could be of value only if switching between two margin criteria proved unsuccessful in simulator experiments.

C. IMPLICATIONS FOR THE EXPERIMENTAL INVESTIGATION

The survey of various flight reference implementation concepts thus described did not result in a list of candidates which were likely to be totally satisfactory in a safety margin system role. From the possibilities considered — dynamic safety margin, ten static safety margin combinations, and lift margin — none appeared to meet all requirements. As illustrated by the summary in Table III-6, good controllability could only be obtained at the expense of good safety margin status information or the ability to directly regulate safety margin excursions, and vice versa. In most cases, there was also a significant difference in characteristics when switching from the condition where speed margin was critical to the condition where vertical gust margin was critical.

REPRODUCIBILITY OF THE
ORIGINAL PAGE IS POOR

TABLE III-6

SUMMARY OF THE SURVEY OF FLIGHT REFERENCE IMPLEMENTATION CONCEPTS

FLIGHT REFERENCE BASIS	IMPLEMENTATION	CONTROLLABILITY	STATUS INFORMATION	MARGIN REGULATION
DSM	1 input	Fair	Ideal	Good
	3 inputs	Fair	Ideal	Good
SSM _{u,w}	1 input	Fair	Ideal	Good
	1+ input	Fair	Good	Good
SSM _{u,θ}	1 input	Fair	Ideal	Good
	2 inputs	Good	Poor	Fair
SSM _{u,d}	1 input	Fair	Ideal	Good
	2 inputs	Unacceptable X	Poor	--
SSM _{u,δ}	1 input	Fair	Ideal	Good
	2 inputs	Poor	Poor	--
SSM _{w,θ}	2 inputs	Good	Poor	Nil
	1+ input	Fair	Good	Good
SSM _{w,d}	2 inputs	Good	Poor	Nil
	1+ input	Fair	Good	Good
SSM _{w,δ}	2 inputs	Good	Poor	Good
	1+ input	Fair	Good	Good
SSM _{θ,d}	2 inputs	Good	Poor	Nil
	2 inputs	Fair	--	--
SSM _{θ,δ}	2 inputs	Ideal	Nil	Nil
	2 inputs	Ideal	Nil	Nil
SSM _{d,δ}	2 inputs	Unacceptable X	--	--
	2 inputs	Unacceptable X	--	--
IM	3+ inputs	Fair	Fair	Good

-- Indicates that no analysis was performed.

The upper line of a table entry refers to an airspeed margin critical condition (high thrust) and the lower line refers to a vertical gust margin critical condition (low thrust).

The general implication of the analytic results was that there were some possibilities that should be evaluated, but they likely would not be suitable for use in a safety margin system without modification. Thus, it would be necessary to carry out development of flight reference schemes as part of the simulator experiments.

Two flight reference schemes were considered to be worth exploring experimentally although neither was expected to be satisfactory without modification. These two were:

- Dynamic safety margin
- Static safety margin based on airspeed and pitch attitude.

Dynamic safety margin was regarded as the most important scheme to evaluate on the simulator. It provided the ideal safety margin status information. Hence, regulation of safety margin excursions would be possible to the limit of manual or automatic controllability. In addition, we believed that it was important to establish the magnitude of likely controllability problems as DSM switched back and forth between margin criteria. Also, we were not sure that DSM would alternate just between the two margin criteria believed most critical (20 kt speed margin from V_{min_m} and 20 kt vertical gust margin); the other three margin criteria mentioned in Section II.A might have unexpectedly come into play under non-steady conditions.

Static safety margin based on airspeed and pitch attitude ($SSM_{u,\theta}$) was the other flight reference scheme we considered worth investigating on the simulator. It offered the hope of improving controllability when vertical gust margin was critical, although status information would be degraded. Most important, it was suspected that a $u - \theta$ combination could be used to alleviate the adverse $\gamma - \theta$ cross coupling when speed margin was critical. Specifically, we envisioned a cross between a constant θ flight reference and a constant airspeed flight reference.

Thus, as we shall discuss next, the experimental investigation began by exploring DSM, $SSM_{u,\theta}$, and subsequently variations of each. This ultimately led to development of a useful hybrid flight reference scheme involving DSM plus a linear function of pitch attitude.

PRECEDING PAGE BLANK NOT FILMED

SECTION IV

EXPERIMENTAL INVESTIGATION

The objectives of the experimental investigation were threefold. First, we desired to explore a limited number of interesting implementation concepts based on the results of the prior analysis effort. Second, we needed to investigate certain specific system features which could be of use in configuring and tuning a final solution such as adding pitch rate or pitch attitude compensation. Last, we wanted to set forth and test the most promising candidate for a final solution. Hence, the experimental effort was mainly developmental in nature.

In the following pages we shall describe the experimental procedure and the results obtained from the various investigations. We will conclude by presenting the results of the evaluation of a refined safety margin system design.

A. EXPERIMENTAL PROCEDURE

The experiments conducted during this program involved manned and unmanned use of the STOLAND airborne hardware simulator located at NASA Ames Research Center. This is a fixed base simulator of the NASA Augmentor Wing research airplane and its associated STOLAND system hardware. The latter is described in Ref. 9. The major components involved in the experiment are shown diagrammatically in Fig. IV-1.

The simulator was used in a head-down IIS approach scenario. Approaches were made both manually and automatically through various wind profiles consisting of a combination of random and deterministic components. Runs started with the aircraft trimmed for descent on a 7.5 deg glide slope at approximately 2000 ft altitude and terminated at 200 ft. No configuration changes were involved.

The specific loading configuration and atmospheric conditions used in this study were:

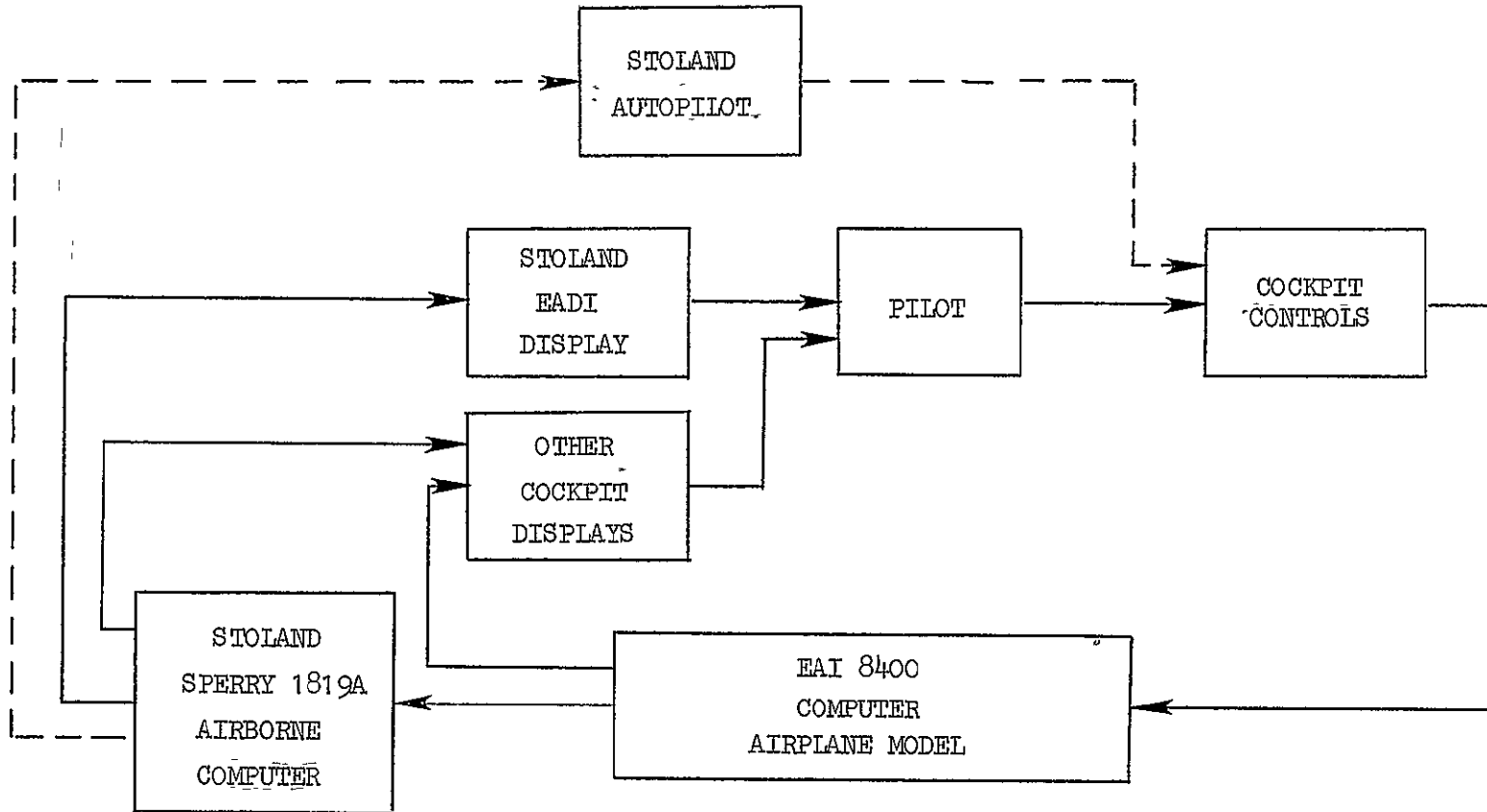


Figure IV-1. Simulator Block Diagram

Weight 40,000 lb
cg FS 341.2
Flap Deflection 65 deg
Nozzle Deflection 70 deg
Atmosphere sea level, standard day
Maximum engine rpm (for this study) 98.5%
Pitch, roll, and yaw SAS on

The cockpit controls included:

Longitudinal control column
Throttle
Lateral wheel
Rudder pedals

The pilot employed a backside control technique in controlling flight path and flight reference, i.e., $\epsilon_{GS} \rightarrow \delta_T$ and $FR \rightarrow \theta_c$.

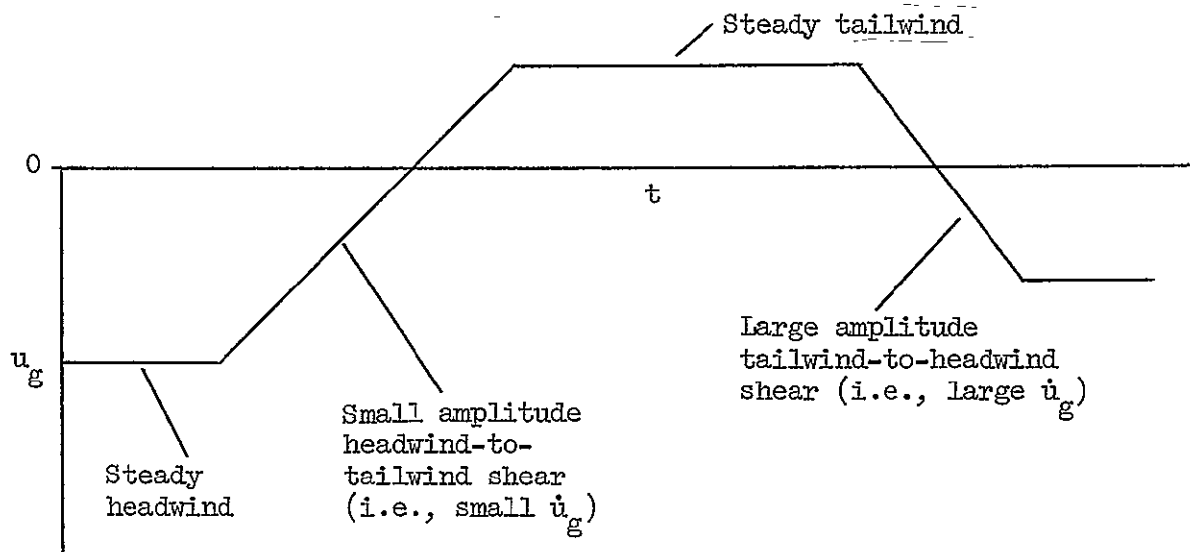
It was necessary to constrain the operational variables (configuration, loading, atmosphere, and piloting technique) in order to study the safety margin system features in an efficient and systematic manner. The effect of changing some operational variables was studied briefly and will be discussed in Section IV.F.

The simulator wind model was the primary tool used for exploring safety margin system designs. The model itself and the procedure for using it was patterned after the simulator experiments reported in Ref. 10 which addressed wind shear hazard for powered-lift aircraft.

The wind model consisted of a combination of random and deterministic components. The random components were computed using the standard MIL-F-8785B Dryden model as described in Ref. 4. The level typically used was based on $\sigma_{UG} = 3$ ft/sec.

The deterministic wind component provided the main pilot-vehicle disturbance and was composed of a series of linear, time-dependent changes in longitudinal and vertical gusts. Normally, during a simulator run, the

deterministic wind component consisted of a profile such as shown in the following sketch:



The main metric of gust severity was considered to be longitudinal gust rate, that is, \dot{u}_g . A magnitude of 3 ft/sec^2 was regarded as relatively large based on Ref. 10, and, indeed, based on pilot opinion during this experiment. In general, the duration of wind shears was sufficiently long to allow for closed loop pilot response to flight reference error (15 to 20 sec). Only limited use was made of deterministic vertical gusts because the aircraft heave response was too rapid to allow significant pilot regulation. The random w_g component provided the main vertical gust component.

Three forms of data were acquired during the experiments including:

- Analog strip chart recordings
- Digital end-of-run printouts
- Tape recordings of pilot commentary.

The pilot tapes, transcribed after each simulator session, were regarded as the most valuable resource. The analog strip charts (3 recorders — 40 channels) provided the most detailed account of simulator runs and

were monitored frequently during simulator runs. Table IV-1 lists the strip chart recorder assignments. Digital printout was used to record only the simulator model variables which were subject to change from run to run depending upon the experiment.

An on-line pilot control technique identification scheme was implemented in an attempt to correlate pilot commentary with measured pilot technique. It was of particular importance to obtain some quantitative measure of flight reference loop tightness in order to verify the prior analysis. Although a relatively low priority was put on development of such an identification scheme, a limited degree of success was obtained.

The method used to identify pilot action consisted of (i) assuming a specific loop structure model as in Fig. IV-2 then (ii) solving for loop structure model parameters by a least squares fit of the simulator data. This was accomplished on-line in real time through use of a running least squares fit, i.e., continually updating the accumulated data. The method is similar to that described in Ref. 11. A summary of the on-line identification scheme is given in Appendix D.

B. INVESTIGATION OF DISPLAY FEATURES

The first step in the simulator investigation was to establish a display format which would serve throughout the remainder of the experimental program.

1. Flight Reference Indication

As a starting point, the flight reference was assigned to the STOLAND EADI speed error indicator. This consisted of a diamond symbol moving on a vertical scale as shown below:

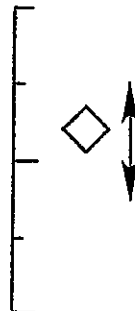


TABLE IV-1

STRIP CHART RECORDER ASSIGNMENTS

VARIABLE	RANGE	VARIABLE	RANGE
Altitude (cyclic)	0 to 250 ft	Flight Reference Standard Deviation	$\pm 50\%$
Altitude Rate (cyclic)	± 25 ft/sec	Flight Reference Mean	$\pm 50\%$
Angle of Attack	-20 to +30 deg	Safety Reference Standard Deviation	$\pm 50\%$
Column Displacement	-5 to +5 deg	Safety Reference Mean	$\pm 50\%$
Longitudinal Gust	± 50 ft/sec	Lateral Displacement	± 500 ft
Glide Slope Error	± 5 deg	Flight Path Angle	-20 to +5 deg
Vertical Gust	± 50 ft/sec	Lateral Path Angle	65 to 115 deg
Engine RPM	75 to 100%	Localizer Error	± 5 deg
Equivalent Airspeed (cyclic)	0 to 50 kt	Heading	65 to 115 deg
Pitch Attitude (cyclic)	± 5 deg	Yaw Rate	± 25 deg/sec
Safety Reference Index	± 5	Roll Attitude	± 25 deg
Safety Reference (cyclic)	25 to 75%	Roll Rate	± 25 deg/sec
Flight Reference Index	± 5	Pitch Loop Gain	± 0.5 deg/deg
Flight Reference (cyclic)	25 to 75%	Integral Flight Reference Gain	± 0.05 deg/ $\frac{1}{2}$ -sec
Dynamic Safety Margin Index	± 5	Flight Reference Error	$\pm 50\%$
Dynamic Safety Margin (cyclic)	25 to 75%	Pitch Attitude	± 12.5 deg
Lateral Gust	± 50 ft/sec	Control Column	± 5 deg
Wheel Deflection	± 12.5 deg	Glide Slope Error Gain	$\pm 12.5\%$ /deg
Distance from Glide Slope	± 125 ft	Glide Slope Error	± 2.5 deg
Lift Margin	0 to 1 g	Throttle Deflection	$\pm 12.5\%$

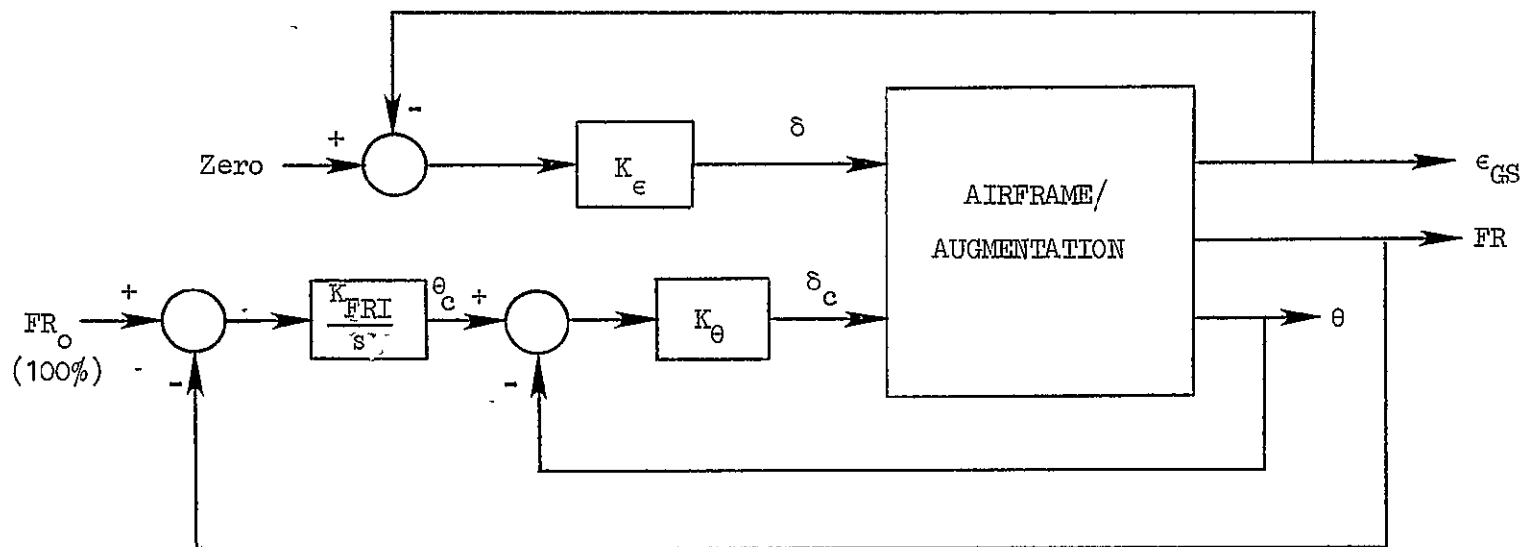
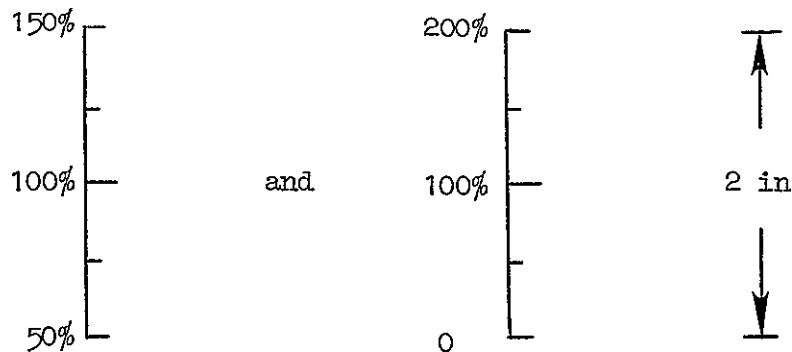


Figure IV-2. Assumed Loop Structure for Pilot Identification

This had the obvious advantage of maintaining the same function for this part of the display as with the original STOLAND system.

The scale markings on the EADI could not be arbitrarily set because they were drawn by hardware circuitry rather than by digital computer program software. Thus, two scalings were considered:

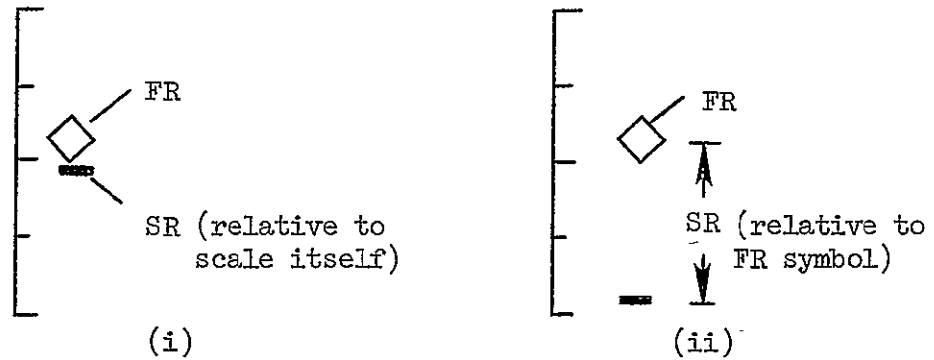


The more sensitive scale on the left corresponded well to the original STOLAND speed error scale which was ± 10 kt. (Recall that in the airspeed margin range $\pm 50\%$ of safety margin corresponds to ± 10 kt.) In contrast, the scale on the right presented a greater range which included zero margin — clearly more desirable if large margin excursions were likely.

Two pilots evaluated the scaling alternatives and considered both to be acceptable. The $\pm 100\%$ scale was preferred by the pilot having no prior experience using the STOLAND displays. The other pilot found that the increased sensitivity of the $\pm 50\%$ scale aided in easier detection of small margin changes and rates of change. Further, it was discovered that margin variations in excess of 50% were unlikely. The sensitive scale was finally selected as the better alternative.

2. Safety Reference Indication

The next display format feature established was the safety reference indication. The two possibilities considered were (i) to have an SR symbol moving on the safety margin scale along with the FR bug, or (ii) to have the SR symbol represented as a kind of floor with respect to the FR bug, i.e.,



In the second case, the SR symbol could be viewed as a shrinking or enlarging of the bottom of the vertical scale. Hence, even if the FR bug indicated 100%, if the SR line moved upward from the bottom scale mark it would indicate a lessening of actual safety margins. Conversely, if it moved downward it would indicate an actual safety margin in excess of that indicated by the FR.

The simulator evaluation of these two cases led to the adoption of the second. The SR line near the bottom of the scale was preferred because it was far enough removed as to not interfere with the FR bug yet was close enough to monitor easily. Also, since the SR line was placed relative to the FR bug (the indicated SR was the distance between the line and the bug) the line did not move radically as long as the FR corresponded well to the actual safety margin.

3. Flight Reference Status Lights

Another display feature adopted was a pair of lights immediately to the left of the FR scale (normally used as marker beacon lights) which indicated the status of the FR, i.e., whether it was operating in the high thrust region or the low thrust region. It was believed that such information could be of value if any significant adjustments in control strategy or technique were involved. As the simulator experiments progressed the flight reference status lights did, in fact, prove to be a useful feature and were adopted as a part of the final safety margin system configuration.

4. Other Features

Miscellaneous other features incorporated into the EADI display format were:

- Engine rpm (digital)
- STOLAND flight path angle bar
- Maximum available flight path angle bar.

The overall display format is summarized in Fig. IV-3.

C. PRELIMINARY EVALUATION OF SAFETY MARGIN SYSTEM CONCEPTS

Several relatively complete safety margin system packages were investigated experimentally. This was done to explore concepts within the full context of FR switching (high thrust region versus low thrust region) and auxiliary use of the SR. The results of these studies formed the main foundation for the refined system ultimately tested and described in Subsection F.

Two basic flight reference schemes were involved, but several variations of each were tried. The two basic flight references were:

- FR[DSM]
- FR[SSM_{u,θ}]

The first of these was based on dynamic safety margin and was considered important to test because of its directness. At the same time, based on analyses, the FR[DSM] appeared to have potential controllability problems which deserved experimental verification.

The second basic flight reference scheme tested, FR[SSM_{u,θ}], represented a system which had good controllability potential but possible problems in providing status information — the converse of the FR[DSM].

The variations which were applied to the two basic flight reference schemes included:

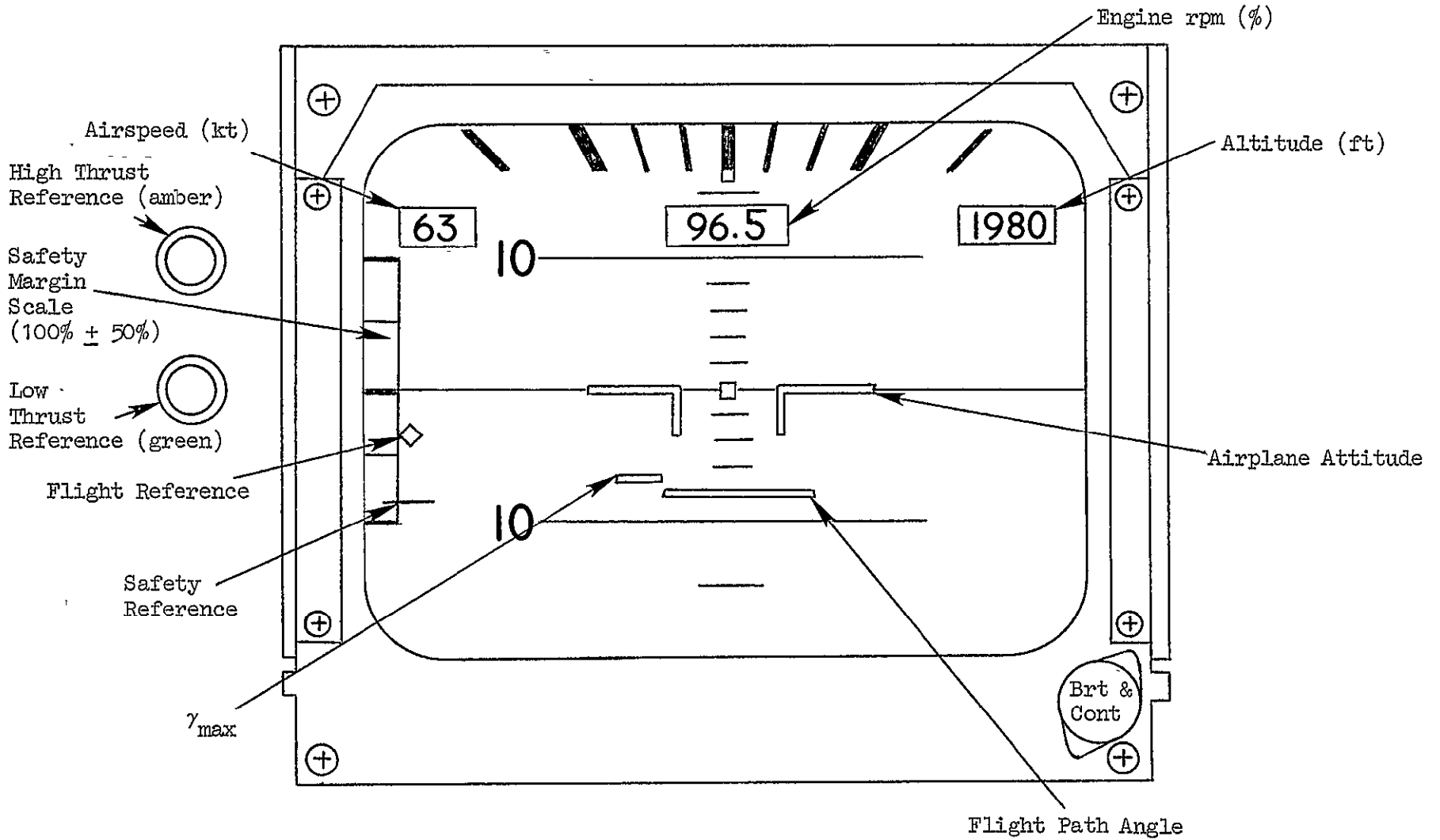


Figure IV-3. STOLAND EADI Display for Safety Margin Evaluation

- Addition of a safety reference for enhanced safety margin status information
- Addition of pitch rate equalization for improved controllability.

These variations involved minor changes in the system logic but had the potential for large differences in pilot perception. Therefore, they were evaluated within the context of the overall safety margin system as opposed to the design adjustments described in the subsequent Subsection IV.D.

1. Evaluation of FR[DSM]

A safety margin system comprised only of a flight reference based on dynamic safety margin was evaluated and found to be an effective system except for some anticipated controllability aspects.

The FR[DSM] was studied on the simulator by adjusting the mean headwind to obtain initial operating points for the conditions of speed margin critical and vertical gust margin critical — normally 20 kt and zero, respectively. Wind shears were introduced to sometimes produce excursions back and forth between the two critical margin conditions and sometimes remain within one critical margin condition.

Based on the analytic results, we expected to find manual controllability problems for both DSM margin conditions. Recall that for speed margin critical, control of speed margin involved adverse $\gamma - \theta$ cross coupling. Also, control of vertical gust margin involved the possibility of an oscillatory tendency if controlling too tightly. Only the former problem appeared to be of any magnitude.

On the matter of adverse $\gamma - \theta$ cross coupling, the main evaluation pilot believed that $\gamma - \theta$ cross coupling should be proverse or, at worst, limited to zero. That is, no downward pitch correction should be required to hold flight reference when making an upward flight path correction. (This belief may have been compounded by the presence of strong proverse $\gamma - \theta$ coupling when vertical gust margin was critical.) We should add, however, that two other pilots who viewed FR[DSM] briefly did not express concern over the adverse $\gamma - \theta$ cross coupling. Nevertheless, this feature

was identified as one for which a remedy should be studied. This is addressed in Subsection D.

Controllability of the angle-of-attack-like dynamics when vertical gust margin was critical was found not to be the problem anticipated. All three pilots evaluating this system restricted their loop crossover frequency to approximately 0.15 rad/sec. This appeared to provide them with an acceptable level of flight reference (and safety margin) precision in even the largest shears encountered, thus an overcontrol tendency was not observed. One pilot hypothesized that the angle-of-attack-like flight reference may have been more acceptable because of the strict exclusion by the DSM of low airspeed, extreme backside operation at higher thrust settings.

In general, control of the FR[DSM] required fairly long term regulation involving initial correction then eventual cross-checking. Hence, it was not regarded as a particularly low workload task even though the specific controllability features discussed above were not as severe as anticipated. There was, therefore, some interest in pursuing flight reference configurations with improved control response.

There was direct evidence that the pilot was regulating dynamic safety margin during sustained wind shears. As shown in Fig. IV-4, he was able to arrest the change in DSM produced by a long term \dot{u}_g , and, in fact, had to stop the DSM excursion in the opposite direction when the shear stopped.

It was difficult to obtain statistically significant safety margin precision measurements in order to compare FR[DSM] effectiveness with other flight reference schemes. Therefore, we had to rely on a combination of analysis and simulator measurements as the main indicator of potential safety margin precision. Consequently our summary of results may sound qualitative.

The reason for difficulty in measuring statistically significant precision directly was the relatively small data sample which could be obtained within the scope of this program and the involvement of primarily only one pilot. Although discrete, deterministic wind shears were used as the primary disturbance forcing function, there was considerable

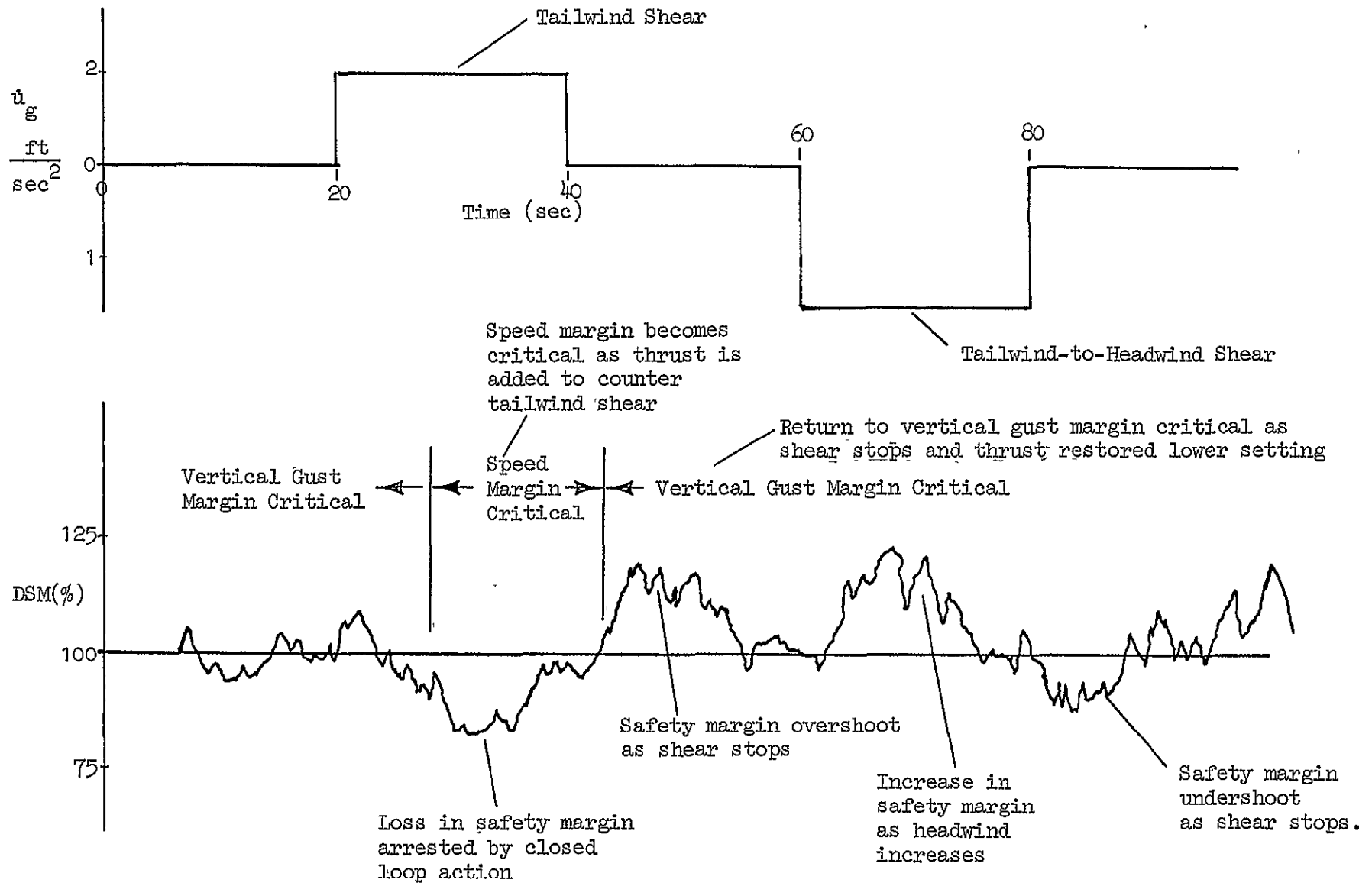


Figure IV-4. Illustration of DSM Regulation in Sustained Wind Shears

randomness in the resulting safety margin excursions. Part of the randomness was due to the low level superimposed random turbulence, and part was due to randomness associated with pilot action in controlling flight path.

Because of the limited sample of data, the procedure for estimating potential effectiveness of any flight reference was (i) to use the pilot loop gain measurements to establish approximate crossover frequency ranges, then (ii) to infer the effect of such crossover frequencies from the simple closed loop models used in the system analyses.

For FR[DSM] the above procedure led to direct use of the closed loop responses shown in Fig. III-5 of the analysis section since measured crossover frequencies were approximately 0.15 rad/sec. In fact, in the case of FR[DSM] a fairly strong closed loop effect was evident in the simulator data and fair direct comparison with analytically modeled response was possible.

One feature of FR[DSM] which could not be handled well analytically was the action of DSM switching back and forth between speed-margin-critical, and vertical-gust-margin-critical conditions. All that was known was that a common set of feedback gain and compensation could be used in the autopilot loop without a significant variation in crossover frequency even though the controlled element dynamics were varying between airspeed and angle of attack.

The simulator evaluation showed that the effect of DSM switching did not, in fact, present any particular problem. The pilot claimed that the flight reference status lights (Section IV.B.3) may have contributed to his impression of the smoothness in switching.

2. Evaluation of FR[SSM_{u,θ}]

A safety margin system composed of a flight reference based on static safety margin was evaluated to examine its anticipated improved controllability over FR[DSM] but degraded safety margin status information. Because this scheme was equivalent to dynamic safety margin with speed margin critical, the nominal operating point evaluated corresponded to a low thrust condition, where the vertical gust margin was critical.

Controllability of FR[SSM_{u,θ}], by itself, was preferred over FR[DSM]. The pilot noted that smaller pitch attitude excursions were made when tracking FR[SSM_{u,θ}], and that these smaller excursions seemed to have a favorable effect on flight path tracking. This appeared to reflect the difference in γ/δ response with FR regulated which is discussed in the analysis of SSM_{u,θ}.

The FR[SSM_{u,θ}] did not provide good DSM status information as predicted, but this shortcoming was not readily apparent to the pilot without careful examination of FR response to known wind profiles and to throttle inputs. A better evaluation of this feature was made when a dynamic safety margin was provided in the form of a safety reference (to be discussed subsequently). The main lesson learned was that, without a direct reference, the pilot cannot easily judge safety margin status, per se. He is, therefore, likely to regard mistakenly his flight reference as safety margin status even though it might be inherently a poor indicator of such status.

3. Evaluation of FR[SSM_{u,θ}] and SR[DSM]

A safety reference was provided as an auxiliary display to the flight reference based on SSM_{u,θ} in order to give the pilot better safety margin status information. Thus, the pilot could track the relatively easy FR[SSM_{u,θ}] while monitoring the true SR[DSM]. This combination proved so incompatible that the effectiveness of both the FR and SR was cancelled.

The problem in using this combination was that when a disturbance was encountered the short term responses of FR and SR were frequently opposite. This led to understandable pilot confusion, and the controllability advantage of FR[SSM_{u,θ}] was effectively lost.

This FR - SR combination supported the notion that if a safety reference is to be used, then the flight reference must correspond reasonably well. The implication is that the flight reference must be a reasonable facsimile of dynamic safety margin if the latter is truly the quantity to be maintained. This was the basis for the flight reference ultimately tried and described in Subsection F.

4. Evaluation of FR[DSM+f($\dot{\theta}$)]

A flight reference was constructed using DSM as a basis and adding a component derived from pitch rate in the hope of improving controllability in the vertical-gust-margin-critical region. The function was defined as shown in Table IV-2. Thus in the steady state FR = DSM, but in the low thrust region where vertical gust margin was critical, the linearized FR numerator was:

$$\begin{aligned} N_{\theta}^{\text{FR}} & \doteq \frac{1}{V} k_w^- \left[s^2 - X_u s - \frac{g}{V} Z_u \right] \\ & \quad + k_{\theta}^* s \\ & = \frac{1}{V} k_w^- \left[s^2 + \left(\frac{V k_{\theta}^*}{k_w^*} - X_u \right) s - \frac{g}{V} Z_u \right] \end{aligned}$$

In effect the low damping ratio in the control numerator could be artificially increased by the parameter k_{θ}^* .

The parameter k_{θ}^* was adjusted so that the damping ratio of the numerator zeros became 0.7. The closed loop response, therefore, would always be well damped unless the pitch attitude itself was overcontrolled by the pilot and driven unstable.

This flight reference was not readily discernible by the pilot from the basic FR[DSM], and his normal flight reference loop gain was unchanged.

In order to produce noticeable degradation in controllability, the N_{θ}^{FR} numerator zeros were driven into the right half plane by changing the sign on k_{θ}^* . With the numerator damping ratio set to -.2 the pilot was able to detect the oscillatory dynamics only if he intentionally tightened up the loop by increasing his control gain.

For the system ultimately to be discussed under Subsection F, a nearly identical placement of zeros was used for N_{θ}^{FR} with vertical gust margin critical, but the system was found significantly easier to control, and a much higher crossover frequency was used. It appeared, then, that in

TABLE IV-2

FLIGHT REFERENCE BASED ON DSM AND $f(\dot{\theta})$

$$FR = \text{MIN}(FR_1, FR_2)$$

$$\text{where } FR_1 = DSM_1 = \frac{V - V_{\min}}{20 \text{ kt}}$$

$$FR_2 = DSM_2 + f(\dot{\theta})$$

$$= \frac{\alpha_{\max} - \alpha}{\arcsin \frac{V}{20 \text{ kt}}} + \frac{k_{\dot{\theta}} s \theta}{\left(s + \frac{1}{T_1}\right)\left(s + \frac{1}{T_2}\right)}$$

- Notes:
- 1) If θ is held fixed then $FR = DSM$
 - 2) $1/T_1$ and $1/T_2$ set to nominal values of airframe $1/T_{\theta 1}$ and $1/T_{\theta 2}$
 - 3) $k_{\dot{\theta}}$ determines damping ratio of FR_2 numerator zeros.

the case of FR[DSM+f($\dot{\theta}$)] the low bandwidth dynamics of the speed-margin-critical N_{θ}^{FR} prevented the pilot from taking advantage of the improved vertical-gust-margin-critical N_{θ}^{FR} .

5. Evaluation of FR[DSM+f($\dot{\theta}$)] and SR[DSM]

A brief evaluation was made using the previously discussed flight reference and a safety reference. Although there was no measurable improvement in controllability, we wanted to evaluate quantitatively the magnitude of disparity between FR and SR to find if even a small disparity were permissible. In the FR--SR case previously discussed (FR[SSM_{u, θ], and SR[DSM]) the difference was so large as to be clearly impractical.}

The finding was that the $k_{\dot{\theta}}$ term amounted to only 10% net difference between FR and SR. With this level the SR appeared to be a useful device for monitoring true safety margins while tracking a flight reference with slightly different dynamics.

6. Evaluation of a Flight Path Reference, GR (Gamma Reference)

A flight path reference indicating the available flight path angle capability, γ_{max} , was added to the displays of FR and SR. The value of the GR display was to tell the pilot how much flight path angle he could produce with the application of maximum thrust at his present flight reference — in effect, the consequences of being too fast or too slow.

The specific GR tested involved a simple steady-state functional relationship between airspeed and thrust derived directly from a $\gamma - V$ curve. A more sophisticated implementation would have included the effects of non-steady gusts (e.g., a tailwind shear would reduce γ_{max}), however, our objective was only to find if an additional displayed parameter could be used in conjunction with the FR and SR.

No problems were perceived by the pilot. The display was easy to use but was regarded as relatively unnecessary without the non-steady effect of wind shear noted above.

7. Conclusions from the Preliminary System Evaluations

As a result of the foregoing experimental investigations several important things were learned which helped in the investigation of design adjustments and in configuring a refined system preparatory to flight testing.

- None of the systems evaluated were satisfactory without refinements.
- The basic FR[DSM] was found to be the most suitable overall.
- All the systems suffered from adverse $\gamma - \theta$ cross coupling, and to rectify it would require a departure from the maximum allowable low speed flight envelope.
- A safety reference was found useful, but only if there was reasonable correspondence to the flight reference.
- The matter of switching between at least two DSM functions presented no apparent problem.

D. INVESTIGATION OF FR DESIGN ADJUSTMENTS

The objective of this line of experiments was to study possible methods for adjusting the flight reference implementation for improved controllability while maintaining reasonable status information. The main topic of study was aimed at alleviating objectionable $\gamma - \theta$ cross coupling. A subsidiary topic involved exploration of a lift-margin-like flight reference.

1. Alleviation of Adverse $\gamma - \theta$ Cross Coupling in High Thrust Region

One of the main objections in all of the basic FR schemes studied was adverse $\gamma - \theta$ cross coupling (nose down pitch when making an upward flight path correction). Thus, it was considered important to devise a way of alleviating the problem.

Since $\gamma - \theta$ coupling was a built-in feature of the given aerodynamic configuration it was necessary to depart from the desired steady state $\gamma - V$ trajectory, i.e., constant airspeed, and to approach a constant pitch attitude trajectory.

Simply configuring the FR to follow a constant pitch attitude was believed unsatisfactory because it would (i) not offer any closed loop regulation of flight reference and (ii) not provide safety margin status information. Hence, it was necessary only to approach a constant θ trajectory as a limit. This was accomplished by making the flight reference a linear combination of airspeed and attitude, i.e.,

$$FR = k_u \Delta u_a + k_\theta \Delta \theta$$

where Δu_a and $\Delta \theta$ were perturbation airspeed and pitch attitude.

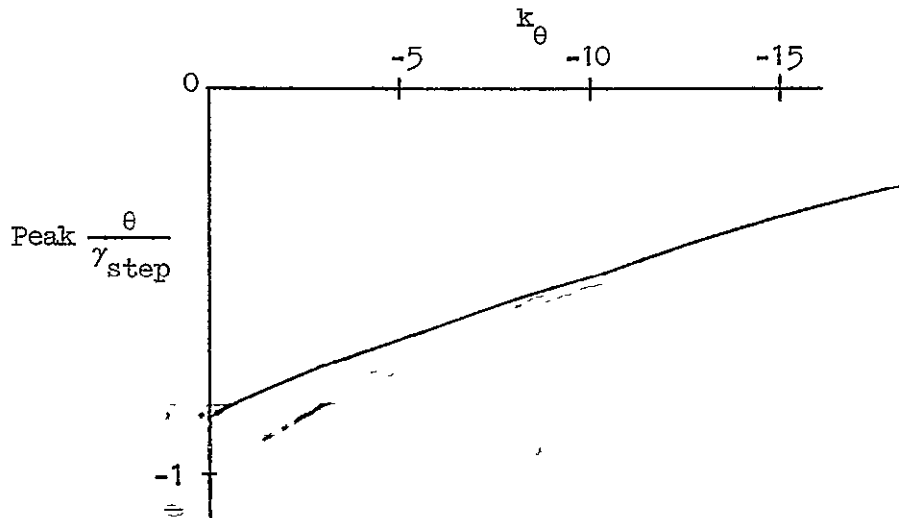
The airspeed coefficient k_u was fixed to maintain the correct sensitivity to horizontal gusts (5%/kt), and k_θ was varied from zero to $-\infty$. Thus for $k_\theta = 0$ the basic FR[DSM] was represented. For $k_\theta = -\infty$ the FR corresponded to constant θ , hence without adverse $\gamma - \theta$ coupling.

For a fixed operating point the pilot was asked to perform the IIS approach task in a variety of turbulence conditions and wind shears. The parameter k_θ was varied from zero to -20%/deg in decrements of 5%/deg. The results were:

k_θ	COMMENTS
Zero	Changes in θ required to track FR were so large that it interfered with flight path tracking.
-5%/deg	No substantial alleviation in adverse $\gamma - \theta$ coupling.
-10%/deg	Marginal — could begin to neglect coordination between θ and throttle.
-15%/deg	Easier to track than -10%/deg and adverse $\gamma - \theta$ coupling reduced to the level of ambient noise.
-20%/deg	Too sensitive to pitch changes — might be susceptible to PIO.

The tradeoff from the pilot's view was mainly between adverse $\gamma - \theta$ coupling and excessive FR/θ sensitivity. But one other factor was present although not directly observable — the degree of correlation between flight reference and safety margin. This last issue forced the tradeoff toward the lowest possible k_θ . Hence, while the pilot preferred $-15\%/deg$, a level of $-10\%/deg$ was considered more widely acceptable.

We should comment on the degree of generality of these numerical results. As for sensitivity to θ excursions and corruption of safety margin information, the values of k_θ mentioned above should be fairly general. With regard to reduction of $\gamma - \theta$ coupling, the numerical values of k_θ cannot be generalized — they are dependent on the specific configuration considered. In order to apply a degree of generality, however, the k_θ 's could be related to a respective θ change during a given flight path angle excursion. Recall that this was done earlier in the analysis section. The approximate relationship between peak θ/γ_{step} and k_θ for the configuration evaluated was:



2. Evaluation of a General u, w Flight Reference (With Implications for the Use of Lift Margin)

A brief experiment was run in which the steady state $\gamma - V$ slope for constant flight reference was varied using a combination of u and w , i.e., airspeed and angle of attack. This experiment also had implications for the use of lift margin because of the similarity in the dynamics.

From the relationships expressed in Table III-2

$$\left. \frac{\partial u}{\partial \gamma} \right|_{FR} = \frac{g}{X_u - \frac{k_u}{k_w} \frac{(X_\alpha - g)}{V}}$$

for a general u,w flight reference. The following range of k_u and k_w , thus $\frac{\partial u}{\partial \gamma}$, was explored:

k_u (%/kt)	k_w (%/kt)	$\frac{\partial u}{\partial \gamma} \left(\frac{kt}{deg} \right)$	Condition
5	0	0	Constant speed
5	-5	-2.4	Intermediate condition — representative of lift margin
0	-5	-4.7	Constant angle of attack

The two extremes in the table above were representative of the basic DSM dynamics for speed margin critical and vertical gust margin critical, respectively. The main objective of this experiment was, therefore, to examine the controllability of the intermediate case.

Prior analysis had shown that the dynamics of a flight reference with $k_u = -k_w$ should be more angle-of-attack-like than airspeed-like (see Section III.B.3). But in using FR[DSM] the pilot had already demonstrated that he controlled angle of attack in essentially the same way as airspeed — rather loosely. Thus we expected that the u-w combination would not produce any unusual results.

A few runs using the intermediate u-w combination showed that this was a usable flight reference, not really distinguishable from FR[DSM]. Measured pilot gains indicated that the closed loop bandwidth was approximately the same as DSM — about 0.15 rad/sec. The implication was that there was a continuum of flight reference possibilities spanning the range of positive k_u and negative k_w combinations which would include lift margin as a special case.

E. COMPATIBILITY OF MANUAL, AUTOMATIC, AND FLIGHT DIRECTOR FUNCTIONS — IMPLEMENTATION AND OPERATION

Another objective of the feasibility study was to address the compatibility of the safety margin system with manual, automatic, and flight director operation. This was accomplished by integrating the components of a safety margin system design into an existing STOLAND autopilot and flight director. The following topics provide a discussion of our investigation.

1. System Implementation

The simulator experiment included the implementation of basic safety margin system components on the STOLAND equipment. Thus it was possible to evaluate directly the impact on the overall software/hardware package as well as certain operational features.

System implementation included the following:

- EADI display functions
- FR and SR functions
- Autopilot and flight director loops.

An example of the Sperry 1819A digital computer coding required for the above functions is included in Appendix E.

Implementation of the display functions had a minimal impact on the existing STOLAND system. Software modifications involved substitution of new signals to drive various existing displays:

- The vertical scale symbol, normally used for airspeed error, was driven by the FR function
- Averaged engine rpm was displayed on the central digital window
- The runway outline was collapsed into a single horizontal line and driven by the SR function

- Two of the marker beacon lights were used to indicate whether airspeed margin or angle of attack margin was more critical
- The flight path acceleration bar was driven by the flight path margin reference, GR.

There was no incompatibility among manual, automatic, and flight director functions so far as the display was concerned.

The general implementation of FR, SR, and GR functions in the Sperry 1819A computer was represented by the specific software implementation of the DSM shown in Appendix E. The DSM was, of course, the heart of the FR and SR functions ultimately recommended. The basic philosophy adopted was to base automatic operation on the preferred manual system. This insured system compatibility with regard to FR and SR functions. Operational problems were encountered, however, and will be discussed shortly.

The magnitude of the impact of the safety margin system on STOLAND software was minimal. As shown in Appendix E, approximately 200 words of the total 32000 word capacity were required to implement the system. The impact on cycle time was also miniscule because many simple arithmetic operations were involved (only one sine function was used, and even this could be eliminated using a small angle approximation).

An angle of attack input is one feature lacking in the present STOLAND system but required to implement a safety margin system. Angle of attack measurements are available on the NASA Augmentor Wing airplane; however, they are not sent to the Sperry 1819A computer. This problem was solved on the simulator by using an existing link from the EAI 8400 digital computer to the 1819A.

2. System Operation

Automatic and flight director operation was investigated by simply replacing the previous airspeed error signal with a suitably scaled flight reference error. Rate and displacement gains were suitably adjusted based on closed loop analysis. Because the basic Sperry STOLAND autopilot and

flight director software were essentially unified it was not necessary to deal with two components of software separately in order to make the system operable.

Autopilot and flight director loops implemented using the basic STOLAND system did produce problems. At the outset it was not clear whether these problems were (i) a result of a basic incompatibility of the preferred manual flight reference with autopilot and flight director operation, or (ii) connected with the specific STOLAND autopilot and flight director being modified.

The main problem encountered involved a limit cycle during an autopilot-controlled approach. The limit cycle produced an engine rpm excursion of approximately $\pm 0.5\%$ which coupled with the flight reference. This ultimately prevented tightening the flight reference loop to the desired level.

It was subsequently found that the thrust response involved not only lags but also a sizable deadband. Effective thrust response could be improved through the use of augmentor wing chokes (essentially a direct lift control), but that feature was not available on the particular STOLAND software being used for this program.

Another problem arose in connection with the STOLAND flight director. Specifically, the flight director command bar was slow in responding to a flight reference error. Thus, the pilot frequently elected to disable the flight director during large wind shear disturbances and proceed under manual control. (Reversion to manual control, however, was accomplished without difficulty.)

The original flight director was designed to control airspeed error, a low frequency regulation task. On the other hand, the flight reference error being sent to the director in place of airspeed was normally regulated at a relatively high frequency (see Subsection F). Thus, to solve the problem of slow response would have required modification of the basic flight director software — a task beyond the scope of this program.

To summarize, for both of the operational problems described here there was no fundamental incompatibility among manual, automatic, and

flight director operation using a safety margin system. There were only those incompatibilities relating to the specific software available.

F. EVALUATION OF A REFINED SYSTEM CONFIGURATION

Based on the results of the simulator experiments and analyses performed, a refined safety margin system was configured and evaluated. The refined system represented a reasonable compromise among the various factors considered important. The major compromises included:

- Enhanced direct flight reference control response at the expense of displaying true safety margin as the flight reference.
- Diminished $\gamma - \theta$ cross coupling at the expense of utilizing the maximum allowable low speed flight envelope.
- Availability of exact safety margin status at the expense of the increased display complexity of an auxiliary safety reference.

1. System Description

The system thus established is described in Table IV-3. It was composed of a flight reference and safety reference combination. Both functions were based on dynamic safety margin. The safety reference was equivalent to dynamic safety margin exactly; the flight reference contained an additional function of pitch attitude to enhance manual and automatic controllability.

The system design was based on the following principles. First, dynamic safety margin should be a predominant component of the flight reference. To the extent that DSM fails to provide adequate controllability, equalization should be added in a way that retains as much of the safety margin status information as possible. Finally, when the flight reference does depart from DSM, it should be backed up by an explicit safety reference which can be easily monitored.

TABLE IV-3
REFINED SAFETY MARGIN SYSTEM

FLIGHT REFERENCE (AUTOMATIC AND MANUAL):

$$\begin{aligned} FR &= FR[DSM+k_g \theta] \\ &= \min (FR_1, FR_2) \end{aligned}$$

$$FR_1 = \frac{DSM_1 + g(\theta)}{0.5 s + 1}$$

$$FR_2 = \frac{DSM_2 + g(\theta)}{0.5 s + 1}$$

where $DSM_1 = 100\% \times \frac{V - V_{min_m}}{20 kt}$

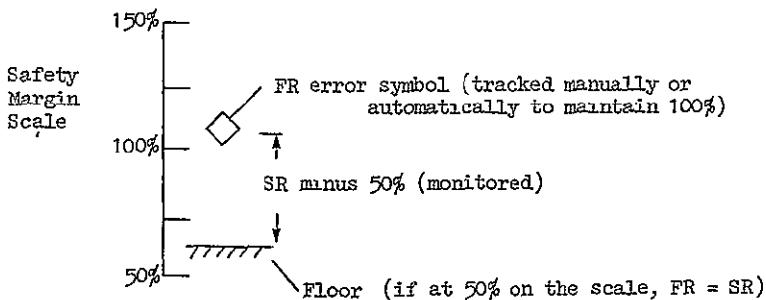
$$DSM_2 = 100\% \times \frac{\alpha_{max} - \alpha}{\sin^{-1} \frac{20 kt}{V}}$$

$$g(\theta) = -10 \frac{\%}{deg} \times (\theta + 5.83 deg)$$

SAFETY REFERENCE:

$$SR = \min (DSM_1, DSM_2)$$

DISPLAY FORMAT:



REPRODUCIBILITY OF THE
ORIGINAL PAGE IS POOR

One of the key factors in determining the flight reference form used, $DSM + k_{\theta} (\theta - \theta_0)$ (which we shall refer to as $FR[DSM+k_{\theta}\theta]$), was that essential DSM dynamics could be observed simply by the pilot's holding his pitch attitude — itself the primary flight reference control. On the other hand, if the pilot were closing a loop on flight reference, the $k_{\theta}\theta$ term would tend to dominate the response and provide something that approaches a simple proportional control (i.e., $\frac{FR}{\theta} \doteq K$). This latter feature would also lessen the disparity between the two critical safety margin conditions.

It was established earlier in the experimental program that in the high thrust region, $FR[DSM+k_{\theta}\theta]$ would alleviate $\gamma - \theta$ cross coupling if the k_{θ} could be set sufficiently high without encountering excessive sensitivity. This, in fact, was the determining factor in the value of k_{θ} picked for the refined system, $-10\%/deg$.

The other parameter, θ_0 , was chosen specifically to guarantee that $FR = 100\%$ would always be greater than or equal to $DSM = 100\%$. Thus θ_0 corresponded to the pitch attitude at the intersection of the 100% DSM trajectory and the minimum required flight path angle (steepest trim approach flight path minus 4 deg for the flight path control power). In this case θ_0 equaled -5.83 deg at $DSM = 100\%$ and $\gamma = -11.5$ deg (trim γ is -7.5) as shown in Fig. IV-5.

Other features of the refined system which resulted from the chosen values of k_{θ} and θ_0 included:

- A controlled element transfer function that was nearly the same in both the speed-margin-critical and vertical-gust-margin-critical regions.
- A loss of available low speed flight envelope equal to about 25% DSM or 5 kt
- Approximately one-half the DSM regulation effectiveness compared to tracking DSM directly.

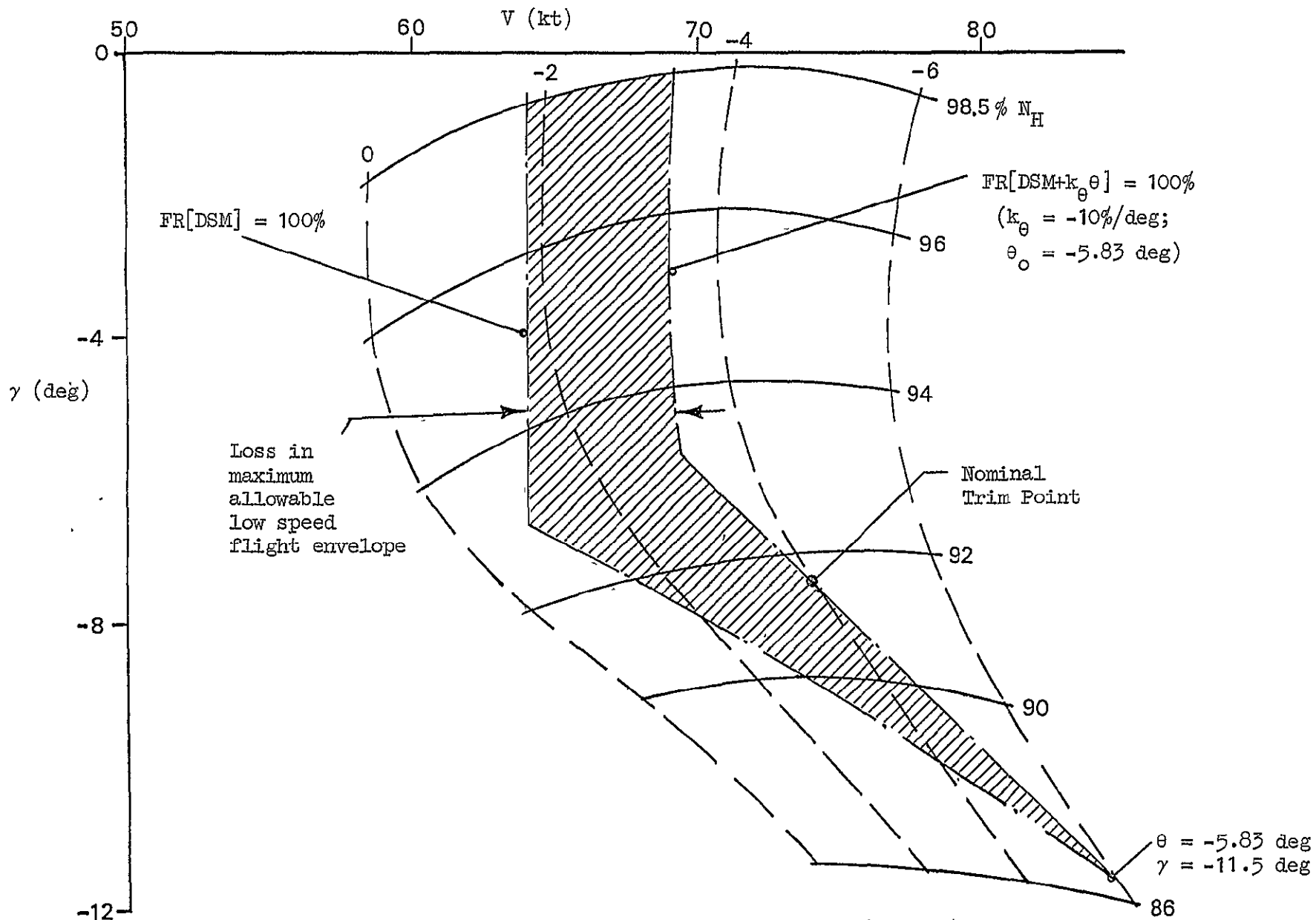


Figure IV-5. $\gamma - V$ Plot Showing Trajectory for $FR[DSM+k_{\theta}\theta] = 100\%$

2. System Analysis

Prior to discussing simulator results for the refined system we shall describe some of its features which are made visible by linear system analysis.

The controllability of the flight reference is indicated by the numerator N_{θ}^{FR} which can be approximated for the two critical safety margin conditions by the following expressions:

For speed margin critical:

$$N_{\theta}^{FR} = k_{\theta} \left\{ s^2 + \left[\frac{k_u^*}{k_{\theta}} (X_{\alpha} - g) - X_u - Z_w \right] s + \frac{k_u^*}{k_{\theta}} g Z_w + X_u Z_w - X_w Z_u \right\}$$

For vertical gust margin critical (assuming that k_w^* is the dominant DSM partial derivative):

$$N_{\theta}^{FR} = k_{\theta} \left(1 + \frac{k_w^* V}{k_{\theta}} \right) \left\{ s^2 + \left[-\frac{Z_w}{1 + \frac{k_w^* V}{k_{\theta}}} - X_u \right] s + \frac{\frac{-k_w^*}{k_{\theta}} g Z_u + X_u Z_w - X_w Z_u}{1 + \frac{k_w^* V}{k_{\theta}}} \right\}$$

With nominal stability derivative values substituted into these expressions,

$$N_{\theta}^{FR} = -10[0.87; 0.39]\%/deg$$

and $= -16[0.70; 0.27]\%/deg$, respectively.

Aside from the numerical similarity it was also significant that both of the numerators contained a complex pair of zeros with a high damping ratio. Thus, unlike an angle-of-attack-like system, the flight reference could be aggressively tracked without an oscillatory tendency.

The refined system had the potential for partially maintaining dynamic safety margin through regulation of flight reference. The measure of closed loop effectiveness (explained in Appendix C) is the following:

$$1 - \frac{N_{u_g}^{FR} N_{\theta}^{DSM}}{N_{u_g}^{DSM} N_{\theta}^{FR}}$$

Referring to Table III-2, we can see that

$$N_{u_g}^{FR} = N_{u_g}^{DSM} \quad \text{for} \quad FR = DSM + k_{\theta} \theta$$

also

$$N_{\theta}^{FR} = N_{\theta}^{DSM} + k_{\theta} \Delta$$

thus,

$$1 - \frac{N_{u_g}^{FR} N_{\theta}^{DSM}}{N_{u_g}^{DSM} N_{\theta}^{FR}} = \frac{k_{\theta} \Delta}{N_{\theta}^{FR}}$$

For both critical margin conditions the $DSM + k_{\theta} \theta$ flight reference appeared to be equally effective — about 50% of the effectiveness of a pure DSM flight reference as shown in Fig. IV-6.

3. Simulator Results

The results from the simulator evaluation of the refined safety margin system configuration generally corresponded to the features described analytically above.

The controllability was, in fact, judged by the evaluation pilot to be much easier than for the basic DSM flight reference. The pilot clearly perceived the nearly one-to-one correspondence between pitch attitude and flight reference and took advantage of it by closing a significantly tighter loop than with FR[DSM]. The crossover frequencies inferred from measurements of pilot gain were approximately 0.15 rad/sec for FR[DSM] and approximately 0.75 rad/sec for FR[DSM+k_θ]. In other words, the flight reference was not regulated in the usual low frequency outer loop sense. Instead, the flight reference was treated more like a flight director command and tracked nearly as tightly as pitch attitude itself. The primary evaluation pilot characterized the ease of flying the Augmentor

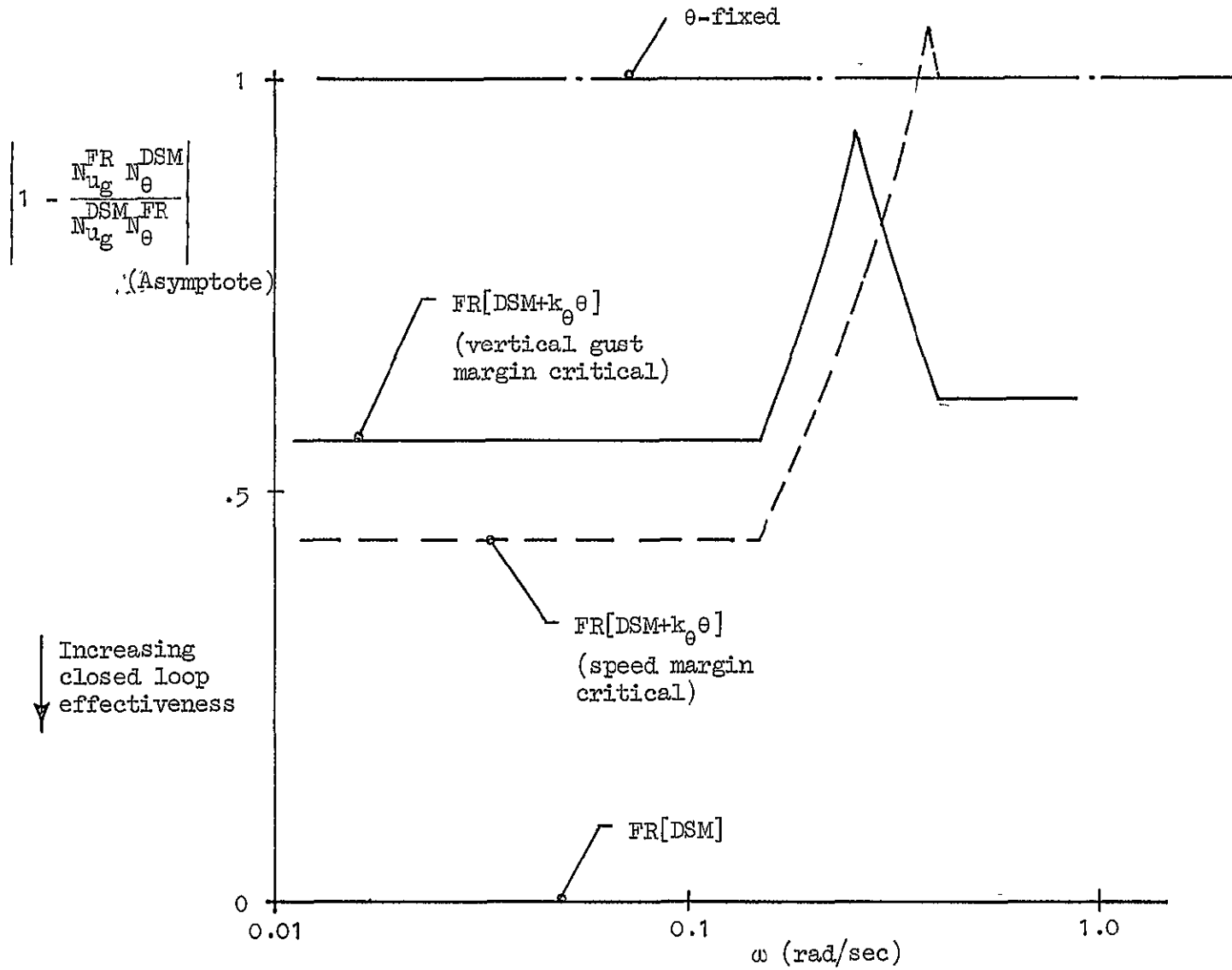


Figure IV-6. Relative Effectiveness of $FR[DSM+k_{\theta}]$ in Maintaining Dynamic Safety Margin

Wing aircraft using $FR[DSM+k_{\theta}]$ as being comparable to flying a CTOL airplane in the approach using raw data (glide slope and indicated airspeed).

The safety reference was considered to be an important part of the safety margin system. The evaluation pilot commented that he could use the SR indication to reduce the amount of pitch attitude commanded by cross-checking SR against FR. If the safety reference indicated that safety margins were within bounds, then the pilot might choose to ignore a given flight reference error and simply hold his attitude. The level of disparity between FR and SR, therefore, was not excessive.

The precision of regulating DSM via the $FR[DSM+k_{\theta}]$ was not adequately determined in the presence of wind shear. With the FR loop closed, some reduction in DSM excursions was discernible; but the high frequency components of disturbances (which could not be well regulated) interfered with obtaining statistically significant measurements. Such measurements would require larger samples of wind shear encounters and pilot subjects than were possible in this program.

Therefore, it was necessary to infer potential effects on DSM precision by combining some results of the analysis with measured pilot loop gains. Figure IV-7 shows the comparative effectiveness of $FR[DSM+k_{\theta}]$ in minimizing DSM excursion in horizontal wind shears. Combine Fig. IV-7 with the fact that crossover frequencies inferred from measured pilot loop gains were approximately 0.15 rad/sec using $FR[DSM]$ and 0.75 rad/sec using $FR[DSM+k_{\theta}]$; therefore, a reasonable benefit of $FR[DSM+k_{\theta}]$ could be directly measured in terms of precision, given an adequate sample.

4. Departure From a Fixed Configuration System

Brief consideration was given to how easily the results of the fixed configuration experiment conducted here could be extended to a wider range of operating conditions. Utilization of the nozzle control was especially of interest.

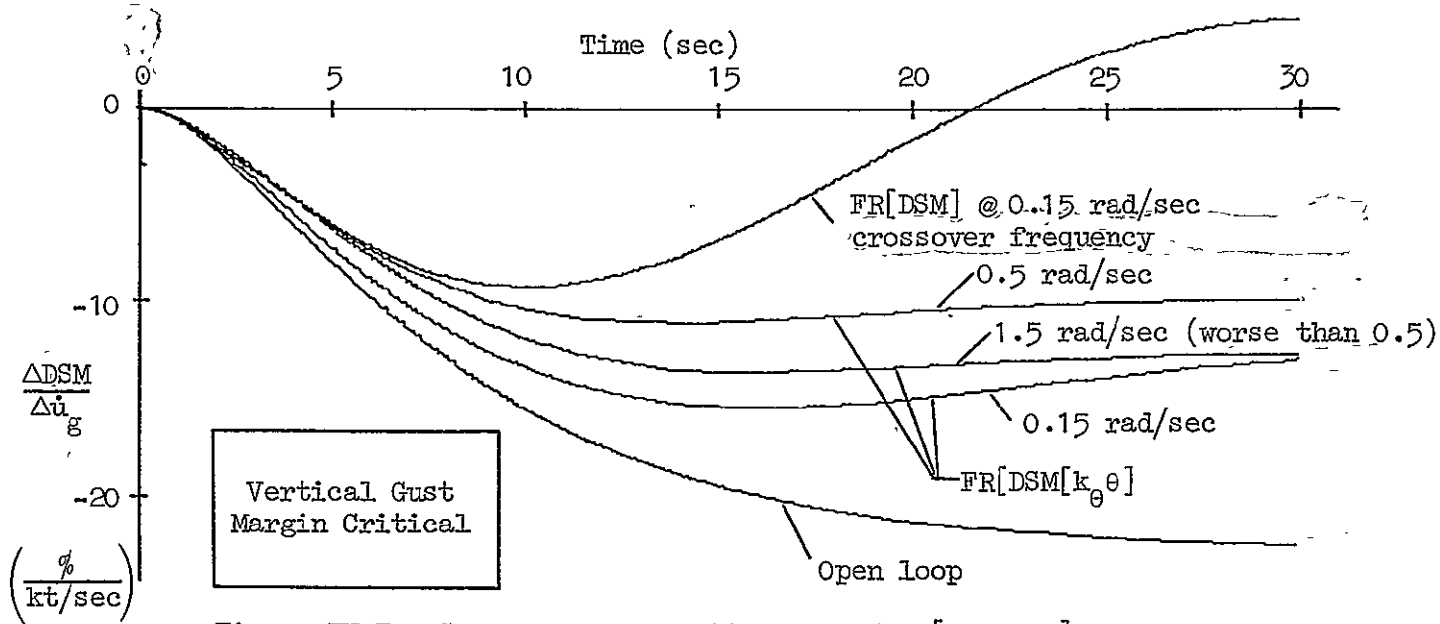
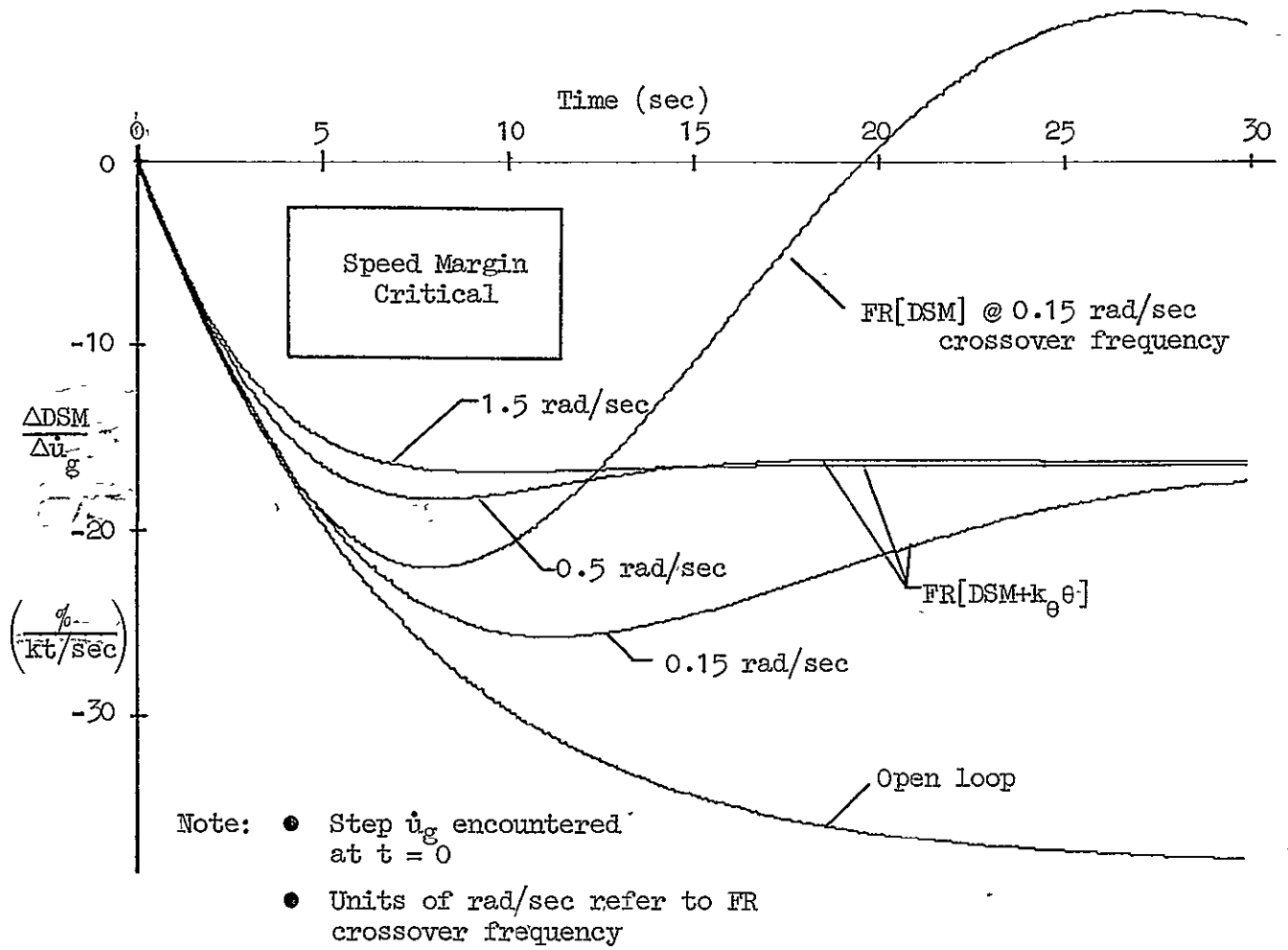
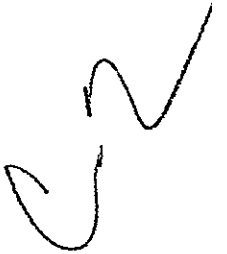


Figure IV-7. Comparative Effectiveness of FR[DSM+k_θ] in Regulating DSM in Wind Shears

The impact of varying configuration was inferred by considering the various parameters involved:

- V_{\min_m}
- $\alpha_{\max} (N_H)$
- k_θ
- θ_o

For variations in nozzle deflection about the 70 deg trimmed angle used here, none of the above parameters appeared sensitive. V_{\min_m} and $\alpha_{\max} (N_H)$ were assumed invariant because of the relatively indirect effect of nozzle on aerodynamic stall. k_θ was set on the basis of controllability and therefore not related to nozzle. Finally, θ_o was determined from trimming at $\gamma = -11.5$ deg and DSM = 100% for ± 20 deg nozzle deflection and found to vary only ± 0.3 deg. On the other hand, variation of flap deflection could be expected to have a direct impact on V_{\min_m} and α_{\max} and thus require scheduling of parameters. Gross weight, likely, would affect only V_{\min_m} .



SECTION V

CONCLUSIONS AND RECOMMENDATIONS

A. SUMMARY OF SYSTEM OBJECTIVES AND DESIGN CONSTRAINTS

The purpose of a powered-lift airplane safety margin system is to enable maximum use of the allowable low speed flight envelope with reasonable ease of control. Factors which contribute to the effectiveness include precision in maintaining safety margins under adverse conditions and the quality of safety margin status information. Consideration must also be given to compatibility between manual and automatic operation and the cost and ease of implementation.

In this study we found that it was necessary to strike a compromise among all of the design objectives and considerations mentioned above, but that acceptable compromises were, in fact, possible.

The degree of acceptability depended upon observing a number of important constraints:

- The normal guides of controllability apply to the flight reference — pitch attitude relationship which includes (i) direct response resembling a pure gain or rate command, (ii) minimum of adverse cross coupling with other controls, and (iii) absence of a PIO tendency if aggressively tracked.
- Effective elimination of adverse cross coupling between pitch attitude and flight path angle (a nose-down correction required for upward flight path change) proved to be the most troublesome constraint and required a reduction in the allowable low speed flight envelope.
- The flight reference itself cannot differ substantially from the dynamic safety margin in its sensitivity to

gusts without confusing the pilot. Also, the use of a safety reference is not acceptable unless there is a reasonable correspondence between the flight reference and the safety reference.

- The value of a safety margin system is questionable unless appropriate variables are sensed. If an airspeed margin criterion is involved, then relative airspeed must be supplied as an input; correspondingly, if an angle of attack or vertical gust margin is involved, then an angle of attack sensor must be employed. Inertial velocity inputs alone are inadequate in both cases.

B. DEFINITION OF RECOMMENDED SAFETY MARGIN SYSTEM

The safety margin system ultimately developed in this study and found to be effective in meeting all objectives consisted of a combination display of flight reference (for tracking) and safety reference (for monitoring).

The flight reference was composed of a linear combination of dynamic safety margin and pitch attitude with mild low pass filtering.

$$FR = \frac{DSM + k_{\theta} (\theta - \theta_0)}{(T_f s + 1)}$$

$$\text{where } k_{\theta} = -10\%/deg$$

$$\theta_0 = -5.83 \text{ deg}$$

$$\text{and } T_f = 0.5 \text{ sec}$$

The parameter k_{θ} was used to enhance controllability at the expense of losing allowable low speed flight envelope. The absolute usable range of k_{θ} was found to be $-15\%/deg$ to zero. The parameter θ_0 was set for a given k_{θ} and minimum required flight path angle. Specifically, θ_0 was equal to

the trim pitch attitude at the minimum flight path angle. (In this case $\theta_0 = -5.83$ deg for $\gamma = -11.5$ deg.)

The safety reference was set exactly equal to dynamic safety margin:

$$SR = DSM$$

A sliding floor display was used in order to displace the SR symbol from the FR symbol. (The value of SR corresponded directly to the distance between the FR and SR symbols.)

Two colored lights adjacent to the FR-SR display were used to indicate the instantaneous critical safety margin — airspeed or angle of attack. This was auxiliary information, but judged useful by the pilot for modifying throttle-to-pitch-attitude crossfeed strategy.

The autopilot loop structure was made to correspond to the manual control strategy ($FR \rightarrow \theta_c$ and $\epsilon_{GS} \rightarrow \delta$).

C. SYSTEM BENEFITS

A number of significant benefits were confirmed both for the general concept of a safety margin system and for the specific design ultimately developed.

- The safety margin system flight reference represents a rational approach to combining multiple margin criteria in a single, normalized indication — this is useful in both manual and automatic operation.
- The safety reference, implemented as a sliding "floor," provides a useful means of monitoring actual safety margin status while tracking a flight reference — also useful in both manual and automatic operation.
- The flight reference ultimately developed ($FR = DSM + k_\theta (\theta - \theta_0)$) offers the advantage that the pilot is always assured of taking correct action when

tracking FR with θ_c , thus he is less inclined to do the wrong thing. Response is rapid, well behaved, and similar in both high thrust and low thrust conditions.

- A minimal number of parameters are involved in the above flight reference, only k_θ and θ_c aside from the definition of DSM itself. Each can be rationally chosen to trade off maximizing the usable low speed flight envelope against ease of control.
- The scheme employed in the NASA Augmentor Wing airplane at a fixed configuration and loading appears to be directly usable for other nozzle deflections, and usable with minor adjustments at other gross weights and flap deflections. Further, the same scheme should be applicable to other powered-lift aircraft for which a backside piloting technique is used.
- If the safety margin excursions can be shown to be improved significantly through use of a safety margin system, it may permit the use of reduced safety margin criteria. This potential benefit was not adequately demonstrated in this study, however.

D. IMPLEMENTATION CONSIDERATIONS

The essential parts of the system described under Heading B were implemented in the existing Augmentor Wing STOLAND system with minor impact.

- Digital computer core storage and cycle time requirements were insignificant — less than 0.6% capacity was utilized and simple arithmetic functions employed (+, ×, ÷).
- For the EADI display it was necessary to borrow an existing line for the SR symbol (in this case the runway perspective was used).

- ⊙ Angle of attack with respect to air mass is currently not an input to STOLAND and would be required in an actual implementation.
- ⊙ An effective system could be configured with a simpler form than that used here with small compromises in the usable flight envelope.

E. RECOMMENDATIONS FOR FURTHER STUDY

Continued study of the safety margin system concept leading to a flight test evaluation is recommended. Based on the results of this feasibility study, a safety margin system offers important benefits in the operation of powered-lift vehicles with minimal added complexity in hardware and software implementation.

The specific tasks which should be carried out in any future work are:

1. Conduct simulator tests to obtain statistically significant measures of safety margin precision for $FR[DSM]$ and $FR[DSM+k_0\theta]$ compared to constant pitch attitude as a baseline. Utilize several pilot subjects to cover likely ranges of piloting technique, precision, and workload capacity.
2. Conduct an additional simulator study to explore the benefits of further optimization and refinement of $FR[DSM+k_0\theta]$ with respect to flight envelope loss versus ease of control, safety margin status, and precision of maintaining safety margins. Again, consider several pilot subjects.
3. Implement the further refined safety margin system obtained from (2) in suitable autopilot and flight director systems and investigate their properties, performance, and potential benefits. In particular, determine whether a longitudinal flight director based on $FR[DSM+k_0\theta]$ offers any advantage over direct regulation of an explicit display of $FR[DSM+k_0\theta]$.

4. Expand the further refined safety margin system concept from (2) and (3) to cover a useful range of airplane configurations, loadings, and atmospheric conditions. Verify operation by simulation.
5. Design a series of experiments to demonstrate the capabilities of the final safety margin system configuration in flight using the NASA Augmentor Wing airplane. Explore possible benefits during visual approaches as well as instrument approaches. Fully exploit naturally-occurring adverse atmospheric disturbances, and, if possible, introduce artificial disturbances, using the STOLAND computer in conjunction with x- and z-force generators.
6. Utilizing the developments of this program, consider safety margin system applications to conventional and VTOL aircraft as well as to STOL aircraft operating in other flight regimes employing other powered-lift concepts, or involving other piloting techniques.

It is believed that use of an effective safety margin system can contribute significantly to the overall safety and ease of operation of complex aircraft. The work reported here illustrates this and, further, serves as a point of departure for either the implementation of a flight test system package or the generalization to other powered-lift aircraft situations.

REFERENCES

1. Scott, Barry C., Paul W. Martin, Charles S. Hynes, and Ralph B. Bryder, Progress Toward Development of Civil Airworthiness Criteria for Powered-Lift Aircraft, FAA-RD-76-100 (NASA TM X-73,124), May 1976.
2. Innis, Robert C., Curt A. Holzhauser, and Hervey C. Quigley, Airworthiness Considerations for STOL Aircraft, NASA TN D-5594, Jan. 1970.
3. Allison, R. L., M. Mack, and P. C. Rumsey, Design Evaluation Criteria for Commercial STOL Transports, NASA CR-114454, June 1972.
4. Heffley, Robert K., Robert L. Stapleford, and Robert C. Rumold, Airworthiness Criteria Development for Powered-Lift Aircraft, NASA CR-2791 (FAA-RD-76-195), Feb. 1977.
5. Heffley, Robert K., John M. Lehman, Robert C. Rumold, Robert L. Stapleford, Barry C. Scott, and Charles S. Hynes, A Simulator Evaluation of Tentative STOL Airworthiness Criteria. Simulation Results and Analysis (Final Report), NASA TM X-73,093 (FAA-RD-75-222), Nov. 1975; Heffley, Robert K., John M. Lehman, Robert L. Stapleford, Barry C. Scott, and Charles S. Hynes, A Simulator Evaluation of Tentative STOL Airworthiness Criteria. Background Information (Final Report), NASA TM X-73,094 (FAA-RD-75-222), Nov. 1975.
6. Stapleford, Robert L., The Conceptual Design of a Safety Margin System for the Augmentor Wing, Systems Technology, Inc., TR-1073-1, Jan. 1976.
7. Key, David L., Review of the Yellow Book and Suggested New Regulatory Format for Tentative Airworthiness Standards for Powered Lift Transport Category Aircraft, Part XX, Subpart B — Flight (Final Report), Calspan Report No. TB-3011-F-3, Sept. 1973.
8. McRuer, Duane, Irving Ashkenas, and Dunstan Graham, Aircraft Dynamics and Automatic Control, Princeton University Press, Princeton, N. J., 1973.
9. Grgurich, John, and Peter Bradbury, STOLAND Final Report, NASA CR-137972, Nov. 1976.
10. Hoh, Roger H., and Wayne F. Jewell, Investigation of the Vulnerability of Powered Lift STOL's to Wind Shear, Systems Technology, Inc., TR-1063-1, Oct. 1976.
11. Wingrove, Rodney C., Comparison of Methods for Identifying Pilot Describing Functions from Closed-Loop Operating Records, NASA TN D-6235, Mar. 1971.

APPENDIX A

AERODYNAMIC CHARACTERISTICS OF THE NASA AUGMENTOR WING AIRPLANE

The characteristics of the airplane involved in this study are summarized here. The numerical values were derived directly from the STOLAND Augmentor Wing simulator model used in the experimental phase.

A fixed configuration and loading were assumed, specifically:

Weight	40,000 lb
cg	FS 341.2
Flap Deflection	65 deg
Nozzle Deflection	70 deg
Atmosphere	sea level, standard day
Maximum engine rpm	98.5%
Pitch, roll, and yaw SAS	on

The essential longitudinal aerodynamic stability derivatives relevant to the study are listed in Table A-1. In cases where approximate factors were used to compute aircraft and flight reference dynamics, the following set of representative stability derivatives were assumed:

$$X_u = -.07 \text{ (1/sec)}$$

$$X_w = 0.10 \text{ (1/sec)}$$

$$Z_u = -.30 \text{ (1/sec)}$$

$$Z_w^{\text{eff}} = -.50 \text{ (1/sec)}$$

$$X_\delta = 0$$

$$Z_\delta = -2 \text{ (ft/sec}^2\text{/}\%)$$

$$V = 120 \text{ ft/sec}$$

PRECEDING PAGE BLANK NOT FILMED

TABLE A-1

BASIC FLIGHT CONDITION PARAMETERS — NASA AUGMENTOR WING AIRPLANE
(40,000 lb, Sea Level Standard Day, Flaps 65 deg, Nozzles 70 deg)

DSM (%)	100(A) [†]	→			100(B) ^{††}	→			125	126	118.6
FR* (%)	58.1	58.9	56.1	58.0	85.5	100(B)	100(A) ^{†††}	→	100(B)		
γ (deg)	0	-2.5	-5.0	-7.5	-10	-11.5	-2.5	-5	-7.5		
V (kt)	64	→			68.3	79	84.5	69.0	69.1	74.2	
N _H (%)	101.0	96.83	94.29	91.69	88.43	86.37	96.06	93.79	91.38		
θ (deg)	-1.64	-1.72	-1.44	-1.63	-4.30	-5.83	-3.39	-3.13	-4.0		
α (deg)	-1.64	.78	3.56	5.87	5.70	5.67	-0.89	1.87	3.50		
α _{max} (deg)	(26.84)	(25.44)	(24.52)	22.88	20.48	19.3	(24.40)	(23.56)	22.05		
X _u (1/sec)	-0.056	-0.059	-0.064	-0.068	-0.087	-0.091	-0.064	-0.069	-0.074		
X _w (1/sec)	.083	.103	.096	.115	.112	.112	.091	.096	.120		
Z _u (1/sec)	-0.250	-0.283	-0.317	-0.315	-0.294	-0.317	-0.244	-0.255	-0.302		
Z _w [†] (1/sec)	-0.574	-0.561	-0.503	-0.526	-0.560	-0.570	-0.572	-0.531	-0.555		
X _δ ** (ft/sec ² -deg)	.0683	.0959	.0727	-0.0103	-0.0114	.0086	.1268	.1067	.0446		
Z _δ (ft/sec ² -deg)	-0.308	-0.602	-0.939	-1.381	-1.059	-1.055	-0.739	-1.109	-1.367		

*FR = DSM - 10 (θ + 5.83 deg)

** $(\partial N_H / \partial \delta)$ = .722%/deg

†† (A) implies critical airspeed margin, (B) critical vertical gust margin

APPENDIX B

SUMMARY OF MULTILOOP SYSTEM RELATIONSHIPS

The following is a summary of multiloop system relationships that were useful in the closed loop pilot-vehicle analysis performed in this study. For a more complete treatment the reader should consult Chapter 3-5 of Ref. B1.

Consider the following example of a set of linearized equations of motion involving four states and three controls (or disturbances):

$$\begin{bmatrix} a_{11}(s) & a_{12}(s) & a_{13}(s) & a_{14}(s) \\ a_{21}(s) & a_{22}(s) & a_{23}(s) & a_{24}(s) \\ a_{31}(s) & a_{32}(s) & a_{33}(s) & a_{34}(s) \\ a_{41}(s) & a_{42}(s) & a_{43}(s) & a_{44}(s) \end{bmatrix} \begin{bmatrix} x_1(s) \\ x_2(s) \\ x_3(s) \\ x_4(s) \end{bmatrix} = \begin{bmatrix} b_{11}(s) & b_{12}(s) & b_{13}(s) \\ b_{21}(s) & b_{22}(s) & b_{23}(s) \\ b_{31}(s) & b_{32}(s) & b_{33}(s) \\ b_{41}(s) & b_{42}(s) & b_{43}(s) \end{bmatrix} \begin{bmatrix} \delta_1(s) \\ \delta_2(s) \\ \delta_3(s) \end{bmatrix}$$

Note that each element in the above matrices can be a polynomial of s .

The characteristic determinant is given by:

$$\Delta(s) = \det \begin{bmatrix} a_{11} & a_{12} & a_{13} & a_{14} \\ a_{21} & a_{22} & a_{23} & a_{24} \\ a_{31} & a_{32} & a_{33} & a_{34} \\ a_{41} & a_{42} & a_{43} & a_{44} \end{bmatrix}$$

Examples of numerators and coupling numerators are:

$$N_{\delta_1}^{x_1}(s) = \det \begin{bmatrix} b_{11} & a_{12} & a_{13} & a_{14} \\ b_{21} & a_{22} & a_{23} & a_{24} \\ b_{31} & a_{32} & a_{33} & a_{34} \\ b_{41} & a_{42} & a_{43} & a_{44} \end{bmatrix} \quad (\text{Type 0 numerator})$$

$$N_{\delta_1 \delta_3}^{x_1 x_4}(s) = \det \begin{bmatrix} b_{11} & a_{12} & a_{13} & b_{13} \\ b_{21} & a_{22} & a_{23} & b_{23} \\ b_{31} & a_{32} & a_{33} & b_{33} \\ b_{41} & a_{42} & a_{43} & b_{43} \end{bmatrix} \quad (\text{Type 1 numerator})$$

$$N_{\delta_3 \delta_1 \delta_2}^{x_2 x_4 x_1}(s) = \det \begin{bmatrix} b_{12} & b_{13} & a_{13} & b_{11} \\ b_{22} & b_{23} & a_{23} & b_{21} \\ b_{32} & b_{33} & a_{33} & b_{31} \\ b_{42} & b_{43} & a_{43} & b_{41} \end{bmatrix} \quad (\text{Type 2 numerator})$$

The largest type coupling numerator is limited by the number of independent variables such as controls and gust disturbances — e.g., Type 1 is the maximum for one control and one disturbance or two controls, Type 2 is the maximum for two controls and one disturbance or three controls, etc.

Also, by way of example, useful numerator identities include:

$$\frac{x_1 x_2}{N_{\delta_1 \delta_2}} = \frac{x_2 x_1}{N_{\delta_2 \delta_1}} = -\frac{x_1 x_2}{N_{\delta_2 \delta_1}}$$

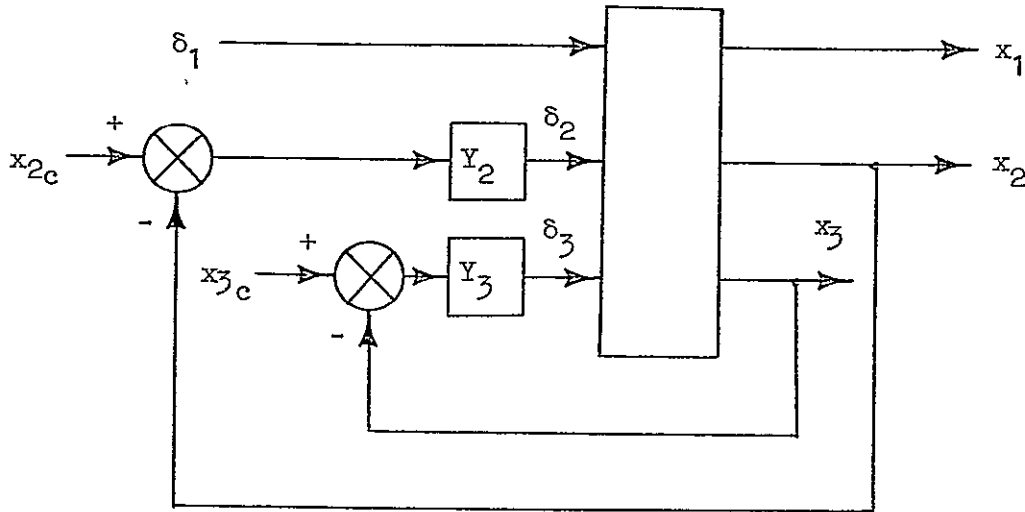
$$\frac{x_1 x_1}{N_{\delta_1 \delta_2}} = \frac{x_1 x_2}{N_{\delta_1 \delta_1}} = 0$$

$$\frac{x_1 x_2}{N_{\delta_1 \delta_2}} = \frac{\det \begin{bmatrix} x_1 & x_1 \\ N_{\delta_1} & N_{\delta_2} \\ x_2 & x_2 \\ N_{\delta_1} & N_{\delta_2} \end{bmatrix}}{\Delta} = \frac{1}{\Delta} \left(\begin{matrix} x_1 & x_2 \\ N_{\delta_1} & N_{\delta_2} \end{matrix} - \begin{matrix} x_1 & x_2 \\ N_{\delta_2} & N_{\delta_1} \end{matrix} \right)$$

$$\frac{x_1 x_2 x_3}{N_{\delta_1 \delta_2 \delta_3}} = \frac{\det \begin{bmatrix} x_1 & x_1 & x_1 \\ N_{\delta_1} & N_{\delta_2} & N_{\delta_3} \\ x_2 & x_2 & x_2 \\ N_{\delta_1} & N_{\delta_2} & N_{\delta_3} \\ x_3 & x_3 & x_3 \\ N_{\delta_1} & N_{\delta_2} & N_{\delta_3} \end{bmatrix}}{\Delta^2} = \frac{\begin{matrix} x_1 x_2 x_3 \\ N_{\delta_1} N_{\delta_2} \delta_3 \\ + N_{\delta_2} N_{\delta_3} \delta_1 \\ + N_{\delta_3} N_{\delta_1} \delta_2 \end{matrix}}{\Delta}$$

A more general description of the expansion of higher type coupling numerators is given in Ref. B2.

In order to appreciate the application of some of the foregoing numerators and coupling numerators, consider the following block diagram:



The following are examples of transfer functions involving multiloop feedbacks for this block diagram.

The exact x_1/δ_1 transfer function is:

$$\frac{x_1}{\delta_1} \Bigg|_{\substack{x_2 \rightarrow \delta_2 \\ x_3 \rightarrow \delta_3}} = \frac{N\delta_1 + Y_2 N\delta_2 \delta_1 + Y_3 N\delta_3 \delta_1 + Y_2 Y_3 N\delta_2 \delta_3 \delta_1}{\Delta + Y_2 N\delta_2 + Y_3 N\delta_3 + Y_2 Y_3 N\delta_2 \delta_3}$$

The x_1/δ_1 transfer function with x_2 and x_3 constrained by δ_2 and δ_3 , respectively, is:

$$\frac{x_1}{\delta_1} \Bigg|_{x_2, x_3} = \lim_{\substack{y_2 \rightarrow \infty \\ y_3 \rightarrow \infty}} \left(\frac{x_1}{\delta_1} \Bigg|_{\substack{x_2 \rightarrow \delta_2 \\ x_3 \rightarrow \delta_3}} \right) = \frac{N\delta_2 \delta_3 \delta_1}{N\delta_2 \delta_3}$$

APPENDIX B REFERENCES

- B1 McRuer, Duane, Irving Ashkenas, and Dunstan Graham, Aircraft Dynamics and Automatic Control, Princeton University Press, Princeton, New Jersey, 1973.
- B2 Hofmann, L. G., G. L. Teper, and R. F. Whitbeck, "Application of Frequency Domain Multivariable Control Synthesis Techniques to an Illustrative Problem in Jet Engine Control," Systems Technology, Inc., Paper No. 209, Presented at NEC International Forum on Multivariable Control, Chicago, Illinois, October 13-14, 1977.

PRECEDING PAGE BLANK NOT FILMED

APPENDIX C

DETAILED ANALYSIS OF FLIGHT REFERENCES BASED ON STATIC SAFETY MARGIN

In the following pages of this appendix various static safety margin combinations are analyzed in detail. The analysis results are the basis of the summary table in Section III.B.2.

Each static safety margin is a combination of the following measurable state variables or control variables. Note that some variables can be represented in several forms:

u_a	Airspeed
w_a	Body fixed vertical velocity or angle of attack relative to the air mass
\dot{d}	Inertial vertical velocity relative to flight path, flight path angle, or altitude rate
θ	Pitch attitude
δ	Thrust, throttle deflection, or engine rpm.

The analysis is based on the general methods outlined in Section III. The simplified longitudinal equations of motion shown in Table III-2 are used exclusively.

1. SSM_{u,w} (airspeed and angle of attack)

Under all conditions the SSM_{u,w} is nearly equivalent to the DSM as demonstrated by the linearized flight reference gains k_u and k_w in Table III-4.

2. $\underline{SSM}_{u,\theta}$ (airspeed and pitch attitude)

The $\underline{SSM}_{u,\theta}$ was considered to be the most promising flight reference substitute for dynamic safety margin, although the simulator evaluation ultimately revealed serious shortcomings.

For speed margin critical, $\underline{SSM}_{u,\theta}$ was exactly equivalent to DSM. But for vertical gust margin critical, $\underline{SSM}_{u,\theta}$ differed significantly from DSM and showed the promise of enhanced controllability over DSM. The following discussion is therefore limited to the condition of vertical gust margin critical.

Recall from Section III.B.1 that for the vertical gust margin critical, tracking DSM would produce a flight path overshoot condition. It was found that tracking the $\underline{SSM}_{u,\theta}$ would greatly improve the overshoot tendency as shown in Fig. C-1.

The reason for the improvement in closed loop flight path overshoot was traced to the closed loop denominator as characterized by

$$\Delta' = \Delta + Y_{FR} N_{\theta}^{FR}$$

The numerator, N_{θ}^{FR} , was the key factor. For FR = DSM we showed that the numerator contained low damping ratio second order zeros typical of angle of attack. i.e., for FR = DSM:

$$N_{\theta}^{FR} \doteq V k_w \left[s^2 - X_u s - \frac{g}{V} Z_u \right]$$

Using the k_u and k_{θ} relationships previously derived for the $\underline{SSM}_{u,\theta}$:

$$\begin{aligned} N_{\theta}^{FR} &\doteq V k_w \frac{g}{X_{\alpha}} \left[s^2 - Z_w s - X_w Z_u \right] \\ &\doteq V k_w \frac{g}{X_{\alpha}} \left(s - Z_w \right) \left(s - \frac{X_w Z_u}{Z_w} \right) \end{aligned}$$

- Note:
- Vertical gust margin critical
 - FR regulated with 0.15 rad/sec crossover frequency
 - Step ΔN_H applied

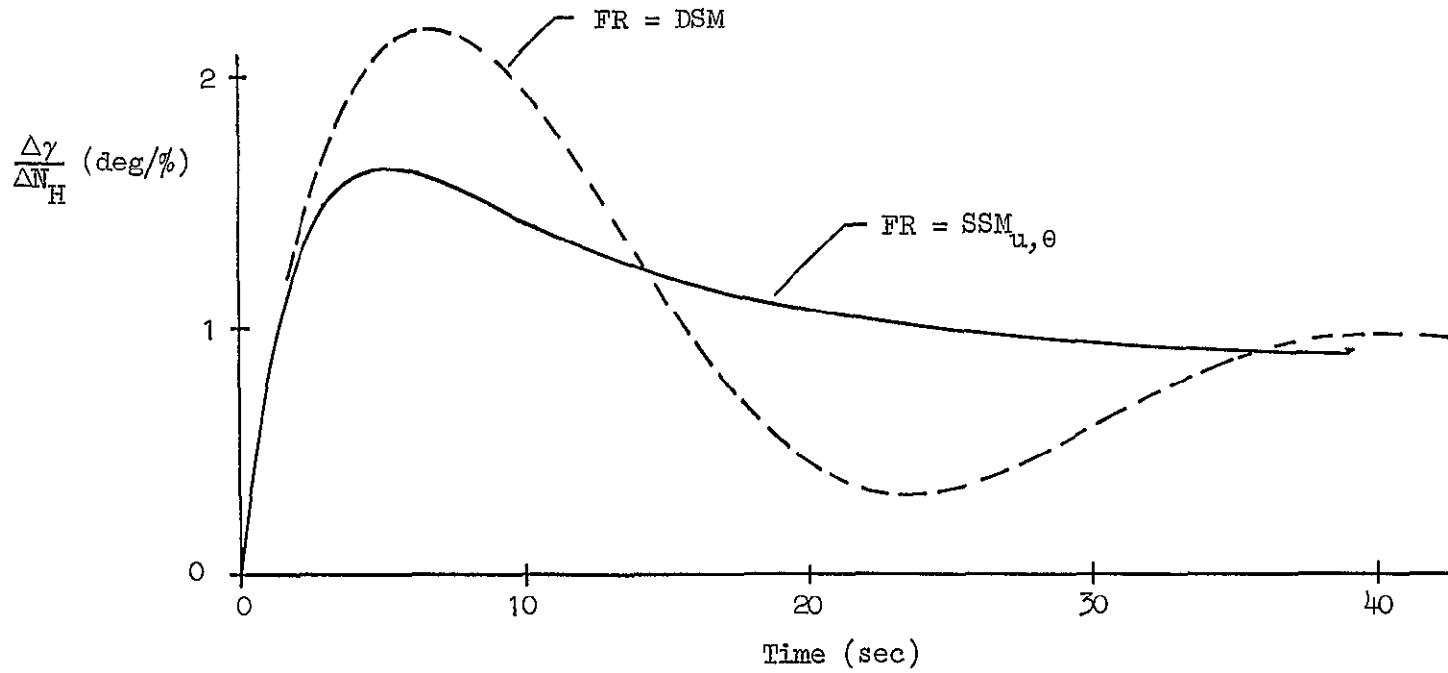


Figure C-1. Reduction in Flight Path Overshoot Using u-θ Static Safety Margin

Thus there is no oscillatory tendency in the $FR \rightarrow \theta_c$ loop with $FR = SSM_{u,\theta}$. This fact was of potential interest in the event that flight path overshoot using DSM was found to be a problem in the experimental investigation.

As for safety margin performance, the vertical-gust-margin-critical $SSM_{u,\theta}$ was found to be effective although less so than using DSM. For an input of a unit horizontal wind shear, \dot{u}_g , the following peak excursions were computed assuming $FR \rightarrow \theta_c$ at 0.15 rad/sec and $\epsilon_{GS} \rightarrow \delta$ at 0.5 rad/sec:

FLIGHT REFERENCE	PEAK DSM EXCURSION
DSM	-6%/kt/sec
$SSM_{u,\theta}$	-20%/kt/sec
Constant θ	-30%/kt/sec

The main shortcoming of using $SSM_{u,\theta}$ was its incorrect sensitivity to gusts when the vertical gust margin was critical. This was apparent from the flight reference gains themselves (Table III-4b).

FLIGHT REFERENCE	u_g SENSITIVITY	w_g SENSITIVITY
DSM	+0.7%/kt	-4.9%/kt
$SSM_{u,\theta}$	-3.3%/kt	0

For a horizontal gust a reverse margin indication would be produced initially and for a vertical gust there would be no initial indication. This is shown more completely by Fig. C-2. This was ultimately found to be the most unfavorable characteristic of this static safety margin formulation in the simulation experiments.

3. $SSM_{u,d}$ (airspeed and flight path angle)

This static safety margin formulation was found to be unacceptable purely on the basis that regulation using pitch attitude would destabilize the pilot-vehicle system. This was indicated by the presence of a positive real zero in the flight reference numerator, N_{θ}^{FR} .

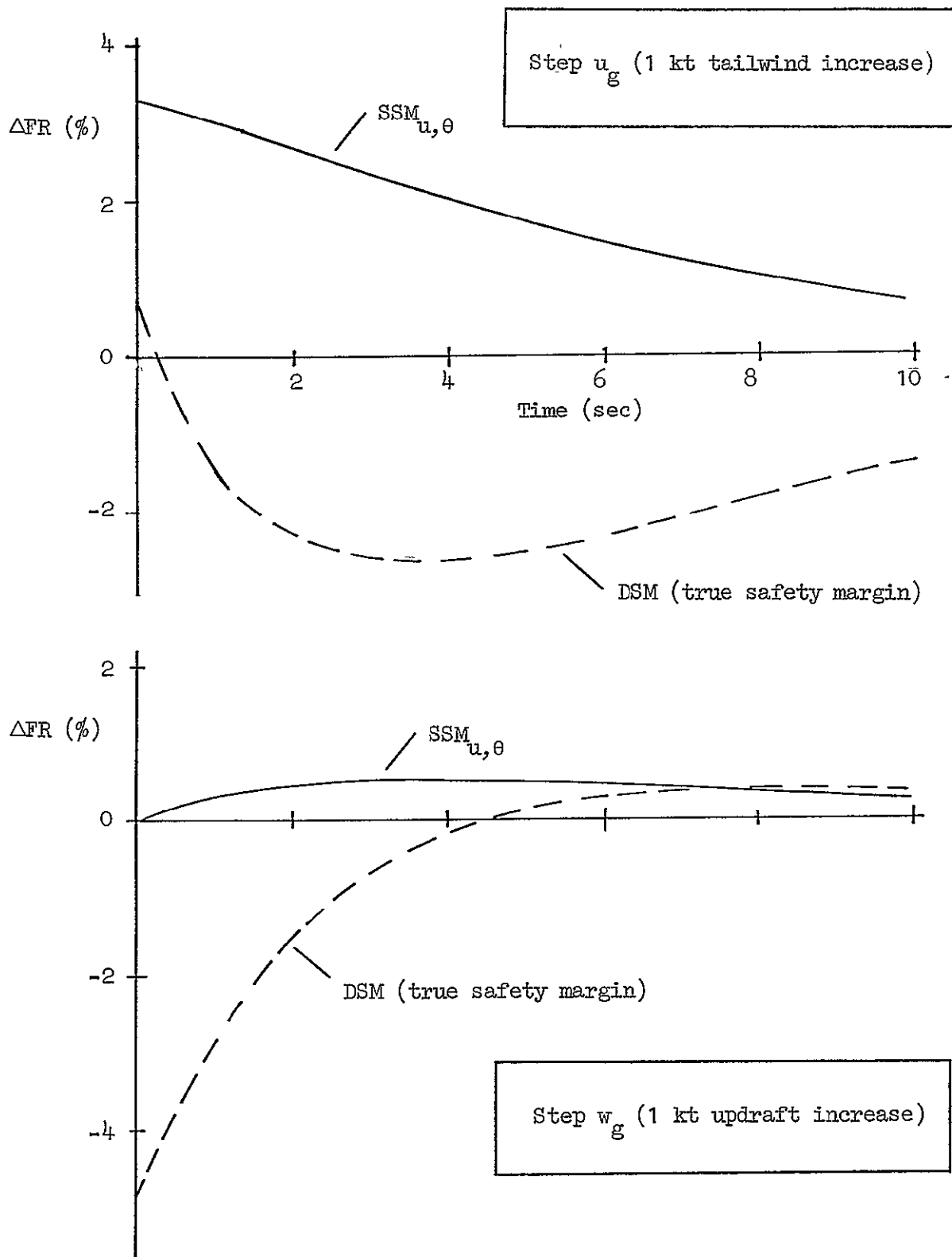


Figure C-2. Behavior of $SSM_{u,\theta}$ to Gusts with Pilot Holding Pitch Attitude Where the Vertical Gust Margin is Critical

Unfortunately, the positive real zero was shown to be a feature always present in $SSM_{u,d}$. Using the method demonstrated earlier, we estimated the k_u and k_d for $SSM_{u,d}$ and found:

$$k_u \doteq - \frac{k_w^* X_u V}{(X_\alpha - g)}$$

and
$$k_d \doteq \frac{k_w^* g}{(X_\alpha - g)}$$

Inserting these into the general form of N_θ^{FR} ,

$$N_\theta^{FR} \doteq k_w^* \frac{g Z_\alpha}{X_\alpha - g} \left(s + \frac{Z_u (X_\alpha - g)}{Z_\alpha} \right)$$

Hence, the zero would always be positive real for realistic values of Z_u , X_α , and Z_α .

4. $SSM_{u,\delta}$ (airspeed and thrust)

The static safety margin based on airspeed and thrust had two main problems when vertical gust margin was critical. First, there was no direct indication of the vertical gust component since angle of attack was not sensed directly; and second, there was a strong influence of thrust (large k_δ) which resulted in significant cross-coupling with flight path control.

The linearized flight reference gains were computed as functions of linearized dynamic safety margin coefficients:

$$k_u \doteq k_u^r - \frac{Z_u}{Z_w} k_w^r$$

and
$$k_\delta \doteq k_\delta^r - \frac{Z_\delta}{Z_w} k_w^r$$

As in cases considered previously the k_u^+ terms dominated when the speed margin was critical, and the k_w^+ dominated when vertical gust margin was critical. The k_δ^- term had only a second-order effect. Nevertheless, the throttle sensitivity for this static safety margin, k_δ , was relatively large (approximately $+15\%/ \Delta N_H$).

The substantial k_δ produced a washout of flight path response similar to that of the dynamic safety margin. In effect, when thrust was applied, a considerable increase in flight reference occurred. This, in turn, led to a pitch down and a subsequent reversal of flight path. The effect is demonstrated in Fig. C-3.

A second view of the throttle-to-flight-reference cross coupling characteristics was obtained by comparing FR/δ with DSM/δ , i.e., the actual FR response to throttle compared to the actual safety margin response to throttle. In general,

$$\left. \frac{FR}{DSM} \right|_\theta = \frac{N_\delta^{FR}}{N_\delta^{DSM}} = \frac{k_u X_w + (k_w - k_d)(s - X_u) + \frac{k_\delta}{Z_\delta} \left[(s - X_u)(s - Z_w) - X_w Z_u \right]}{k_u X_w + k_w^* (s - X_u) + \frac{k_\delta^+}{Z_\delta} \left[(s - X_u)(s - Z_w) - X_w Z_u \right]}$$

If, for the vertical gust margin critical case, we neglect k_u^+ and k_δ^+ , we can then show that

$$\frac{N_\delta^{FR}}{N_\delta^{DSM}} = \frac{s}{-Z_w} + 1$$

Therefore, the flight reference would be overly sensitive to throttle inputs in the short term, i.e., $t < \frac{1}{-Z_w} \doteq 2$ sec.

This static safety margin combination appeared to offer no clear advantage over dynamic safety margin. It lacked direct w_g response and involved potentially troublesome cross coupling. It did, however, involve one less sensor.

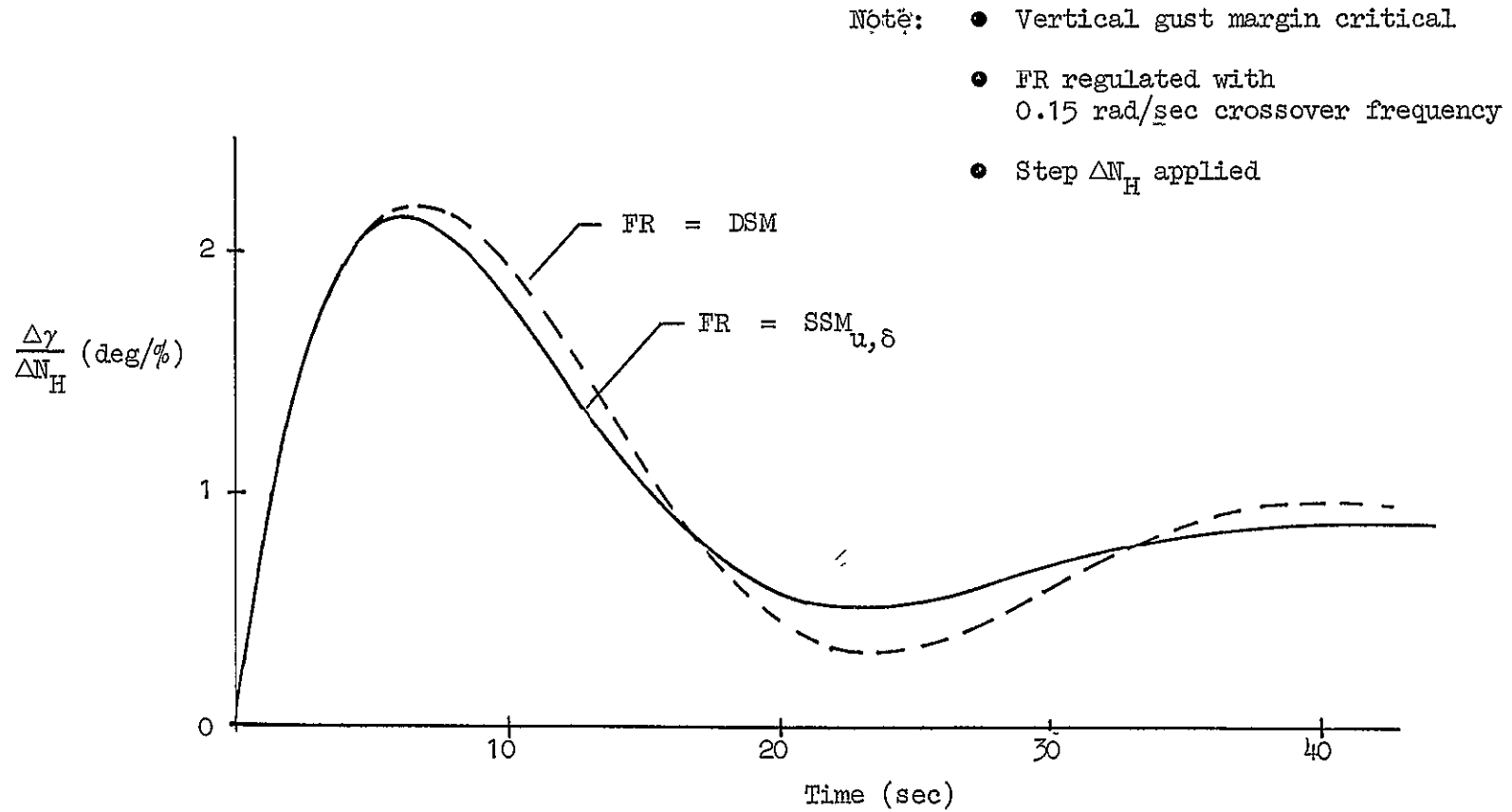


Figure G-3. Ineffectiveness of SSM_{u,δ} in Eliminating Flight Path Overshoot

5. $\underline{SSM}_{w,\theta}$ (angle of attack and pitch attitude)

In this and the following static safety margins involving angle of attack (w), the main area of interest was in the region where airspeed margin was critical. Otherwise, any SSM involving w was essentially equivalent to dynamic safety margin.

For the $\underline{SSM}_{w,\theta}$ in the speed margin critical range, the flight reference gains (as calculated in Section III.B.2) are:

$$k_w \doteq -\frac{X_w}{X_u} k_u^*$$

$$\text{and } k_\theta \doteq \frac{g}{X_u} k_u^*$$

When these gains were substituted into the expression for N_θ^{FR} it was apparent that the flight reference responded nearly in proportion to pitch attitude in the frequency range below 0.5 rad/sec:

$$\begin{aligned} \frac{\text{FR}}{\theta} &\doteq \frac{N_\theta^{\text{FR}}}{\Delta} \doteq \frac{-(X_\alpha - g)(s - X_u) \left(s + \frac{Z_w g}{X_\alpha - g} \right)}{\left(s + \frac{1}{T_{\theta 1}} \right) \left(s + \frac{1}{T_{\theta 2}} \right)} \\ &\doteq \frac{35(0.07)(0.8)}{(0.15)(0.4)} \text{ (\%/deg)} \end{aligned}$$

Thus, direct controllability was judged not to be a problem.

The adverse $\gamma - \theta$ cross coupling still remained a factor in this flight reference implementation just as it had with dynamic safety margin and static safety margins containing airspeed. That is, it was still necessary to depress pitch attitude when making an upward flight path correction. This feature was present in all static safety margin implementations where holding constant speed (or speed margin) was the objective.

The most serious problem with $SSM_{w,\theta}$ (and all the remaining SSMS, in fact) was that there was an incorrect indication of horizontal gusts. Recall from Table III-2 that for the DSM:

$$\frac{\dot{FR}}{\dot{u}_g} = \frac{N_{u_g}^{FR}}{s\Delta} = \frac{-k_u^* \left(\frac{s - Z_w}{s + \frac{1}{T_{\theta_1}}} \right) \left(\frac{s - \frac{1}{T_{\theta_2}}}{s + \frac{1}{T_{\theta_2}}} \right)}{\left(s + \frac{1}{T_{\theta_1}} \right) \left(s + \frac{1}{T_{\theta_2}} \right)} = \frac{-5 (0.5)}{(0.15)(0.4)}$$

In this case, i.e., $SSM_{w,\theta}$,

$$\frac{\dot{FR}}{\dot{u}_g} = \frac{\frac{X_w}{X_u} Z_u k_u^*}{\left(s + \frac{1}{T_{\theta_1}} \right) \left(s + \frac{1}{T_{\theta_2}} \right)} = \frac{+2.4}{(0.15)(0.4)}$$

For cases in which airspeed was not directly involved in the flight reference, it was necessary to examine closely the potential for regulating airspeed, thus DSM, via the flight reference. The general procedure was to use the closed loop response of DSM to u_g . This indicated the effectiveness in reducing DSM excursions by regulation of an indirect flight reference. Starting with the general expression for dynamic safety margin response to horizontal gusts with flight reference regulated:

$$\begin{aligned} \left. \frac{DSM}{u_g} \right|_{FR} &= \frac{N_{u_g}^{DSM} + Y_{FR} N_{\theta}^{FR} \frac{DSM}{u_g}}{\Delta + Y_{FR} N_{\theta}^{FR}} \\ &= \frac{\frac{N_{u_g}^{DSM}}{\Delta} \left(1 + \frac{Y_{FR} N_{\theta}^{FR}}{\Delta} \left(1 - \frac{N_{u_g}^{FR} N_{\theta}^{DSM}}{N_{u_g}^{DSM} N_{\theta}^{FR}} \right) \right)}{\left(1 + \frac{Y_{FR} N_{\theta}^{FR}}{\Delta} \right)} \end{aligned}$$

The term $\frac{N_{ug}^{DSM}}{\Delta}$ is the open loop gust response and $\frac{Y_{FR} N_{\theta}^{FR}}{\Delta}$ is the open loop pilot-vehicle response to flight reference. Note that if the remaining expression

$$1 - \frac{N_{ug}^{FR} N_{\theta}^{DSM}}{N_{ug}^{DSM} N_{\theta}^{FR}}$$

is unity there is no modification of the open loop $\frac{DSM}{u_g}$ response — pitch attitude might just as well be held constant. If the expression is zero, then the $\frac{DSM}{u_g}$ response is reduced as if DSM were regulated directly.

Consider the results for $FR = SSM_{w,\theta}$. For the case where speed margin is critical, $k_w^r = k_{\theta}^r = 0$ for DSM; and $k_w = -X_w/X_u k_u^r$; $k_{\theta} = g/X_u k_u^r$ for $SSM_{w,\theta}$. Hence, from Table III-2?

$$\begin{aligned} N_{ug}^{FR} &= -k_w Z_u s = \frac{X_w}{X_u} k_u^r Z_u s \\ N_{ug}^{DSM} &= -k_u^r s (s - Z_w) \\ N_{\theta}^{FR} &= k_w V \left[s^2 - X_u s - \frac{g}{V} Z_u \right] \\ &\quad + k_{\theta} \left[(s - X_u)(s - Z_w) - X_w Z_u \right] \\ &= -\frac{X_{\alpha}}{X_u} k_u^r \left[s^2 - X_u s - \frac{g}{V} Z_u \right] \\ &\quad + \frac{g}{X_u} k_u^r \left[(s - X_u)(s - Z_w) - X_w Z_u \right] \\ &= -\frac{(X_{\alpha} - g)}{X_u} k_u^r (s - X_u) \left(s + \frac{gZ_w}{X_{\alpha} - g} \right) \\ N_{\theta}^{DSM} &= k_u^r (X_{\alpha} - g) \left(s + \frac{gZ_w}{X_{\alpha} - g} \right) \end{aligned}$$

and,

$$1 - \frac{N_{u_g}^{FR} N_{\theta}^{DSM}}{N_{u_g}^{DSM} N_{\theta}^{FR}} = \frac{s^2 - (X_u + Z_w) s + X_u Z_w - X_w Z_u}{s^2 - (X_u + Z_w) s + X_u Z_w}$$

Figure C-4 shows a plot of the asymptotes of the absolute value of this function for typical values of the stability derivatives involved. As indicated, the function is not as small as desired; rather it is approximately unity. Hence, the $SSM_{w,\theta}$ was expected to be relatively ineffective in maintaining dynamic safety margin. The results are further confirmed by the closed loop DSM/ \dot{u}_g frequency response plot in Fig. C-5. This shows that $FR = SSM_{w,\theta}$ is even less effective than holding attitude regardless of how tight the $FR \rightarrow \theta_c$ loop.

6. $SSM_{w,\dot{\alpha}}$ (angle of attack and flight path angle)

A flight reference based on $SSM_{w,\dot{\alpha}}$ was shown to be equivalent to the $SSM_{w,\theta}$ in all major respects. Controllability, safety margin status information, and dynamic safety margin maintainability were all found identical to $SSM_{w,\theta}$ by virtue of generic transfer function relationships.

Just as for $SSM_{w,\theta}$, the region of interest for $SSM_{w,\dot{\alpha}}$ was when speed margin was critical. For this condition:

$$k_w = - \frac{(X_{\alpha} - g)}{V X_u} k_u^*$$

$$\text{and } k_d = \frac{g}{V X_u} k_u^*$$

Substituting these values into the equations of Table III-2 gives:

$$N_{\theta}^{FR} = \frac{(X_{\alpha} - g)(s - X_u) \left(s + \frac{g Z_w}{X_{\alpha} - g} \right)}{X_u}$$

and

$$N_{u_g}^{FR} = \frac{X_w Z_u s}{X_u}$$

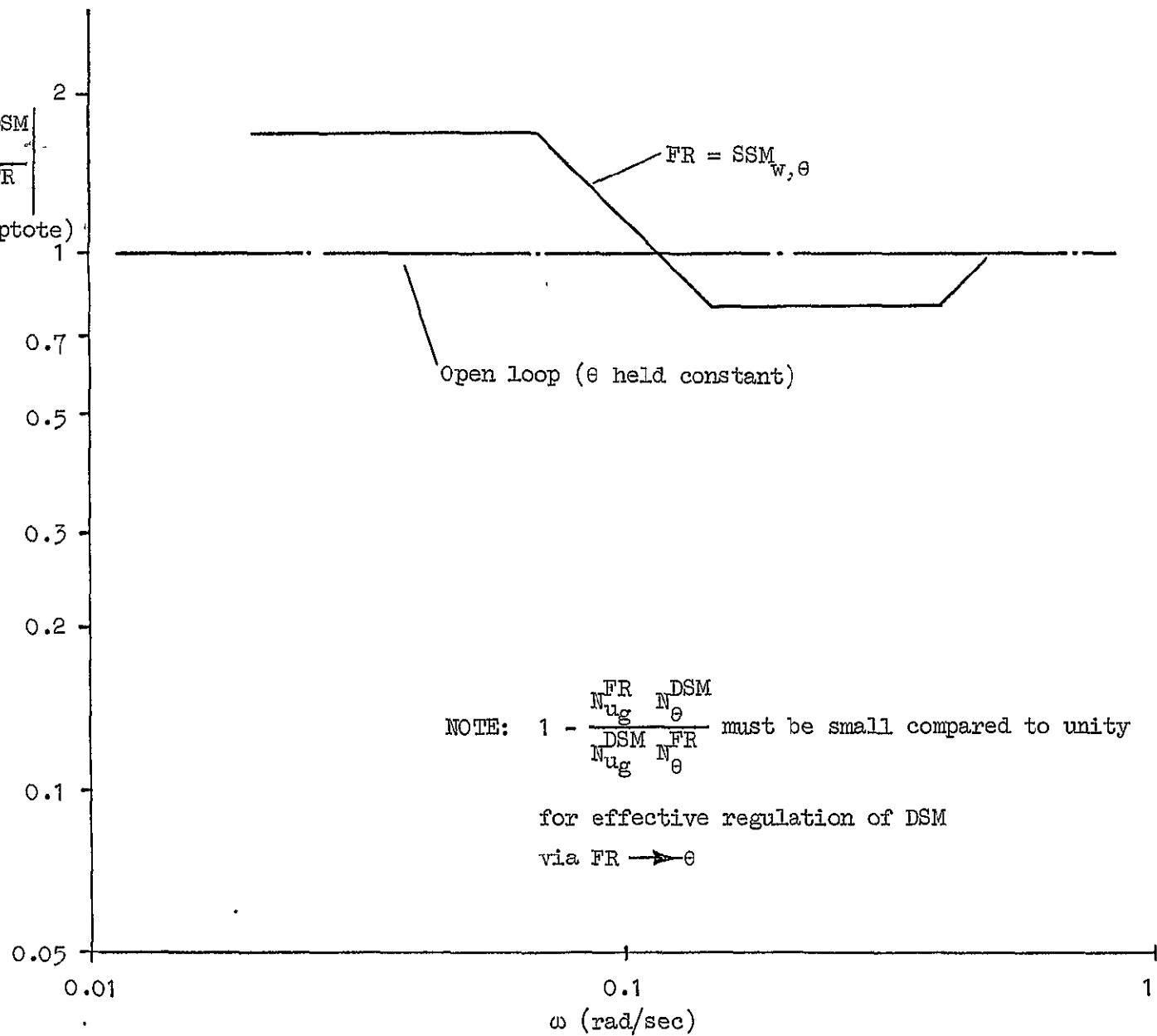


Figure C-4. Ineffectiveness of $SSM_{w,\theta}$ in regulating DSM

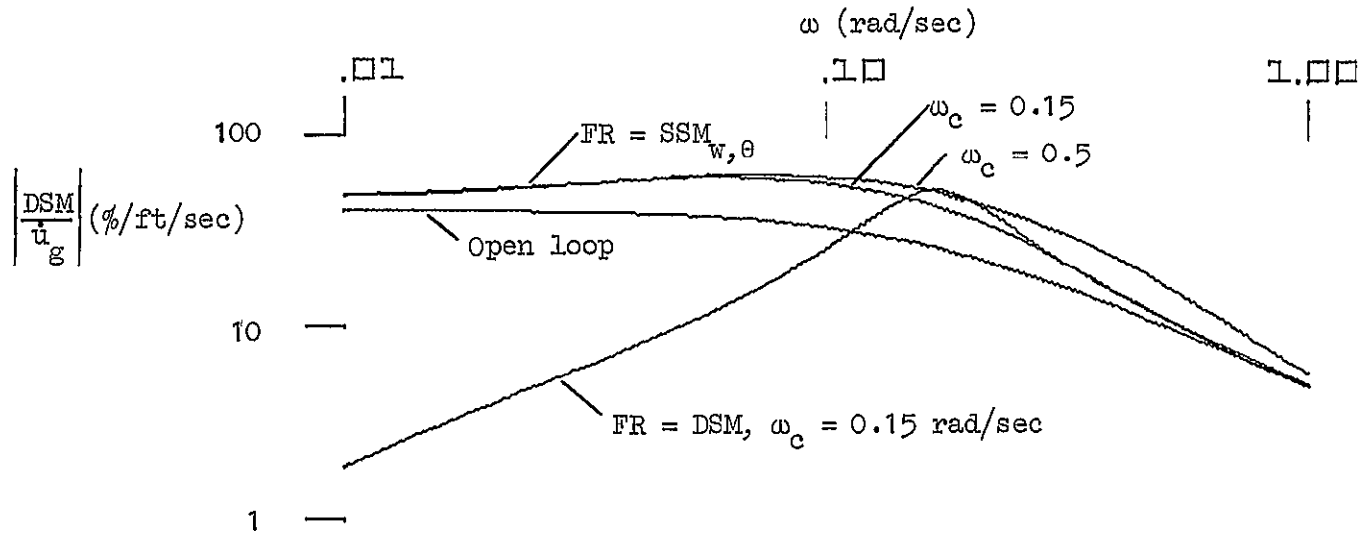


Figure C-5. Frequency Response of $\frac{DSM}{u_g}$ with $FR = SSM_{w, \theta}$ Compared to $FR = DSM$

Since these relationships were identical to those of $SSM_{w,\theta}$, the same conclusions were drawn. Notably:

- Controllability was considered good because of the pure gain response of FR/θ :
- Margin status information was distorted without a direct airspeed input as indicated by FR/u_g
- Dynamic safety margin was not regulated via an $FR \rightarrow \theta$ loop as shown by the closed loop $\frac{DSM}{u_g}$ response.

7. $SSM_{w,\delta}$ (angle of attack and thrust)

The static safety margin based on angle of attack and thrust was found to provide a reasonably direct indication of dynamic safety margin even when airspeed margin was critical. Further, it had the potential for effectively regulating dynamic safety margin. There was, however, a controllability problem when transitioning from the vertical-margin-critical region to the speed-margin-critical region. Also, adverse throttle-to-flight-reference cross coupling was evident.

The static safety margin partial derivatives derived for $SSM_{w,\delta}$ were:

	k_w	k_δ
High Thrust (speed margin critical)	$-\frac{Z_w}{Z_u} k_u^*$	$-\frac{Z_\delta}{Z_u} k_u^+$
Low Thrust (vertical gust margin critical)	$k_w^* - \frac{Z_w}{Z_u} k_u^*$	$k_\delta^- - \frac{Z_\delta}{Z_u} k_u^-$

Based on these derivatives, the FR/θ numerator was computed for both high and low thrust conditions:

$$\text{High thrust: } N_\theta^{FR} \doteq -\frac{Z_w}{Z_u} V k_u^* \left[s^2 - X_u s - \frac{g}{V} Z_u \right]$$

$$\text{Low thrust: } N_\theta^{FR} \doteq k_w^* V \left[s^2 - X_u s - \frac{g}{V} Z_u \right]$$

Since $k_u^r \doteq -k_w^*$ for the two conditions there would be a net gain change of approximately $Z_w/Z_u \doteq 1.7$. The potential danger in this gain change coupled with the low damping ratio of the complex pair of zeros would be the tendency to over-control or to produce a pilot-induced oscillation following a switch from the low thrust condition to the high thrust condition.

The other undesirable feature of $SSM_{w,\delta}$ was a large magnitude adverse cross coupling between throttle and flight reference. This was directly evident from the speed margin critical partial derivative,

$$k_\delta \doteq -\frac{Z_\delta}{Z_u} k_u^* \doteq -20\%/ \% \Delta N_H$$

According to this, a 1% increase in engine rpm would indicate an instantaneous safety margin loss of 20% — a contradiction since thrust normally increases margins.

A flight reference based on w and δ was used during the powered-lift simulator experiment reported in Ref. C1. The flight reference partial derivatives in terms used here were:

$$k_w = -4.9\%/kt$$

$$k_\delta = +0.9\%/ \%$$

These were approximately equivalent to the $SSM_{w,\delta}$ for vertical gust margin critical.

The w,δ flight reference from Ref. C1 was considered usable with the essential features of angle of attack clearly visible. The piloting technique involved making an initial pitch change, waiting, then making additional attitude corrections as speed and angle of attack slowly changed. The direct effect of thrust on FR was noted but was not objectionable since it was in the correct sense ($k_\delta > 0$).

8. $\underline{SSM}_{\theta, \dot{d}}$ (pitch attitude and flight path angle)

This static safety margin combination was shown similar to dynamic safety margin in terms of controllability but failed to provide adequate safety margin status and margin regulation.

The $\underline{SSM}_{\theta, \dot{d}}$ partial derivatives were derived for both critical safety margins:

	k_{θ}	$k_{\dot{d}}$
High Thrust Condition	$\dot{=} - \frac{(X_{\dot{\alpha}} - g)}{X_u} k_u^*$	$\frac{X_w}{X_u} k_u^*$
Low Thrust Condition	$V k_w^*$	$-k_w^*$

The lack of status information in both high thrust and low thrust conditions was apparent by the absence of a k_u and a k_w . The inability of regulating DSM via an FR $\rightarrow \theta_c$ loop was shown by the high-thrust-condition, near-unity value of

$$1 - \frac{N_{u_g}^{FR} N_{\theta}^{DSM}}{N_{u_g}^{DSM} N_{\theta}^{FR}} = \frac{s^2 - (X_u + Z_w) s + X_u Z_w - X_w Z_u}{s^2 - (X_u + Z_w) s + X_u Z_w}$$

Note that this expression was identical to those of $\underline{SSM}_{w, \theta}$ and $\underline{SSM}_{w, \dot{d}}$, and therefore unsatisfactory for the same reasons.

9. $\underline{SSM}_{\theta, \delta}$ (pitch attitude and thrust)

This static safety margin implementation represented the extreme in terms of control ease and lack of safety margin information or direct margin regulation. The reason for this was that $\underline{SSM}_{\theta, \delta}$ was a function of only control variables — state variables were totally absent.

The ease of control can be shown in a general manner by considering the FR/ θ transfer function. First, the partial derivatives were determined:

$$k_{\theta} \doteq \frac{g}{X_u Z_w - X_w Z_u} (Z_w k_u^* - Z_u k_w^*)$$

$$\text{and } k_{\delta} \doteq k_{\delta}^* + \frac{X_w Z_{\delta}}{X_u Z_w - X_w Z_u} k_u^* - \frac{X_u Z_{\delta}}{X_u Z_w - X_w Z_u} k_w^*$$

Substituting these into the expressions in Table III-2

$$\frac{FR}{\theta} = \frac{N_{\theta}^{FR}}{\Delta} \doteq \frac{g (Z_w k_u^* - Z_u k_w^*)}{X_u Z_w - X_w Z_u}, \text{ a pure gain.}$$

The lack of flight reference response to gusts is evident from the absence of k_{θ} and k_{δ} in the gust numerators, $N_{u_g}^{FR}$ and $N_{w_g}^{FR}$ (in Table III-2).

A version of a θ, δ flight reference was also evaluated experimentally and described in Ref. C1. The partial derivatives were similar to the low thrust $SSM_{\theta, \delta}$ considered here, i.e.,

$$k_{\theta} = -5.4\%/deg$$

$$k_{\delta} = +3.8\%/%$$

The ease of controlling this implementation was readily apparent, but it was realized that any indication of gust or wind shear hazard was completely lacking.

10. SSM_{d, \delta} (flight path angle and thrust)

A static safety margin based on flight path angle and thrust is unsuitable for any aircraft operating near $\frac{\partial \gamma}{\partial V} = 0$. Thus it is unsuitable for most aircraft during landing approach.

As mentioned earlier, the $k_{\dot{d}}$ and k_{δ} partial derivatives were excessively sensitive. The source of the problem could be demonstrated by deriving the implicit general expression for the partial derivatives:

$$k_{\dot{d}} = \left. \frac{\partial \text{DSM}}{\partial \dot{d}} \right|_{\delta} = \frac{N_{\theta}^{\text{DSM}}(s=0)}{N_{\theta}^{\dot{d}}(s=0)}$$

and

$$k_{\delta} = \left. \frac{\partial \text{DSM}}{\partial \delta} \right|_{\dot{d}} = \frac{N_{\delta}^{\text{DSM}} \dot{d}(s=0)}{N_{\theta}^{\dot{d}}(s=0)}$$

$N_{\theta}^{\dot{d}}(s=0)$ is the common denominator in both equations and is also proportional to $\frac{\partial \gamma}{\partial V}$. When $\frac{\partial \gamma}{\partial V}$ approaches zero, $k_{\dot{d}}$ and k_{δ} will therefore approach infinity.

APPENDIX C REFERENCE

- C1 Heffley, Robert K., John M. Lehman, Robert C. Rumold, Robert L. Stapleford, Barry C. Scott, and Charles S. Hynes, A Simulator Evaluation of Tentative STOL Airworthiness Criteria. Simulation Results and Analysis (Final Report), NASA TM X-73,093 (FAA-RD-75-222), Nov. 1975; Heffley, Robert K., John M. Lehman, Robert L. Stapleford, Barry C. Scott, and Charles S. Hynes, A Simulator Evaluation of Tentative STOL Airworthiness Criteria. Background Information (Final Report), NASA TM X-73,094 (FAA-RD-75-222), Nov. 1975.

PRECEDING PAGE BLANK NOT FILMED

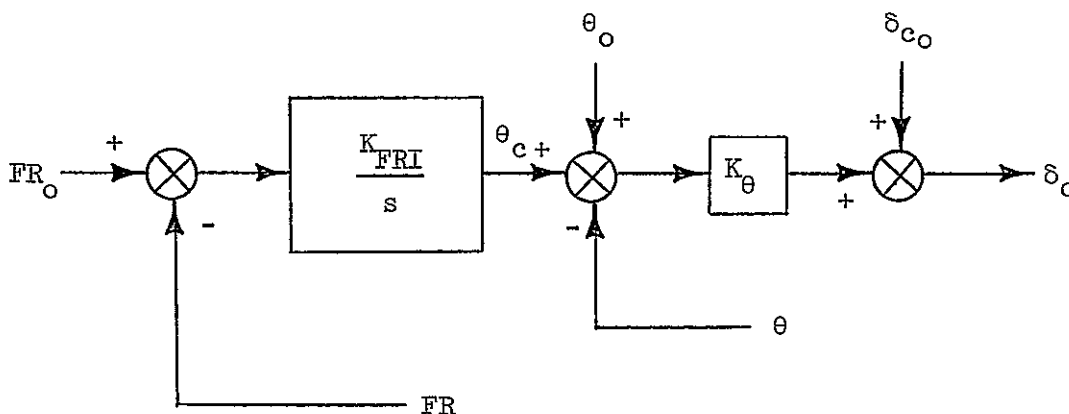
APPENDIX D

FLIGHT REFERENCE LOOP PARAMETER COMPUTATION

System: Powered-lift STOL aircraft with pitch SAS

Assumed Control Strategy: STOL technique, i.e., flight path regulated by throttle and flight reference regulated by pitch attitude — no control crossfeed.

Block Diagram of Flight Reference Loop:



$$\text{i.e., } \delta_c - \delta_{c_0} = -K_\theta (\theta - \theta_0) - \frac{K_\theta K_{FRI}}{s} (FR - FR_0)$$

$$\text{or } \Delta\delta_c = -K_\theta \Delta\theta - \frac{K_\theta K_{FRI}}{s} \Delta FR$$

Difference Equation:

$$\Delta\delta_c(z) = -K_\theta \Delta\theta(z) - \frac{K_\theta K_{FRI} T z^{-1}}{1 - z^{-1}} \Delta FR(z)$$

$$\text{or } \Delta\delta_c(n) - \Delta\delta_c(n-1) = -K_\theta [\Delta\theta(n) - \Delta\theta(n-1)] - K_\theta K_{FRI} T \Delta FR(n-1)$$

or, in the form $y = H a$

where $y \triangleq$ vector of measurements

$a \triangleq$ vector of unknown parameters

$H \triangleq$ matrix of measurements

$$\underbrace{\begin{bmatrix} [\Delta\delta(1) - \Delta\delta(0)] \\ [\Delta\delta(2) - \Delta\delta(1)] \\ \vdots \\ [\Delta\delta(n) - \Delta\delta(n-1)] \end{bmatrix}}_y = \underbrace{\begin{bmatrix} [\Delta\theta(1) - \Delta\theta(0)] & [T \Delta FR(0)] \\ [\Delta\theta(2) - \Delta\theta(1)] & [T \Delta FR(1)] \\ \vdots & \vdots \\ [\Delta\theta(n) - \Delta\theta(n-1)] & [T \Delta FR(n-1)] \end{bmatrix}}_H \underbrace{\begin{bmatrix} -K_\theta \\ -K_\theta K_{FRI} \end{bmatrix}}_a$$

Least Squares Solution:

for $y = H a$

$$\hat{a} = [H^T H]^{-1} H^T y$$

where \hat{a} is least squares estimate of a

Running Solution:

For a running solution of \hat{a} compute $H^T H$ and $H^T y$ by storing appropriate summations, i.e.,

$$H^T y = \begin{bmatrix} \sum [\Delta\delta(n) - \Delta\delta(n-1)] [\Delta\theta(n) - \Delta\theta(n-1)] \\ \sum [\Delta\delta(n) - \Delta\delta(n-1)] [T \Delta FR(n-1)] \end{bmatrix}$$

$$H^T H = \begin{bmatrix} \sum [\Delta\theta(n) - \Delta\theta(n-1)]^2 & \sum [(\Delta\theta(n) - \Delta\theta(n-1)) T \Delta FR(n-1)] \\ \sum [(\Delta\theta(n) - \Delta\theta(n-1)) T \Delta FR(n-1)] & \sum [T \Delta FR(n-1)]^2 \end{bmatrix}$$

Result:

The unknown parameters K_{θ} and K_{FRI} can be computed and displayed on-line using the two dimensional arrays of stored summations of column deflection, pitch attitude, and flight reference.

APPENDIX E

SPERRY 1819A DIGITAL COMPUTER SOFTWARE MODIFICATIONS

The following is a description of the software modifications made to existing STOLAND software*. Most of the modifications were made to implement the flight reference scheme described in this report. In addition, some program changes were required to update the pitch SAS and to correct a computer timing problem.

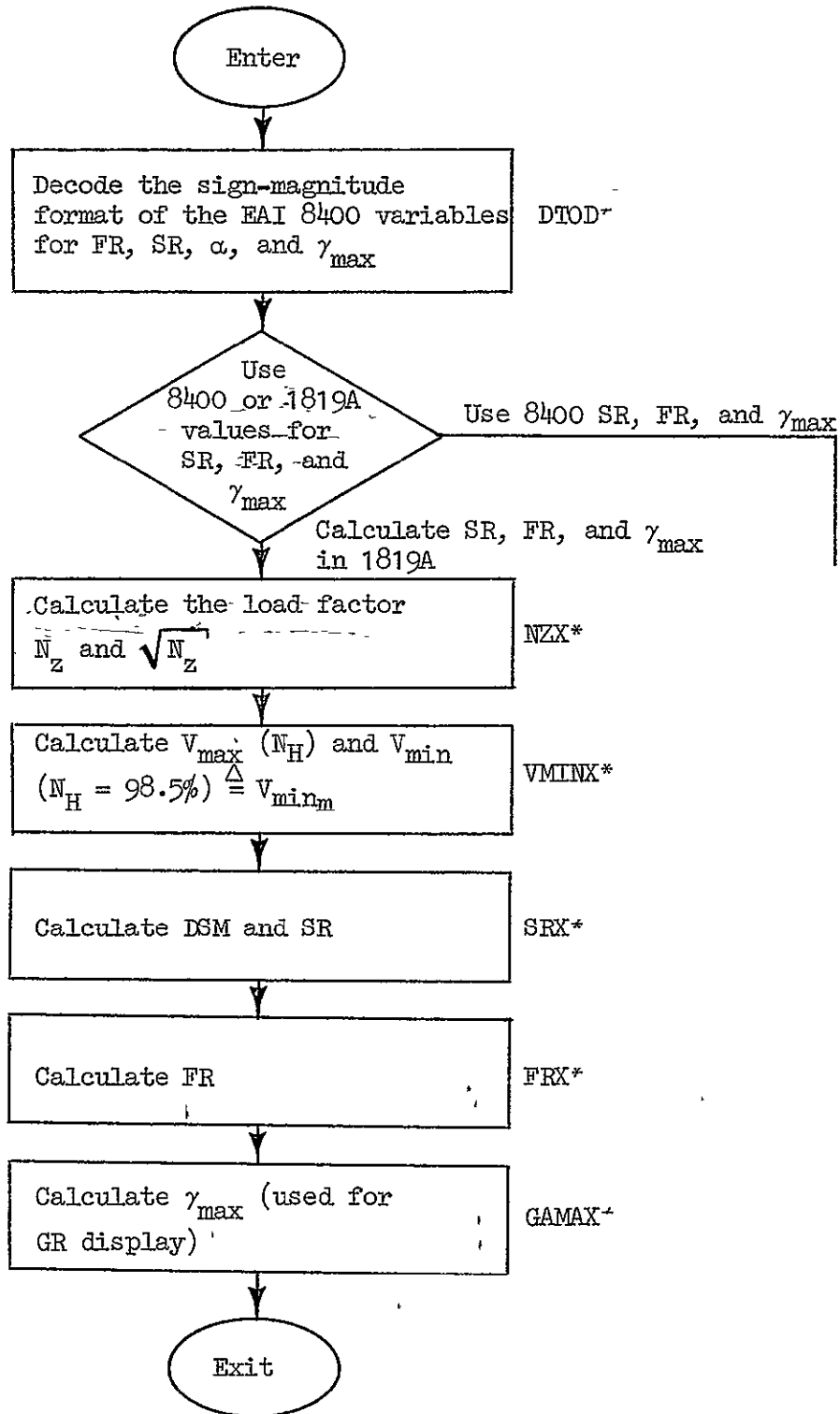
The program changes are listed according to their specific function which include:

- (i) Calculation of SR, FR, and GR
- (ii) Display of FR
- (iii), Display of SR
- (iv) Display of GR
- (v) Display of N_H
- (vi) Modification of pitch SAS
- (vii) Elimination of timing problem
- (viii) Modification of autopilot.

1. CALCULATE SR, FR, AND GR

The flow chart of Fig. E-1 depicts the calculations required to obtain the SR, FR, and GR variables. Note that an option for using SR, FR, and GR functions generated in the EAI 8400 has also been provided. (The EAI 8400 "D-to-D" software program was modified to pass the variables SR, FR, α , and γ_{\max} to the 1819A.) This was done because some experimental safety margin schemes were more easily programmed in FORTRAN and implemented on

* Modifications apply specifically to the Augmentor Wing STOLAND tape AWXA-1 dated 20 April 1977.



* Subroutine name.

Figure E-1. Flow Chart of 1819A Computer Program for Calculating SR, FR, and GR

the EAI 8400. Angle of attack (α) was provided by the EAI 8400 for calculation of DSM_2 (true angle of attack is not presently available in the Sperry 1819A digital computer).

Table E-1 contains a listing of the 1819A assembly language code used to realize the flow chart of Fig. E-1. Program variables start at core location 33743 and constants at 37123. Some of the subroutines have been placed at the end of bank 4 (i.e., 47557), others pre-empted a portion of the runway display code (the runway display program was used to display SR as described in Section E-3).

2. FLIGHT REFERENCE (FR) DISPLAY

The speed bug symbol on the EADI was used to display FR. The display was programmed to be centered when FR = 100%, and have a sensitivity of 50%/in. The required code is shown below. The format of the changes is [core location], new instruction, (old instruction).

[4 2607]	ENTAL'FR	=	12 3744	(12 2616)
[4 2610]	SUBAL'D10000	=	16 4373	(24 4360)
[4 2611]	MULAL'D81	=	24 4154	(26 4373)
[4 2612]	DIVA'D5000	=	26 4337	(50 6100)
[4 2613]	NOOP'	=	50 4000	(10 4154)
[4 2614]	NOOP'	=	50 4000	(76 5331)

3. SAFETY REFERENCE (SR) DISPLAY

The runway perspective on the EADI was used to display the difference between FR and SR. The existing code was modified such that the "runway" appeared as a solid horizontal line approximately 1/4 inch wide. The line was biased to the left so that it would line up with the speed bug, and down such that when FR - SR = 0 the line would be at the bottom of the speed bug display. (Figure IV-3 in the main body of the report depicts the resulting display.) The sensitivity was set to 50%/in.

TABLE E-1. LISTING OF SPERRY 1819A ASSEMBLY LANGUAGE CODE

INTERMETRICS 1819A ASSEMBLER 01/12/78 PAGE	1 STI SR AND FR SYSTEM FOR THE AUG. WING
200 000000 000000	ALLOC
300 000000 034073 ONEZ	ALLOC 34073
400 000000 034111 D10	ALLOC 34111
500 000000 034217 D360	ALLOC 34217
600 000000 032724 VCAL	ALLOC 32724 .1 KT/BIT
700 000000 034157 D100	ALLOC 34157
800 000000 031044 THET	ALLOC 31044 (1/360) DEG/BIT
900 000000 032147 NH	ALLOC 32147 .01%/BIT
1000 000000 043543 BLANKE	ALLOC 43543
1100 000000 031771 ERNFLG	ALLOC 31771
1200 000000 032760 THPO	ALLOC 32760
1300 000000 034337 D5000	ALLOC 34337
1400 000000 032617 XR1	ALLOC 32617
1500 000000 032620 XR2	ALLOC 32620
1600 000000 032621 XR3	ALLOC 32621
1700 000000 032622 XR4	ALLOC 32622
1800 000000 032623 YR1	ALLOC 32623
1900 000000 032624 YR2	ALLOC 32624
2000 000000 032625 YR3	ALLOC 32625
2100 000000 032626 YR4	ALLOC 32626
2200 000000 034160 M100	ALLOC 34160
2300 000000 036727 THETSC	ALLOC 36727
2400 000000 036732 ZMAX	ALLOC 36732
2500 000000 033023 ZAV	ALLOC 33023
2600 000000 033024 XV	ALLOC 33024
2700 000000 034071 ZERO	ALLOC 34071
2800 000000 037010 SIN00	ALLOC 37010
2900 000000 034203 D250	ALLOC 34203
3000 000000 034302 D2000	ALLOC 34302
3100 000000 043253 RNY60	ALLOC 43253
3200 000000 034257 D1000	ALLOC 34257
3300 000000 034373 D10000	ALLOC 34373
3400 000000 037040 COS0	ALLOC 37040
3500 000000 031002 ACCZB	ALLOC 31002
3600 000000 040035 SQR T	ALLOC 40035
3700 000000 032542 COSPHI	ALLOC 32542
3800 000000 032423 GANMA1	ALLOC 32423
3900 000000 032727 VTAIRF	ALLOC 32727
4000 000000 030763 PSINDT	ALLOC 30763
4100 000000 040034 SINCOA	ALLOC 40034
4200 000000 034420 RADDF5	ALLOC 34420
4300 000000 034154 D81	ALLOC 34154
4400 000000 034252 D900	ALLOC 34252
4500 000000 031274 IASREF	ALLOC 31274

REPRODUCIBILITY OF THE
ORIGINAL PAGE IS POOR

TABLE E-1. (Continued)

INTERMETRICS 1819A ASSFMBLER 01/12/78 PAGE 2 STI SR AND FR SYSTEM FOR THE AUG. WING					
4600	000000	031255	DZC11	ALLOC	31255
4700	000000	032266	THTCOM	ALLOC	32266
4800	000000	014051	NOCROS	ALLOC	14051
4900	000000	033543	XINT	ALLOC	33543
5000	000000	054525	SIGNMG	ALLOC	54525
5100	000000	034232	D500	ALLOC	34232
5200	000000	017511	ZTFLAG	ALLOC	17511
5300	037123	000000		START	37123
PUT CONSTANTS HERE					

INTERMETRICS 1819A ASSEMBLER 01/12/78 PAGE 3 PUT CONSTANTS HERE					
5600	037123	776027	KTIME		-1000D
5700	037124	773727	THENDT		-2088D
5800	037125	202153	KDSM3		66667D
5900	037126	101065	KDSM5		33333D
6000	037127	207654	KMVO		69548D
6100	037130	775440	KMVNH		-1247D
6200	037131	001122	KMVNH2		594D
6300	037132	773365	KAO		-2314D
6400	037133	777406	KAV		-249D
6500	037134	000230	KAV2		152D
6600	037135	000475	KANH		317D
6700	037136	777626	KANH2		-105D
6800	037137	770574	KGO		-3715D
6900	037140	000074	KG1		60D
7000	037141	777750	KG2		-23D
7100	037142	777704	RNSR		-59D
7200	037143	000670	VHM		-440D
7300	037143	000000		START	33743
PUT VARIABLES HERE					

REPRODUCIBILITY OF THE ORIGINAL PAGE IS POOR.

TABLE E-1 (Continued)

INTERMETRICS 181°A ASSEMBLY 01/12/78 PAGE				4 PUT VARIABLES HERE	
7600	033743	000000	SR	0	
7700	033744	000000	FR	0	
7800	033745	000000	FRONT	0	
7900	033746	000000	VHIN	0	10BT/KT
8000	033747	000000	VHINM	0	10BT/KT
8100	033750	000000	ALFAMX	0	360BT/DEG
8200	033751	000000	D5M	0	100BT/%
8300	033752	000000	IDSM	0	1,2,3,4 OR 5
8400	033753	000000	N7	0	MODIFIED L.F., 10000BT/G
8500	033754	000000	SON7	0	SQUARE ROOT OF N7
8600	033755	000000	GMAX	0	MAXIMUM AERO, FPA
8700	033756	000000	FRMSP	0	FR-SR, 100BT/%
8800	033757	000000	ALFA	0	ADA(FROM 8400), 360BT/DEG
8900	033760	000000	GAMA	0	AERO, FPA(FROM 8400), 360 BT/DEG
9000	033761	023422	TP	100000	TFST VARIABLES
9100	033762	035230	TRA	150000	
9200	033763	011610	TRB	50000	
9300	033764	000144	TRAB	1000	
9400	031522	000000	START	31522	LGAIN+43

TABLE E-1 (Continued)

INTERMETRICS 1819A ASSEMBLER 01/12/78 PAGE				5 LGAIN+43		
9700	031522	456316		-1073130	FR	LAG TIME CONSTANT
9800	031523	406243		-1278360	NZ	LAG TIME CONSTANT
9900	047557	000000	START	47557		
10000	047557	017511	FOLAG	0*ZTFLAG		
10100	047560	000000	FRX	0*0	CALC.	FR
10200	047561	360053	ENTBK	43D		
10300	047562	123751	ENTAL	DSM		
10400	047563	307557	IRJP	FOLAG	FILTER	DSM
10500	047564	443744	STRAL	FR		
10600	047565	121044	ENTAL	THET		
10700	047566	167124	SUBAL	THE NOT		
10800	047567	247123	MULAL	KTHE		
10900	047570	264217	DIVA	D360		
11000	047571	143744	ADDAL	FR		
11100	047572	443744	STRAL	FR		
11200	047573	163743	SUBAL	SR		
11300	047574	443756	STRAL	FRMSR		
11400	047575	123744	ENTAL	FR		
11500	047576	244073	MULAL	ONEZ		
11600	047577	264111	DIVA	D10		
11700	047600	443745	STPAL	FROTFN		
11800	047601	557560	IJP	FRX		
11900	047602	054525	CONVRT	0*SIGNMG		
12000	047603	000000	DTOD	0*0		
12100	047604	123543	FNTAL	XINT	SR	
12200	047605	307602	IRJP	CONVRT		
12300	047606	443743	STRAL	SR		
12400	047607	123544	ENTAL	XINT+1	FR	
12500	047610	307602	IRJP	CONVRT		
12600	047611	443744	STRAL	FR		
12700	047612	123546	ENTAL	XINT+3	ALFA	
12800	047613	307602	IRJP	CONVRT		
12900	047614	443757	STRAL	ALFA		
13000	047615	123547	FNTAL	XINT+4	GMAX	
13100	047616	307602	IRJP	CONVRT		
13200	047617	443755	STRAL	GMAX		
13300	047620	123744	ENTAL	FR	FR-SR	
13400	047621	163743	SUBAL	SR		
13500	047622	443756	STRAL	FRMSP		
13600	047623	123744	FNTAL	FR		
13700	047624	244073	MULAL	ONEZ		
13800	047625	264111	DIVA	D10		
13900	047626	443745	STPAL	FROTFN		
14000	047627	557603	IJP	DTOD		

FR 1095-1

TABLE E-11 (Continued)

INTERMETRICS 1819A ASSEMBLER 01/12/78 PAGE 6				STI SR AND FR SYSTEM FOR THE AUG. WING	
14100	047630	000000	SRX	0'0	DYNAMIC SAFETY MARGIN AND SR
14200	047631	122724	ENTAL	VCAL	
14300	047632	163747	SUBAL	VMINM	
14400	047633	442765	STRAL	TMPO+5	
14500	047634	244232	MULAL	D500	
14600	047635	264111	DIVA	D10	
14700	047636	442761	STRAL	TMPO+1	DSM(1)
14800	047637	123750	ENTAL	ALFAMX	
14900	047640	163757	SUBAL	ALFA	
15000	047641	244232	MULAL	D500	
15100	047642	264420	DIVA	RADDES	
15200	047643	242724	MULAL	VCAL	
15300	047644	264111	DIVA	D10	
15400	047645	442762	STRAL	TMPO+2	DSM(2)
15500	047646	122724	ENTAL	VCAL	
15600	047647	163746	SUBAL	VMIN	
15700	047650	442764	STRAL	TMPO+4	
15800	047651	247125	MULAL	KDSM3	
15900	047652	263746	DIVA	VMIN	
16000	047653	442763	STRAL	TMPO+3	DSM(3)
16100	047654	122764	ENTAL	TMPO+4	
16200	047655	244157	MULAL	D100	
16300	047656	442764	STRAL	TMPO+4	DSM(4)
16400	047657	122765	ENTAL	TMPO+5	
16500	047660	247126	MULAL	KDSM5	
16600	047661	263747	DIVA	VMINM	
16700	047662	442765	STRAL	TMPO+5	DSM(5)
16800	047663	443751	STRAL	DSM	
16900	047664	360004	ENTBK	4	FIND SMALLEST DSM(I)
17000	047665	423752	STRB	IDSM	
17100	047666	360003	FNTBK	3	
17200	047667	032761	CMALB	TMPO+1	
17300	047670	677673	JPMGR	LOK+3	
17400	047671	132761	ENTALB	TMPO+1	
17500	047672	423752	STRB	IDSM	
17600	047673	727667	RJP	LOK-4	
17700	047674	443751	STRAL	DSM	
17800	047675	443743	STRAL	SP	
17900	047676	123752	ENTAL	IDSM	
18000	047677	710001	ADDALK	1	
18100	047700	443752	STRAL	IDSM	
18200	047701	557630	IJP	SRX	
18300	047702	000000	N7X	0'0	CALC. LOAD FACTOR
18400	047703	124257	ENTAL	D1000	
18500	047704	141002	ADDAL	ACCZB	INCREMENTAL AZ, +UP

132

REPRODUCIBILITY OF THE
ORIGINAL PAGE IS POOR

TABLE E-1 (Continued)

INTERMETRICS 1819A ASSEMBLER 01/12/78 PAGE 7 STI SR AND FR SYSTEM FOR THE AUG. WING				
18600	047705	360054	ENTBK	44D
18700	047706	307557	IRJP	FOLAG
18800	047707	443753	STRAL	NZ
18900	047710	107010	ENTAU	SIN00
19000	047711	300035	IPJP	SQRT
19100	047712	504320	RSHA	16D
19200	047713	244157	MULAL	D100
19300	047714	504302	RSHA	2D
19400	047715	443754	STRAL	SONZ
19500	047716	557702	IJP	N7X
19600	047717	000000	GAMAX	0'0
19700	047720	127140	ENTAL	KG1
19800	047721	243744	MULAL	FR
19900	047722	264157	DIVA	D100
20000	047723	147137	ADDAL	KG0
20100	047724	443755	STRAL	GMAX
20200	047725	127141	ENTAL	KG2
20300	047726	243744	MULAL	FR
20400	047727	264257	DIVA	D1000
20500	047730	243744	MULAL	FR
20600	047731	264257	DIVA	D1000
20700	047732	143755	ADDAL	GMAX
20800	047733	443755	STRAL	GMAX
20900	047734	124373	ENTAL	D10000
21000	047735	163753	SURAL	NZ
21100	047736	244420	MULAL	RADDES
21200	047737	264373	DIVA	D10000
21300	047740	143755	ADDAL	GMAX
21400	047741	443755	STRAL	GMAX
21500	047742	557717	IJP	GAMAX
21600	043110	000000	START	43110

TABLE E-1, (Continued)

INTERMETRICS 1819A ASSFMLFR 01/12/78 PAGE 8 STJ SR AND FR SYSTEM FOR THE AUG. WING					
21900	043110	767603	RJP	DTOD	GFT 8400 VARIABLES
22000	043111	763154	PJP	TFETH	SAW TOOTH FUNC. FOR DYNAMIC CHECKS
22100	043112	767702	RJP	N7X	L.F. & SORT L.F.
22200	043113	763177	RJP	VMINX	VMIN & VMINM
22300	043114	763216	RJP	AFMX	ALFMAX
22400	043115	767630	RJP	SRX	DSM, IDSM, SR
22500	043116	767560	RJP	FRX	FR & FR-SR
22600	043117	767717	RJP	GAMAX	GMAX
22700	043120	121771	ENTAL	ERNFLG	
22800	043121	613543	JPALZ	BLANKE	
22900	043122	123756	ENTAL	FRMSP	PUT FR-SR ON RUNWAY PERSP.
23000	043123	164337	SUBAL	D5000	BIAS DOWN 50%
23100	043124	247142	MULAL	PNSR	SCALE AT 50%/IN
23200	043125	264157	DIVA	D100	
23300	043126	442760	STRAL	TMPO	
23400	043127	244160	MULAL	M100	
23500	043130	266727	DIVA	THEISC	
23600	043131	146732	ADDAL	ZMAX	
23700	043132	443023	STPAL	7AV	
23800	043133	124071	ENTAL	7ERD	
23900	043134	443024	STRAL	XV	
24000	043135	124337	ENTAL	D5000	RUNWAY CORNERS
24100	043136	442617	STRAL	XR1	
24200	043137	442622	STRAL	XR4	
24300	043140	144203	ADDAL	D250	LENGTH
24400	043141	442620	STRAL	XR2	
24500	043142	442621	STRAL	XR3	
24600	043143	700031	ENTALK	25D	W/2
24700	043144	164302	SUBAL	D2000	Y
24800	043145	442623	STRAL	YR1	
24900	043146	442624	STRAL	YR2	
25000	043147	707746	FNTALK	-25D	-W/2
25100	043150	164302	SUBAL	D2000	Y
25200	043151	442625	STRAL	YR3	
25300	043152	442626	STRAL	YR4	
25400	043153	343252	JP	RNY60-1	
25500	043154	000000	TEETH	0'0	SAW TOOTH FUNCTION
25600	043155	123761	ENTAL	TR	SET SR IC TO 1000
25700	043156	023767	CMAL	TRA	SET SRA TO 15000
25800	043157	653167	JPMLEQ	LOK+3	
25900	043160	023763	CMAL	TRB	SET SRB TO 1000
26000	043161	653166	JPMLEQ	LOK+5	
26100	043162	123764	ENTAL	TRAB	SET SRAB TO 100
26200	043163	506100	CPAL		CHANGE SIGN OF DELTA IF

TABLE E-1 (Continued)

INTERMETRICS 1819A ASSEMBLER 01/17/78 PAGE			9 STI SR AND FR SYSTEM FOR THE AUG. WING		
26300	043164	443764	STRAL	TRAB	OUTSIDE BOUNDS
26400	043165	123761	ENTAL	TR	
26500	043166	143764	ADDAL	TRAB	INCREMENT SR
26600	043167	443761	STRAL	TR	
26700	043170	443743	STRAL	SR	
26800	043171	553154	IJP	TEFTII	
26900	043172	000000	VMINX	O'D	MINIMUM AIRSPEED
27000	043173	127130	FNTAL	K'VMNH	
27100	043174	247147	MULAL	NH	
27200	043175	264157	DIVA	D100	
27300	043176	147127	ADDAL	KMVO	
27400	043177	443746	STRAL	VMIN	
27500	043200	127131	ENTAL	KMVNH2	
27600	043201	242147	MULAL	NH	
27700	043202	264257	DIVA	D1000	
27800	043203	242147	MULAL	NH	
27900	043204	264257	DIVA	D1000	
28000	043205	143746	ADDAL	VMIN	
28100	043206	243754	MULAL	SON7	
28200	043207	267040	DIVA	COSO	
28300	043210	443746	STRAL	VMIN	MIN, A/S
28400	043211	127143	FNTAL	VMM	
28500	043212	243754	MULAL	SONZ	
28600	043213	264373	DIVA	D10000	
28700	043214	443747	STPAL	VMINH	MIN. A/S AT MAX. POWER
28800	043215	553172	IJP	VMINX	
28900	043216	000000	AFMX	O'D	MAX, AOA
29000	043217	127133	FNTAL	KAV	
29100	043220	242724	MULAL	VCAL	
29200	043221	264111	DIVA	D10.	
29300	043222	147132	ADDAL	KAO	
29400	043223	443750	STRAL	ALFAMX	
29500	043224	127134	ENTAL	KAV2	
29600	043225	242724	MULAL	VCAL	
29700	043226	264157	DIVA	D100	
29800	043227	242724	MULAL	VCAL	
29900	043230	264157	DIVA	D100	
30000	043231	143750	ADDAL	ALFAMX	
30100	043232	443750	STRAL	ALFAMX	
30200	043233	127135	ENTAL	KANH	
30300	043234	242147	MULAL	NH	
30400	043235	264157	DIVA	D100	
30500	043236	143750	ADDAL	ALFAMX	
30600	043237	443750	STRAL	ALFAMX	
30700	043240	127136	ENTAL	KANH2	

REPRODUCIBILITY OF THE ORIGINAL PAGE IS POOR

TABLE E-11 (Continued)

INTERMETRICS 1819A ASSEMBLER 01/12/78 PAGE 10 STI SR AND FR SYSTEM FOR THE AUG. WING					
30800	043241	242147	MULAL	NH	
30900	043242	264257	DIVA	D1000	
31000	043243	242147	MULAL	NH	
31100	043244	264257	DIVA	D1000	
31200	043245	143750	ADDAL	ALFAMX	
31300	043246	443750	STRAL	ALFAMX	
31400	043247	553716	IJP	AFMX	
31500	042527	000000	START	42527	USE FPA FOR GR

INTERMETRICS 1819A ASSEMBLER 01/12/78 PAGE 11 USE FPA FOR GR					
31800	042527	123755	ENTAL	GMAX	MAY, AERO FPA
31900	042530	162423	SUBAL	GAMMAI	
32000	042531	244157	MULAL	D100	
32100	042532	264252	DIVA	D900	
32200	042533	504000	NOOP		
32300	042607	000000	START	42607	USE SPEED BUG FOR FR
32400	042607	123744	ENTAL	FR	FLIGHT REF.
32500	042610	164373	SUBAL	D10000	BIAS TO CENTER
32600	042611	244154	MULAL	D81	SCALE AT 91 RTS/IN
32700	042612	264337	DIVA	D5000	50%/IN
32800	042613	504000	NOOP		
32900	042614	504000	NOOP		

REPRODUCIBILITY OF THE
ORIGINAL PAGE IS POOR

TABLE E-1. (Continued)

INTERMETRICS 1819A ASSEMBLER 01/12/78 PAGE 12 USE SPEED BUG FOR FR

CROSS REFERENCE BLOCK NUMBER = 1										
AFMX	LINE	28900	LOC	043216	REF	-22300	31400			
ALFA	LINE	8800	LOC	033757	REF	-12200	14900			
ALFAMX	LINE	8100	LOC	033750	REF	14800	-29400	30000	-30100	30500 -30600 31200 -31300
CONVPT	LINE	11900	LOC	047602	REF	-12200	-12500	-12800	-13100	
DSM	LINE	8200	LOC	033751	REF	10300	-16800	-17700		
DTOD	LINE	12000	LOC	047603	REF	14000	-21900			
FOLAG	LINE	10000	LOC	047557	REF	-10400	-18700			
FR	LINE	7700	LOC	033744	REF	-10500	11000	-11100	11400	-12600 13300 13600 19800
		20300		20500						32400
FRMSR	LINE	8700	LOC	033756	REF	-11300	-13500	22900		
FROTEN	LINE	7800	LOC	033745	REF	-11700	-13900			
FRX	LINE	10100	LOC	047560	REF	11800	-22500			
GAMA	LINE	8900	LOC	033760	IS NOT REFERENCED.					
GAMAX	LINE	19600	LOC	047717	REF	21500	-22600			
GMAX	LINE	8600	LOC	033755	REF	-13200	-20100	20700	-20800	21300 -21400 31800
IDSM	LINE	8300	LOC	033752	REF	-17000	-17500	17900	-18100	
KA0	LINE	6300	LOC	037132	REF	29300				
KANH	LINE	6600	LOC	037135	REF	30200				
KANH2	LINE	6700	LOC	037136	REF	30700				
KAV	LINE	6400	LOC	037133	REF	29000				
KAV2	LINE	6500	LOC	037134	REF	29500				
KDSM3	LINE	5800	LOC	037125	REF	15800				
KDSM5	LINE	5900	LOC	037126	REF	16500				
KGO	LINE	6800	LOC	037137	REF	20000				
KG1	LINE	6900	LOC	037140	REF	19700				
KG2	LINE	7000	LOC	037141	REF	20200				
KMVO	LINE	6000	LOC	037127	REF	27300				
KMVNH	LINE	6100	LOC	037130	REF	27000				
KMVNH2	LINE	6200	LOC	037131	REF	27500				
KTRE	LINE	5600	LOC	037123	REF	10800				
NZ	LINE	8400	LOC	032753	REF	-18800	21000			
NZX	LINE	18300	LOC	047702	REF	19500	-22100			
RNSP	LINE	7100	LOC	037142	REF	23100				
SQNZ	LINE	8500	LOC	033754	REF	-19400	28100	28500		
SR	LINE	7600	LOC	033743	REF	11200	-12300	13400	-17800	-26700
SRX	LINE	14100	LOC	047630	REF	18200	-22400			
TEETH	LINE	25500	LOC	043154	REF	-22000	26800			
THENOT	LINE	5700	LOC	037124	REF	10700				
TR	LINE	9000	LOC	033761	REF	25600	-26400	-26600		
TPA	LINE	9100	LOC	033762	REF	25700				
TRAB	LINE	9300	LOC	033764	REF	26100	-26300	26500		
TRB	LINE	9200	LOC	033763	REF	25900				
VHIN	LINE	7900	LOC	033746	REF	15600	15900	-27400	28000	-28300

TR 1095-1

137

TABLE E-1 (Continued)

TR 1095-1

INTERMETRICS 1819A ASSEMBLER 01/12/78 PAGE 13 USE SPEED BUG FOR FR									
VMINM	LINE	8000	LOC 033747	REF	14300	16600	-28700		
VMINX	LINE	26900	LOC 043172	PEF	-22200	28900			
VMM	LINE	7200	LOC 037143	REF	28400				

INTERMETRICS 1819A ASSEMBLER 01/12/78 PAGE 14 USE SPED BUG FOR FR

CROSS REFERENCE FOR GLOBAL LABELS

ACCZR	LINE	3500	LOC 031002	REF	18500							
BLANKE	LINE	1000	LOC 043543	REF	22800							
C050	LINE	3400	LOC 037040	PEF	28200							
C05PHI	LINE	3700	LOC 032542	IS NOT REFERENCED.								
D10	LINE	400	LOC 034111	REF	11400	13800	14600	15300	29200			
D100	LINE	700	LOC 034157	REF	16200	19200	19900	23200	27200	29700	29900	30400
		32000										
D1000	LINE	3200	LOC 034257	REF	18400	20400	20600	27700	27900	30900	31100	
D10000	LINE	3300	LOC 034373	REF	20900	21200	23600	32500				
D2000	LINE	3000	LOC 034302	REF	24700	25100						
D250	LINE	2900	LOC 034203	REF	24300							
D260	LINE	500	LOC 034217	REF	10900							
D500	LINE	5100	LOC 034232	REF	14500	15000						
D5000	LINE	1300	LOC 034337	REF	23000	24000	32700					
D81	LINE	4300	LOC 034154	REF	32600							
D900	LINE	4400	LOC 034252	REF	32100							
DZC11	LINE	4600	LOC 031255	IS NOT REFERENCED.								
ERNFLG	LINE	1100	LOC 031771	REF	22700							
GAMMAI	LINE	3800	LOC 032423	REF	31900							
IASREF	LINE	4500	LOC 031274	IS NOT REFERENCED.								
M100	LINE	2200	LOC 034160	REF	23400							
NH	LINE	900	LOC 032147	REF	27100	27600	27800	30300	30800	31000		
NOCROS	LINE	4800	LOC 014051	IS NOT REFERENCED.								
ONEZ	LINE	300	LOC 034073	REF	11500	13700						
PST00T	LINE	4000	LOC 030763	IS NOT REFERENCED.								
RADDES	LINE	4200	LOC 034420	REF	15100	21100						
RNY60	LINE	3100	LOC 043253	REF	25400							
SIGNMG	LINE	5000	LOC 054525	REF	11900							
SIN00	LINE	2800	LOC 037010	PEF	18900							
SINCHA	LINE	4100	LOC 040034	IS NOT REFERENCED.								
SQRT	LINE	3600	LOC 040035	REF	-19000							
THET	LINE	800	LOC 031044	REF	10600							
THETSC	LINE	2300	LOC 036727	PEF	23500							
THTCOM	LINE	4700	LOC 032266	IS NOT REFERENCED.								
TMPO	LINE	1200	LOC 032760	REF	-14400	-14700	-15400	-15700	-16000	16100	-16300	16400
		-16700	17200	17400	-23300							
VCAL	LINE	600	LOC 032724	REF	14200	15200	15500	29100	29600	29800		
VTATRF	LINE	3900	LOC 032727	IS NOT REFERENCED.								
XINT	LINE	4900	LOC 033543	REF	12100	12400	12700	13000				
XR1	LINE	1400	LOC 032617	REF	-24100							
XR2	LINE	1500	LOC 032620	REF	-24400							
XR3	LINE	1600	LOC 032621	REF	-24500							
XR4	LINE	1700	LOC 032622	REF	-24200							

138

TABLE E-1 (Concluded)

INTERMETRICS 1819A ASSEMBLER 01/12/78 PAGE 15 USE SPEED BUG FOR FR						
XV	LINE	2600	LOC	033024	REF	-23900
YR1	LINE	1800	LOC	032623	REF	-24800
YR2	LINE	1900	LOC	032624	REF	-24900
YR3	LINE	2000	LOC	032625	REF	-25200
YR4	LINE	2100	LOC	032626	REF	-25200
7AV	LINE	2500	LOC	033023	REF	-23700
ZERO	LINE	2700	LOC	034071	REF	23800
ZMAX	LINE	2400	LOC	036732	REF	23600
7TFLAG	LINE	5200	LOC	017511	REF	10000

INTERMETRICS 1819A ASSEMBLER 01/12/78 PAGE 16 USE SPEED BUG FOR FR

NO ERRORS DETECTED

A portion of the code required to put FR - SR on the runway perspective is shown in the listing of Table E-1. All of the other changes required are delineated below.

[4 3275]	MULAL'TMPO	=	24 2760	(24 1044)
[4 3320]	ENTAL'ZERO	=	12 4071	(12 1327)
[4 3321]	NOOP'	=	50 4000	(71 7671)
[4 3476]	MULAL'ZERO	=	24 4071	(24 1327)

4. GAMMA REFERENCE (GR) DISPLAY

The flight path acceleration bar was used to display γ_{\max} (which is the steady state maximum flight path angle possible at the existing FR). It was displayed with respect to the artificial horizon, and had the same sensitivity as the inertial flight path bar. The required changes are delineated below:

[4 2527]	ENTAL'GMAX	=	12 3761	(12 2571)
[4 2530]	SUBAL'GAMMAI	=	16 2423	(24 4420)
[4 2531]	MULAL'D100	=	24 4157	(26 7027)
[4 2532]	DIVA'D900	=	26 4252	(10 4024)
[4 2533]	NOOP'	=	50 4000	(76 5331)

5. RPM (N_H) DISPLAY

The following changes were made in order to display N_H on the EADI center window:

[3 6740]	1D	=	00 0001	(00 0457)
[3 6745]	10D	=	00 0012	(00 1140)
[4 2722]	ENTIBK'4	=	36 0004	(32 1763)
[4 2770]	STRZ'SGNENA	=	40 0427	(12 2034)
[4 2771]	ENTAL'NH	=	12 2147	(63 2735)
[4 2772]	JP'3002	=	34 3002	(40 0427)

6. PITCH SAS MODIFICATION

The following changes were made to the pitch SAS as per E.O. No. 271a dated 2 April 1976.

[3 2306]	02 5370
[3 2315]	06 4570
[3 2275]	02 7340
[3 1466]	47 0500
[3 7156]	07 2460
[1 4027]	02 7156
[1 4015]	34 7710
[1 7710]	44 2762
[1 7711]	12 2021
[1 7712]	63 4016
[1 7713]	12 2024
[1 7714]	50 4000
[1 7715]	63 4016
[1 7716]	12 7156
[1 7717]	44 2301
[1 7720]	34 4032

7. ELIMINATION OF TIMING PROBLEM

It was discovered that a portion of the MFD code was causing a timing problem. The following patch was made in order to circumvent the errant code.

[6 0622] 34 0647 (50 7313)

8. AUTOPILOT MODIFICATIONS

The standard airspeed-hold autopilot was transformed into an FR-hold autopilot. The approach taken was to calculate an effective speed error from the flight reference error, that is:

$$\Delta V \triangleq \frac{\Delta FR[\%]}{5\%/kt}$$
$$\Delta FR \triangleq FR_c - FR$$

The flight reference command (FR_c) was equated to the standard variable used for airspeed command (IASREF), and the calculation of effective speed error was substituted every place the true speed error was calculated (VCERR or INEDRV). The following patches were required:

a. Convert IASREF to FR_c :

[1 1033]	ENTAL'FROTEN	=	12 3743
[1 1346]			
[1 6317]			
[1 7273]			
[1 7427]			
[2 5402]			
[2 7017]			
[4 2106]			

where FROTEN = $FR/10$

b. Remove IASREF limit calculation and set FR_c limits to 75% and 120%.

[6 4600]	NOCP'	=	50 4000
[3 2400]	750D	=	00 1356
[3 2401]	1200D	=	00 2260

c. Calculate the effective speed error from FR_c and FR.

[4 7611]	XFRERR	0'0	=	00 0000
[4 7612]	ENTAL'IASREF		=	12 1270
[4 7613]	MULAL'D10		=	24 4111
[4 7614]	SUBAL'FR		=	16 3747
[4 7615]	MULAL'ONE		=	24 4073
[4 7616]	DIVA'D50		=	26 4143
[4 7617]	STRAL'VCERR		=	44 2616
[4 7620]	IJP'XFRERR		=	55 7611

- d. Change calculations of VCERR and INTDRV to calculate the effective speed error.

[1 1355]		IRJP'YFRERR	=	30 1357
[1 1356]		JP'LOK+2	=	34 1360
[1 1357]	YFRERR	O'XFRERR	=	04 7611
[1 5025]		IRJP'YFRERR	=	30 1357
[1 5026]		NOOP'	=	50 4000
[1 5027]		NOOP'	=	50 4000
[1 6530]		IRJP'YFRERR	=	30 1357
[1 6531]		NOOP'	=	50 4000
[1 6532]		NOOP'	=	50 4000
[1 6561]		IRJP'YFRERR	=	30 1357
[1 6562]		NOOP'	=	50 4000
[6 4513]		IRJP'ZFRERR	=	30 4515
[6 4514]		JP'LOK+2	=	34 4516
[6 4515]	ZFRERR	O'XFRERR	=	04 7611
[6 4516]		NOOP'	=	50 4000

- e. Inhibit nozzle changes (this was done because the SR, FR scheme described herein was designed for one value of nozzle deflection).

[1 7103]	NOOP'	=	50 4000
[1 7121]	NOOP'	=	50 4000
[1 7306]	NOOP'	=	50 4000

- f. Remove the pitch "feedforward" in the elevator loop (this was done because the variable THHPR would occasionally cause large pitch excursions).

[1 4052]	NOOP'	=	50 4000
[1 4053]	↓		↓
[1 4054]			
[1 4055]			
[1 4056]			

g. Add an option for a pitch-attitude-to-throttle crossfeed (this was done in order to decouple the FR and flight path axes)*.

(1) Calculate the crossfeed

[1 4035]	ADDAL'ZC11	=	14 1271
[1 4036]	NOOP'	=	50 4000
[1 4037]	ENYBK'11D	=	36 0013
[1 4040]	RJP'ZTFWO	=	76 7522
[1 4041]	MULAL'KFRDT	=	24 3757
[1 4042]	DIVA'D360	=	26 4217
[1 4043]	STRAL'THTAX	=	44 3760
[1 4044]	NOOP'	=	50 4000
[1 4045]	NOOP'	=	50 4000
[1 4046]	NOOP'	=	50 4000
[1 4047]	NOOP'	=	50 4000

(2) Define required constants

[3 1602]	130527D	(washout time constant)
[3 3757]	-324D	(X-feed gain)
[3 3760]	0	(X-feed variable)

(3) Add crossfeed to throttle command.

[1 6627]	JP'7735	=	34 7735
[1 7735]	ENTAL'THTAX	=	12 3760
[1 7736]	MULAL'KTHHR	=	24 2141
[1 7737]	ADDA'TMPO	=	20 2760
[1 7740]	STRA'TMPO	=	50 0600
[1 7741]		=	03 2760
[1 7742]	ENTAL'THRTBL	=	12 2162
[1 7743]	JP'6630	=	34 6630

h. Define the proportional and integral flight reference gains.

[3 2303]	KVTHRS	-4	(K_{FR})
[3 2134]	KCRSS1	-4	(K_{FR_I})

* This option was not checked out.